

**Characterising the role of Actin and PI (3) kinases in  
endocytosis in the malaria parasite  
*Plasmodium falciparum***

**Wynand Anton Smythe**

Thesis presented for the degree of

**Masters in Science**

in the Division of Pharmacology

Department of Medicine

**University of Cape Town**

**Supervisor**

Dr Heinrich C Hoppe

February 2007

The copyright of this thesis vests in the author. No quotation from it or information derived from it is to be published without full acknowledgement of the source. The thesis is to be used for private study or non-commercial research purposes only.

Published by the University of Cape Town (UCT) in terms of the non-exclusive license granted to UCT by the author.

## Declaration

I hereby declare that all the work presented in this thesis is my own. This thesis has not been submitted in whole or in part for a degree at any other university.

---

Wynand Smythe

---

Date

University of Cape Town

# Table of Contents

---

<b>ACKNOWLEDGEMENTS</b>	<b>i</b>
<b>ABSTRACT</b>	<b>1</b>
<b>LIST OF ABBREVIATIONS</b>	<b>2</b>
<b>CHAPTER I: General Introduction</b>	<b>3</b>
1.1 Preface	3
1.2 Endocytosis	4
1.3 Model organisms in the study of endocytosis	7
1.3.1 Endocytosis in Amoebozoa	7
1.3.2 Endocytosis in Apicomplexans	7
1.3.3 Endocytosis in <i>Plasmodium falciparum</i>	9
1.4 Objective of this study	12
<b>CHAPTER II: Actin and its role in endocytosis</b>	<b>13</b>
2.1 Introduction	13
2.2 Results	17
2.2.1 The sensitivity of malaria parasites to actin inhibitors (IC <sub>50</sub> )	17
2.2.2 The effect of actin disrupting drugs on red blood cell integrity	18
2.2.3 The effect of actin disrupting drugs on trophozoite morphology	19
2.2.4 The effect of actin disrupting drug treatment on haemoglobin levels in malaria parasites	21
2.2.5 Haemoglobin levels in the presence of protease inhibitors (PrI)	25
2.2.6 The effect of actin disrupting drugs on HRP uptake by malaria parasites	28
2.2.7 Immunofluorescence assay (IFA)	30
2.2.8 Electron microscopy of malaria parasites exposed to actin disrupting drugs	36
2.2.9 The effect of actin disrupting drugs on the localisation of actin in <i>P. falciparum</i> infected erythrocytes as assessed by immunofluorescence assay (IFA)	40
2.3 Discussion	41
<b>CHAPTER III: Phosphoinositides and their role in endocytosis</b>	<b>46</b>
3.1 Introduction	46
3.2 Results	49
3.2.1 The sensitivity of malaria parasites to PI (3) kinase inhibitors (IC <sub>50</sub> )	49
3.2.2 The effect of PI (3) kinase inhibiting drugs on trophozoite morphology	50
3.2.3 The effect of PI (3) kinase inhibiting drug treatment on haemoglobin levels in malaria parasites	52

3.2.4 Haemoglobin levels in the presence of protease inhibitors	55
3.2.5 The effect of PI (3) kinase inhibiting drugs on HRP uptake by malaria parasites	58
3.2.6 Immunofluorescence assay (IFA)	60
3.2.7 Electron microscopy of malaria parasites exposed to the PI (3) kinase inhibiting drug Wortmannin	65
3.2.8 The effect of PI (3) kinase inhibiting drugs on the localisation of actin in <i>P.</i> <i>falciparum</i> infected erythrocytes as assessed by immunofluorescence assay (IFA)	69
3.3 Discussion	71

## **CHAPTER IV: Conclusion** 75

## **CHAPTER V: Materials and methodology** 77

5.1 <i>P. falciparum</i> strain used in this study	77
5.2 Drugs used during this study	77
5.2.1 Actin cytoskeleton disruptors	77
5.2.2 PI (3) kinase inhibitors	78
5.2.3 Malaria endocytosis inhibitor	78
5.2.4 Haemoglobin digesting inhibiting drugs (protease inhibitors (PrI))	78
5.2.5 Horseradish Peroxidase	78
5.3 <i>P. falciparum</i> <i>in vitro</i> cell culture	79
5.4 Parasite synchronisation	80
5.5 Growth inhibition assays (IC <sub>50</sub> )	81
5.6 Enrichment of trophozoite infected erythrocytes	84
5.7 Trophozoite isolation from host erythrocytes by saponin lysis	85
5.8 The effect of actin disrupting drugs on red blood cell integrity	86
5.9 Morphology of parasitised erythrocyte cultures before and after 14 hour actin perturbing drug exposure	86
5.10 Sodium dodecyl sulphate polyacrylamide gel electrophoresis (SDS-PAGE)	87
5.11 Western blotting	87
5.12 Horseradish Peroxidase endocytosis assay	88
5.13 Immunofluorescence assay (IFA)	90
5.14 Electron microscopy	92

## **REFERENCES** 94

## Acknowledgments

To my loving wife Tamara and daughter Kierha, thank you both for all your love and support.

I wish to thank my supervisor Dr. Heinrich Hoppe, for your guidance, supervision and encouragement. Thank you for helping me convey the “story” behind the data.

To my colleagues both past and present, Dale, Dr. Donnelly Van Schalkwyk, Lindy, Noor, Sandy, Sumaya, Dr. Susan Yeh, Dr. Uschi Wichart and Yuan, thank you all very much.

To my parents, brothers and sisters, thank you all for your motivation and belief in me.

In addition I would like to thank the University of Cape Town for their financial support during the completion of my Masters degree.

# Abstract

Endocytosis is a fundamental process performed by eukaryotic cells, whereby particles or solutes, present in the external environment, are taken up into the cell within membrane bound transport vesicles derived by the invagination and pinching-off of pieces of plasma membrane. Currently, published reports are not entirely conclusive or consistent regarding the role of actin in endocytosis. However, actin dynamics is suggested to play several roles during this process, including vesicle formation and subsequent trafficking in mammalian cells. Phosphoinositides (PI), in addition to generating messengers, regulate cell functions that include actin cytoskeleton remodelling and membrane trafficking within mammalian cells. By contrast to mammalian cells, very little is known about endocytosis in the malaria parasite. However, endocytosis via the cytostome is required by the parasite to ingest haemoglobin from its host cytosol which it transports within double membrane vesicles to the digestive vacuole, where digestion occurs and metabolites are used mostly for nutritional purposes. To gain a deeper understanding of the molecular basis and mechanisms of this vital process, a panel of inhibitors was used to inhibit the actin cytoskeleton and PI (3) kinases in the parasite. In this study Cytochalasin D and Latrunculin A, which depolymerise and prevent actin filament formation, Jasplakinolide, which stabilises actin filaments, and Wortmannin and LY294002, which inhibit PI (3) kinase, were used to study actin disrupting and PI (3) kinase inhibiting drug effects on haemoglobin endocytosis and transport vesicle trafficking within the malaria parasite *Plasmodium falciparum*. Using Western blot assays with anti-haemoglobin antiserum, we established actin cytoskeleton disruption (Cytochalasin D) not to alter haemoglobin levels following drug treatment in the presence of protease inhibitors. Similarly, Cytochalasin D did not inhibit horseradish peroxidase uptake from pre-loaded erythrocytes. These results suggest Cytochalasin D does not inhibit endocytosis, and thus that endocytosis is not actin dependent in the malaria parasite. By contrast, similar assays demonstrated PI (3) kinase inhibition to both reduce haemoglobin levels in presence of protease inhibitors, and similarly reduce HRP uptake following drug treatment. These results suggested a requirement for PI (3) kinase activity during endocytosis in the parasite. Additionally, both actin and PI (3) kinase were demonstrated to play a role in vesicle trafficking within the parasite. Immunofluorescence assays, using anti-haemoglobin, in addition to electron microscopy studies, demonstrated significantly elevated transport vesicles with accompanying significantly lowered haemoglobin levels within the digestive vacuole following actin and PI (3) kinase inhibiting drug treatments. These results, together with significantly raised intra-parasitic haemoglobin levels (as assessed by Western blot), suggested a block in haemoglobin trafficking to the digestive vacuole with a resultant accumulation of undigested haemoglobin within transport vesicles. The mechanism by which these drugs block trafficking within the parasite is, however, proposed to occur by two distinct mechanisms. Actin disruption may impede the physical trafficking and transport of vesicles, while PI (3) kinase inhibition may prevent membrane maturation, thereby preventing transport vesicle docking and fusion with the digestive vacuole.

## List of abbreviations

CM	Culture medium
Da	Daltons
DAPI	4',6-Diamidino-2-phenylindole Dihydrochloride
dH <sub>2</sub> O	Distilled deionised water
DMSO	Dimethyl Sulphoxide
IC <sub>50</sub>	Inhibitory concentrations at which 50 % of cells are killed
Haem	Haem B (prosthetic group consisting of iron located in haemoglobin)
Hb	Haemoglobin
Hct	Haematocrit
HEPES	Hydroxyethane Piperazine Sulphonic Acid
HRP	Horseradish Peroxidase
LDH	Lactate dehydrogenase
pLDH	Plasmodium lactate dehydrogenase
m	milli
mA	milli-Amps
MeOH	Methanol
mL	milli-Litre
M	Molar
mM	milli-molar
n	nano
NBT	Nitroblue tetrazolium
nM	nano-Molar
OPD	o-phenylenediamine
pst	Parasitemia
PBS	Phosphate Buffered Saline
PES	Phenazine ethosulphate
PI	Phosphoinositide
PI's	Phosphoinositides
PI (3) kinase	Phosphoinositide (3) kinase
PI (3) P	Phosphoinositide (3) phosphate
pLDH	Parasite lactate dehydrogenase
PrI	Protease inhibitors (ALLN & E64)
RBC's	Red blood cells
rpm	Revolutions per minute
rcf	Relative centrifugation factor
SDS-PAGE	Sodium Dodecyl Sulphate Polyacrylamide Gel Electrophoresis
TV's	Transport vesicles
Tris	Tris (hydroxymethyl) aminomethane
μ	micro
μM	micro-Molar
%	Percent
5 hr	5 hours
14 hr	14 hours

## 1.2 Endocytosis

Endocytosis can best be described as the process whereby particles or solutes, present in the external environment, are taken up into eukaryotic cells within membrane bound transport vesicles derived by the invagination and pinching-off of pieces of plasma membrane (Gagescu *et al.* 2000). Importantly, essential small molecules are able to traverse the plasma membrane through the action of integral membrane protein pumps or channels, whereas macromolecules have to be endocytosed within transport vesicles. Endocytosis can be mechanistically categorised into two groups: phagocytosis and pinocytosis (Figure 1). Phagocytosis, or cell eating, typically involves the uptake of large particles and is usually limited to specialised cells such as mammalian macrophages and *Dictyostelium* amoeba (Araki *et al.* 1996, Seastone *et al.* 1998). Conversely, pinocytosis, also known as cell drinking, occurs in all eukaryotic cell types where fluid and solutes are internalised by at least one of four basic pathways; macropinocytosis, clathrin-mediated endocytosis (CME), caveolae-mediated endocytosis and clathrin- and caveolae-independent endocytosis (Cavalli *et al.* 2001, Kirkham & Parton 2005).

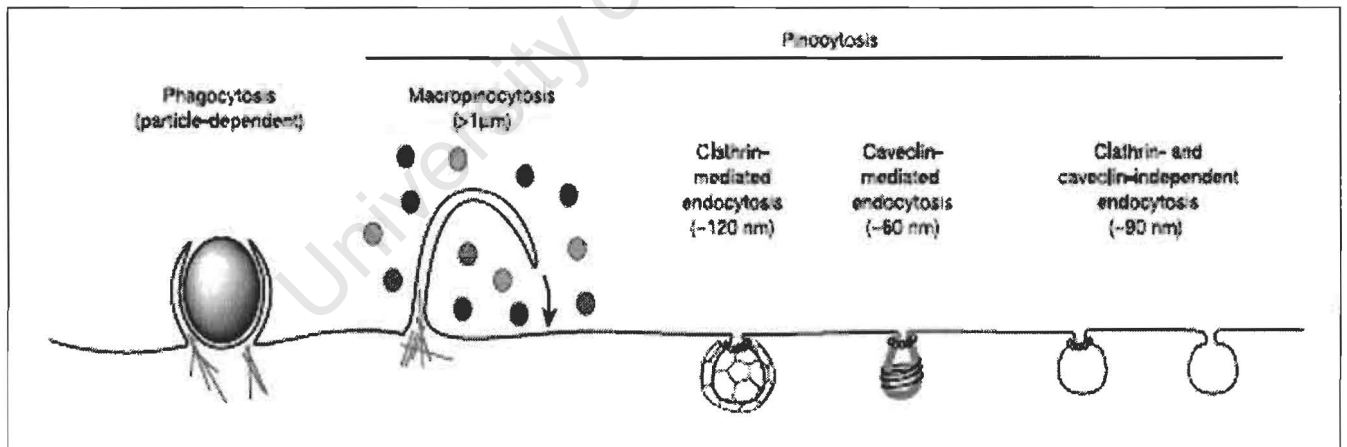


**Figure 1.** Endocytic pathways as described by Conner & Schmid (2003).

Phagocytosis in mammalian macrophages is an active process regulated by cell surface receptors and signalling cascades coordinated by Rho-family GTPases. Signalling cascades result in the formation of cell surface extensions (pseudopods) which engulf particles intended for internalisation. Macropinocytosis similarly involves Rho-family

GTPases which trigger membrane protrusions which then fuse back with the plasma membrane sampling large volumes of the surrounding milieu into large endocytic vesicles termed macropinosomes (Conner & Schmid 2003). Macropinocytosis thus closely resembles phagocytosis in that both internalisation processes involve actin assisted membrane extensions, which ultimately fuse and pinch off as intracellular vesicles (Araki *et al.* 1996, Mukherjee *et al.* 1997). Both phagocytosis and macropinocytosis differ mechanistically from the involution of more selective plasma membrane domains that give rise to smaller pinocytic vesicles. These mechanistically distinct and selective uptake pathways consist of CME and caveolae-mediated endocytosis as well as clathrin- and caveolae-independent endocytic mechanisms (Conner & Schmid 2003).

CME is the best understood pinocytic pathway which, constitutively occurs in all mammalian cells, allowing the continuous uptake of essential nutrients. Transmembrane receptors bound to their specific ligands are concentrated into coated pits on the plasma membrane. These coated pits are formed by the assembly of cytosolic clathrin proteins which invaginate the plasma membrane, pinching off to form clathrin coated vesicles (CCV's). These in turn transport concentrated receptor-ligand complexes into the cell (Mukherjee *et al.* 1997).

The less well understood pinocytic pathways encompass the clathrin independent mechanisms. These clathrin independent pathways are composed of either caveolae dependent or caveolae independent endocytic routes (Singh *et al.* 2003, Nabi & Le 2003, Kirkham *et al.* 2005). Caveolae are present on many cells, demarcating cholesterol and sphingolipid-rich microdomains of the plasma membrane in which signalling and membrane transporting molecules are concentrated (Anderson 1998). Highly ordered and dynamic lipid microdomains, caused by the interaction of sterols and sphingolipids, are termed lipid-rafts or rafts (Brown & London 1998). Caveolae are considered specialised lipid-raft domains, and have been implicated in a variety of cellular functions including endocytic processes and signal transduction (Razani *et al.* 2002). Lipid-raft enriched caveolae are flask-shaped plasma membrane indentations, stabilised by caveolins, which are essential cholesterol-binding membrane proteins (Rothberg *et al.* 1992). Caveolae are morphologically distinct from CCV's in that they are both smaller and "smoother", having

no clathrin coat. The latter appears as an electron dense coat when viewed under the electron microscope (Razani *et al.* 2002).

Other clathrin independent endocytic pathways are also caveolae independent and similarly represent a type of lipid-raft which is thought to constitute a specialised high capacity endocytic route for lipids and fluid (Kirkham & Parton 2005). These caveolae independent lipid-rafts are presumably captured and internalised within any of the endocytic pathways (Conner & Schmid 2003). Damm *et al.* (2005) and colleagues similarly demonstrated a clathrin and caveolae-independent endocytic pathway.

The majority of current knowledge regarding endocytic trafficking is based on clathrin dependent endocytic pathways, where internalised components captured within membrane bound vesicles are delivered to peripherally located early endosomes (EE) (Mukherjee *et al.* 1997). The early endosomal protein EEA1, essential for endosome fusion, is recruited to the early endosomal membrane through binding to the PI (3) kinase product, phosphatidylinositol-3-phosphate (PI (3) P), via a zinc finger referred to as the FYVE domain (Stenmark *et al.* 1996). EEA1 was identified as a new Rab5 effector that is required for endosome fusion (Simonsen *et al.* 1998). From the EE, components are sorted and either recycled back to the plasma membrane directly from the EE, or indirectly via tubule shaped networks collectively termed recycling endosomes (RE) in an actin dependent fashion (Apodaca 2001). Conversely, microtubules (but not actin) are required for the delivery of molecules from early endosomes to late endosomes (Gruenberg *et al.* 1989). This was partly demonstrated by the isolation of endosome carrier vesicles (ECV's) from cells that were treated with the microtubule-disrupting agent nocodazole (Gruenberg *et al.* 1989). ECV's likely represent the vacuolar portion of an early sorting endosome, which would move as a unit towards the centre of the cell in a microtubule dependent fashion and mature into a late endosome. Endocytosed molecules intended for degradation are transported to late endosomes (LE) or lysosomes (LY) inside these transport intermediates (Cavalli *et al.* 2001). A characteristic of all endosomal vesicles along the degradative pathway is the appearance of multiple membranes within their lumen, encapsulated by a limiting membrane forming the ECV (Gagescu *et al.* 2000). As in early endosomes, PI (3) P is also found within the internal membranes of transport intermediates but not within late endosomes (Simonsen *et al.* 1998).

## 1.3 Model organisms in the study of endocytosis

### 1.3.1 Endocytosis in Amoebozoa

The National Institutes of Health has listed *Dictyostelium* as a model system organism for the study of phagocytosis (Cardelli 2001). As regulator and effector molecules involved in uptake and transit are largely conserved between higher and lower eukaryotes, *Dictyostelium* (a soil amoeba) serves as a valuable model system for the study of endocytosed particles and fluid (Maniak 2001). Phagocytosis and macropinocytosis are actin dependent uptake pathways primarily performed by specialist cells (including macrophages and *Dictyostelium*) resulting in particle and fluid-filled phagosomes and macropinosomes respectively (Araki *et al.* 1996, Clarke *et al.* 2002). Actin polymerisation is required for the protrusion of plasma membrane and engulfment of particles and fluid as demonstrated by filamentous actin depolymerising drugs Cytochalasin and Latrunculin (Seastone *et al.* 1998). It is postulated that during phagocytosis and macropinocytosis, actin polymerisation and vesicle recruitment are coupled to extend the plasma membrane, forming the phagocytic and macropinocytic cups respectively (Cardelli 2001). In support of this, actin was observed to accumulate below forming phagocytic cups as verified by the actin filament binding fluorescent phalloidin (Seastone *et al.* 1998). Macropinocytosis is the main route of fluid phase uptake in *Dictyostelium* (Clarke *et al.* 2002). Newly formed actin dependent macropinosomes (mostly between 1 and 2  $\mu\text{m}$  in diameter) containing internalised fluid are, however, dependent on microtubules for their transport within the cell (Clarke *et al.* 2002). Exocytosis, by contrast is actin dependent, as late endocytic vacuoles (coated with filamentous actin) accumulate in presence of actin depolymerising drugs (Maniak 2003). In *Dictyostelium*, Phosphoinositide (3) Kinase (PI (3) K) is required for macropinocytosis, but does not appear essential for phagocytosis (Cardelli 2001).

### 1.3.2 Endocytosis in Apicomplexans

*Toxoplasma gondii*, an obligate intracellular protozoan parasite infecting all nucleated cell types of warm blooded vertebrates, is regarded as a model system for the study of intracellular parasitism (Botero-Kleiven *et al.* 2001). Intracellular forms of apicomplexan parasites such as *Toxoplasma* and *Plasmodium* actively penetrate host cells resulting in the

formation of a fusion resistant parasite vacuole termed the parasitophorous vacuole (PV) (Dobrowolski & Sibley 1996). The PV maintains a neutral pH and remains segregated from the host endocytic and exocytic pathways (Sibley 2003). *Plasmodium* and *Toxoplasma* are purine auxotrophs and consequently cannot synthesise their own purines and are therefore reliant on the uptake of purine containing compounds from their hosts (Wang & Simashkevich 1981). The parasitophorous vacuole membrane (PVM) of apicomplexan parasites is non-fusogenic and thought to be inaccessible to macromolecules (Robibaro *et al.* 2001). In order to gain host cell nutrients, *Toxoplasma* modifies the limiting membrane of the PV allowing free diffusion of small molecules, possibly those of simple sugars, amino acids, nucleobases and cofactors (Sibley 2003). Here, the PV limiting membrane is proposed to have a PVM channel (140pS high capacity channel) which imparts a size-dependent permeability between the host cytosol and the PV with a size exclusion limit of <1300 Da, similar to the PVM channel in *Plasmodium* infected erythrocytes which has a size exclusion limit estimated at <1400 Da (Robibaro *et al.* 2001). Furthermore, the PV of *T.gondii* contains an intravacuolar tubulovesicular network, which in part appears continuous with the parasite plasma membrane (PPM) and forms connections with the PVM (Saliba & Kirk 2001). The parasite is additionally known to target many proteins from its secretory organelles (rhoptries and dense granules) to its vacuole membrane (Hakansson *et al.* 2001).

In comparison to the low molecular weight nutrient uptake pathways, endocytic mechanisms in apicomplexan parasites are poorly understood (Botero-Kleiven *et al.* 2001). In *Toxoplasma*, the cytostome, a cup shaped invagination of the parasite plasma membrane, has a bristle-like appearance on the cytosolic face of the membrane suggestive of a clathrin coat known to be associated with endocytic vesicles in higher eukaryotes (Nichols *et al.* 1994). *Toxoplasma* and *Plasmodium* are proposed to use their cytostome organelles to mediate internalisation of macromolecules (Nichols *et al.* 1994, Aikawa *et al.* 1966). Extracellular tachyzoites of *T. gondii* acquire molecules through both receptor-specific and fluid phase endocytic mechanisms concentrating them inside single tubulo vesicular compartments that become multiple with time (Botero-Kleiven *et al.* 2001).

### 1.3.3 Endocytosis in *P. falciparum*

The *Plasmodium* parasite plasma membrane (PPM) has a full range of transport processes typical of eukaryotic cells (Kirk 2001). Mammalian erythrocyte plasma membranes however, have a reserved range of transport systems which are able to support the moderate nutritional demands of the cell. In some cases the transport capabilities of the host cell membrane meet the nutritional requirement of the intracellular *Plasmodium* parasite (e.g. glucose transport) (Francis *et al.* 1994). However, in other cases the host endogenous transport system is either too slow or is completely lacking, as is the case for glutamate and pantothenic acid transport (Saliba & Kirk 2001). As *Plasmodium* species are auxotrophs and incapable of fatty acid synthesis, they endocytose most of their host cell cytoplasm (Goldberg 1993, Olliaro & Goldberg 1995) and may further supplement their nutritional needs by endocytosing low molecular weight solutes and macromolecules delivered to the parasitophorous vacuole (PV) (Robibaro *et al.* 2001). The malaria parasite is separated from its host's cytoplasm by two membranes namely: the parasitophorous vacuole membrane (PVM) (the outer most membrane) and the parasite plasma membrane (PPM) (the inner membrane). In addition, the parasite is further isolated from the extracellular environment by the erythrocyte plasma membrane. The parasite permeates the host erythrocyte cell membrane by inserting nutrient channels into it, referred to as parasite derived new permeation pathways (NPP) (Ginsburg *et al.* 1984). Nutrients may also gain access to the parasite via an interconnected network of tubulovesicular membranes (TVM) which is thought to be an extension of the PVM (Pouvelle *et al.* 1991, Goodyer *et al.* 1997, Lauer *et al.* 1997). There are three proposed mechanisms of how the TVM could allow access of nutrients to the parasite. Firstly, although doubtful, the TVM is hypothesised to bridge the PVM and the host erythrocyte plasma membrane forming a macromolecule-permeable aqueous channel (parasitophorous duct) allowing the uptake of macromolecules (Pouvelle *et al.* 1991, Goodyer *et al.* 1997). Secondly, the TVM could possibly, without penetrating it, form specialised junctions with its host erythrocyte plasma membrane where NPP channels are located (Martin & Kirk 2006). Thus, the TVM-red cell junction functions as a molecular sieve allowing low molecular weight solutes, but not macromolecules, access to the parasite. Lastly, the increased surface area of the PVM provided by the TVM network, together with its high conductance (140pS) channels, could further allow the intracellular parasite access to nutrients (Robibaro *et al.* 2001). The PVM high capacity channels (140pS) are proposed to act as molecular sieves,

freely allowing diffusion of low molecular weight ions and nutrients (below 1400 Da) between the host cytosol and the parasitophorous vacuole (PV) (Saliba & Kirk 2001).

*Plasmodium* species are known to endocytose large amounts of extracellular material from their host erythrocytes cytoplasm (Goldberg 1993). The intracellular parasite internalises host cytoplasm, consisting primarily of haemoglobin (Hb), via a specialised structure (cytostome or micropore) consisting of invaginations of the parasite plasma and parasitophorous vacuole membrane (Aikawa *et al.* 1966, Olliaro & Goldberg 1995, Bannister *et al.* 2000). A double membrane vesicle pinches off from the cytostome with its inner membrane derived from the parasitophorous membrane and its outer membrane derived from the parasite plasma membrane. These haemoglobin filled endocytic vesicles traffic towards, fuse with and release their parasitophorous membrane encapsulated contents into the digestive vacuole (Goodyer *et al.* 1997, Bannister *et al.* 2000, Fitch 2004). Endocytosed Hb delivered to the large acidic digestive vacuole (presumably equivalents of mammalian lysosomes) contains aspartic, cysteine and metallo-proteases which cleave Hb into peptides (Kolakovich *et al.* 1997, Gavigan *et al.* 2001). Trafficking of proteases, along with endocytosed Hb, is proposed to occur via the parasite plasma membrane to the digestive vacuole (Francis *et al.* 1994). Host cytoplasmic Hb is utilised as an amino acid source and possibly this uptake with subsequent digestion prevents the lytic pressure on the host erythrocyte from being exceeded (Krugliak *et al.* 2002). The digested Hb product haem is converted into insoluble haemozoin or malaria pigment (Slater *et al.* 1991). While little is known about the formation and regulation of the cytostomal pathway, it does not appear to be microtubule dependent, as Taxol treatment (microtubule stabilising agent) does not inhibit the production of haemozoin (Goodyer *et al.* 1997). Cytochalasin D, a drug which depolymerises actin filaments, showed no effect on the internalisation of fluorescent dextrans from the external milieu (Goodyer *et al.* 1997). Interestingly, these extra-erythrocytic endocytic fluorescent dextran tracers were not delivered to the food vacuole as Hb typically is. They are instead conveyed to unknown structures present throughout the parasite cytoplasm, suggesting two separate endocytic pathways which do not converge at the food vacuole (Goodyer *et al.* 1997). Strikingly, Pouvelle *et al.* (1994) demonstrated that host cell membranes of infected erythrocytes do not endocytose. Conversely, uptake of the a fluid phase marker Lucifer

Yellow, has been observed in mature infected red blood cells suggesting that host erythrocyte membranes were indeed capable of pinocytosis (Haldar *et al.* 1989).

*Plasmodium* parasites are known to contain homologues of endocytic machinery including Rab GTPases, clathrin, dynamin and adapter subunit complexes critical for endocytic trafficking. However, their role in haemoglobin and dextran uptake is unknown (Robibaro *et al.* 2001, Quevillon *et al.* 2003). These proteins are known to have additional functions to endocytosis in mammalian cells, thus their presence in malaria parasites (based on gene sequence homologies) does not necessary indicate they function as endocytic proteins. *Plasmodium* parasitised erythrocyte membranes contain lipid rafts which Haldar *et al.* (2001) assume to play a role during endocytosis and macromolecular transport, however, links between the cytoskeleton and lipid rafts are not well understood. It must be recalled that Pouvelle *et al.* (1994) has demonstrated host cell membranes incapable of endocytosis.

## 1.4 Objective of this study

From the previous discussion it is clear that we have only a superficial knowledge of endocytosis in malaria parasites, based predominantly on morphological studies. Endocytosis is a fundamental process in all eukaryotic cells and is required by the parasite to ingest haemoglobin from the infected erythrocyte cytosol, mostly for nutritional purposes. A deeper understanding of the molecular basis and mechanisms of this vital process is required. Experimentally this may be achieved by various approaches. One approach is to use known inhibitors of endocytosis in other eukaryotes and determine their effects (if any) on the parasite. In this study, a panel of inhibitors was used to inhibit the actin cytoskeleton and PI (3) kinases, two elements known to mediate and regulate the endocytic pathway in higher cells. Their roles, if any, in parasite endocytosis was determined using novel endocytic assays.

# Chapter II

## Actin and its role in endocytosis

### 2.1 Introduction

Actin is the most abundant intracellular protein in eukaryotic cells and exists in two states; G-actin, the globular monomer protein, and filamentous actin, composed from a linear chain of G-actin monomers (Prescott 1988). G-actin readily polymerises under physiological conditions to form filamentous actin (F-actin). Similarly, F-actin can depolymerise into monomer G-actin subunits. F-actin is a double-helical filament, able to polymerise and depolymerise from both the barbed and pointed ends. The polymerisation and depolymerisation rates are, however, not equal. The barbed end polymerises faster while the pointed end depolymerises faster. Cytochalasins, a family of chemically related mould metabolites, bind the barbed ends of microfilaments, preventing their elongation and leading to depolymerisation from the pointed end (Goddette & Frieden 1986). Conversely, Jasplakinolide, a cyclic peptide isolated from the marine sponge *Jaspis johnstoni*, binds F-actin competitively with phalloidin thereby stabilising the microfilaments and inducing polymerisation (Bubb *et al.* 1994).

Genetic studies performed on the yeast, *Sacharomyces crevisiae*, have established a functional connection between a dynamic actin cytoskeleton and endocytosis (Engqvist-Goldstein & Drubin 2003). Cortical actin patches support the internalisation pathway within yeast (Ayscough 2004). Actin polymerisation at these cortical sites is proposed to drive endocytic vesicles into the cell (Merrifield *et al.* 2002, Ayscough *et al.* 1997), a process similar to that observed by Merrifield *et al.* (1999) in mammalian cells. The link between endocytosis and actin in mammalian cells is still, however, not as convincing (Qualmann *et al.* 2000). Here the actin cytoskeleton is hypothesised to either regulate the localisation and anchoring of endocytic machinery on the plasma membrane by providing a scaffolding-type support structure, or to generate a driving force provided by actin polymerisation to facilitate membrane invagination, vesicle fission and / or the propulsion

of nascent vesicles away from the plasma membrane into the cell cytosol (Merrifield *et al.* 1999, Taunton *et al.* 2000).

Localised actin polymerisation occurs at endocytic sites in phagocytosis, macropinocytosis, clathrin-mediated endocytosis and caveolae-mediated endocytosis (Engqvist-Goldstein & Drubin 2003). Phagocytosis and macropinocytosis are more convincingly actin dependent compared to clathrin-dependent pathways (Cavalli *et al.* 2001, May & Machesky 2001). Phagocytosis and macropinocytosis accompany membrane ruffling induced in many cell types by growth factors. Rho-family GTPases trigger actin driven membrane protrusions (pseudopods) which result in particles (phagocytosis) or solutes (macropinocytosis) ingested into large endocytic vesicles termed phagosomes or macropinosomes respectively (Niedergang and Chavrier 2004). Additionally, macropinosomes induce actin polymerisation when they separate from the plasma membrane (Merrifield *et al.* 1999), using the force generated by actin polymerisation to drive them through the dense cytocortex away from the plasma membrane into the cell (Merrifield *et al.* 2002).

As in yeast, mammalian cells may require the actin cytoskeleton for clathrin-dependent receptor-mediated endocytosis (May & Machesky 2001). Supporting this, Latrunculin A, a membrane permeable drug which selectively sequesters actin monomers, thereby depolymerising actin filaments by shifting the equilibrium from the polymerised to the depolymerised state (Coue *et al.* 1987, Ayscough *et al.* 1997, Oliveira *et al.* 1997), was found to inhibit formation of clathrin-coated vesicles at the plasma membrane (Lamaze *et al.* 1997). Actin may function as a scaffold for caveolae similarly to that seen in clathrin coated vesicle formation. In support of the requirement of actin during caveolae mediated endocytosis, this uptake pathway was impeded following disruption of actin assembly (Conner & Schmid 2003).

In mammalian cells Latrunculin A arrests the endocytic pathway at the invaginated coated pit stage (Lamaze *et al.* 1997). This provides support for the possible role of actin polymerisation required to generate the force for vesicle fission from the plasma membrane. As stated above, multiple roles may be performed by the polymerisation of the actin cytoskeleton during endocytosis. These include induction of membrane

invaginations, pinching off and fission of endocytic vesicles, and propulsion of nascent vesicles away from the plasma membrane. The latter is supported by experimental reports of endosomes, pinosomes, clathrin coated vesicles and secretory vesicles associated with actin tails or plumes (comet tails) in the cytoplasm (Merrifield *et al.* 1999, Taunton *et al.* 2000) as are lysosomes in *in vitro* systems (Quallman *et al.* 2000). Phagosomes are similarly hypothesised to use actin comet tails to propel them through the cytoplasm as they retain proteins within their membranes which interact with the actin cytoskeleton (May & Machesky 2001). The actin cytoskeleton may support endocytic vesicle transport into the cytosol by assembling actin nucleating machinery on the surface of endocytic vesicles, ultimately leading to organelle migration (Merrifield *et al.* 1999).

Despite the requirement for actin polymerisation required during these endocytic events, actin may also negatively regulate endocytosis (Quallman *et al.* 2000) as it does in exocytosis (Eitzen 2003). Importantly, all endocytic pathways require remodelling of the cell cortex (Ayscough 2004). A rigid cortical actin cytoskeleton may act as a physical barrier to endocytosis and thus will require its removal in order to allow passage for nascent vesicles into the cytoplasm (Schafer 2002). Cytochalasin D (CD) binds and caps the faster growing barbed ends of F-actin (Goddette & Frieden 1986), causing the depolymerisation of actin microfilaments that are actively turning over (predominantly stress fibres). Conversely, cortical actin filaments appear more resistant to disruption by CD (Cassimeris *et al.* 1990), possibly explaining ambiguous results yielded by this drug in studies on endocytosis in mammalian cells (Lamaze *et al.* 1997).

Once extracellular compounds are endocytosed and the vesicles have been propelled from the plasma membrane, actin filaments may further facilitate their trafficking within the cell (Gruenberg 2001, Schafer 2002). Actin motor proteins may link endocytosed cargo to actin filaments via rhodopsin or via linker proteins referred to as CLIPs (cytoplasmic linker proteins) (Goode *et al.* 2000). Some studies on mammalian cells are in agreement regarding the requirement of actin further along the degradative endocytic pathway (Durrbach *et al.* 1996, Clague 1998). By contrast, studies in yeast have demonstrated trafficking events between intermediate endosomes and lysosomes to be actin independent (Clague 1998). Transport along the recycling pathway is both actin and myosin motor

dependent. These could play a mechanical role in the biogenesis and dynamics of recycling tubules (Gruenberg 2001).

In summary, although published reports are as yet not entirely conclusive or consistent, actin dynamics may play several roles in eukaryotic vesicle formation and subsequent trafficking in mammalian cells. In this study, Cytochalasin D and Latrunculin A (depolymerise and prevent actin filament formation) and Jasplakinolide (stabilises actin filaments) were used to study haemoglobin endocytosis and transport vesicle behaviour in malaria parasites.

University of Cape Town

## 2.2 Results

### 2.2.1 The sensitivity of malaria parasites to actin inhibitors (IC<sub>50</sub>)

To ensure that malaria parasites are sensitive to commonly used actin inhibitors and to determine the concentrations of inhibitors required for examining the role of actin in parasites, growth inhibition assays, based on the measurement of parasite lactate dehydrogenase activity, were performed. The concentrations of the various study drugs which yield 50% parasite growth inhibition (IC<sub>50</sub>) are summarised in Table 1. Working concentrations for the various classes of drug were derived from the IC<sub>50</sub> values and are summarised together with their solvent concentrations in Table 1. Final working concentrations for each drug were for most drugs 5 - 10 times that of their respective IC<sub>50</sub> values in an attempt to ensure observed parasite effects are the result of drug exposure and avoid non-specific effects by overdosing. However, Latrunculin A and Jasplakinolide were used at 10 and 1  $\mu$ M respectively as shown in Table 1. As IC<sub>50</sub> values for all drugs were in the nanomolar range, it is apparent that malaria parasites require a dynamic actin cytoskeleton for their survival. Similarly, actin filament stabilising and destabilising drugs have been shown to inhibit apicomplexan motility, in agreement with the requirement for actin filament dynamics in erythrocyte invasion (Kappa *et al.* 2004).

**Table 1.** IC<sub>50</sub> values generated for each drug together with their 95 % confidence intervals and final working and solvent concentrations used during experimentation.

Drug	IC <sub>50</sub>	95 % Confidence Interval	Final working concentration used	Solvent concentration
Cytochalasin D	10.98 nM	9.63 – 12.51	50 nM	0.0005 % DMSO
Latrunculin A	9.85 nM	6.76 – 14.36	10 $\mu$ M	0.1 % DMSO
Jasplakinolide	74.26 nM	61.61 – 89.50	1 $\mu$ M	0.1 % DMSO
Mefloquine	21.44 nM	14.87 – 30.91	156 nM	0.006 % MeOH
Dimethyl-sulphoxide	0.84 %	0.65 – 1.07	0.0005 – 0.1 %	0.0005 – 0.1 %
Methanol	1.01 %	0.61 – 1.68	0.006 %	0.006 %

## 2.2.2 The effect of actin disrupting drugs on red blood cell integrity

As 5 hours of Cytochalasin D treatment has been reported to cause frog red blood cell swelling (Sauviat *et al.* 2006), erythrocyte integrity assays were conducted to investigate whether actin disrupting drugs cause lysis of human erythrocytes membranes which possess a rigid actin cytoskeleton. Erythrocyte numbers and shape were observed by light microscopy prior to and after treatment with either 50 nM Cytochalasin D or 1  $\mu$ M Jasplakinolide over a 5 hour period.

As no significant differences were found in erythrocyte numbers (Table 2) or shape (data not shown) before and after drug treatment, observed parasite effects in following studies were assumed to be due to actin cytoskeleton disruption within the malaria parasite. In future studies, this assumption may be strengthened by a more thorough examination of erythrocyte membrane integrity and general morphology by scanning electron microscopy. Erythrocyte numbers before and after actin disrupting drug treatment are summarised in Table 2.

**Table 2.** Normalised erythrocyte counts before & after 5 hours of 50 nM Cytochalasin D and 1  $\mu$ M Jasplakinolide treatment. Erythrocytes were suspended in culture medium with a final haematocrit of 2 %. Erythrocytes were counted before and after incubation with the various treatment regimens by means of a haemocytometer and light microscope. The mean of three erythrocyte counts performed before and after treatment exposure were compared. Significance was set at  $\alpha = 0.05$ . n = number of observations.

Treatment regimen	Before	After	% Change	n	Statistical test	Two-tailed P value	Outcome
[50 nM] Cytochalasin D	100 $\pm$ 7.71	96.82 $\pm$ 9.55	3 % $\downarrow$	15	Unpaired T test	p = 0.7973	NO significant change
[1 $\mu$ M] Jasplakinolide	100 $\pm$ 11.95	99.23 $\pm$ 10.02	1 % $\downarrow$	15	Unpaired T test	p = 0.961	NO significant change

### **2.2.3 The effect of actin disrupting drugs on trophozoite morphology**

Infected red blood cell membranes are conceivably more susceptible to cytoskeleton disruption compared to non-infected erythrocyte membranes due to additional lytic pressures brought about by the intracellular parasite. Parasite and erythrocyte morphologies were observed by light microscopy of Giemsa-stained thin blood smears following drug and solvent control exposure of *in vitro* trophozoite infected red blood cells.

No major morphological differences were detected between control and drug-treated trophozoite stage parasites and erythrocytes (Figure 2). Nonetheless, punctate structures were peripherally located in the majority of drug-treated treated parasites (Figure 2, black arrows), while malaria pigment was more readily identifiable in control treated parasites (Figure 2, white arrows). Malaria pigment was easily identifiable due to the presence of shiny haemozoin crystals formed from haem moieties released during haemoglobin digestion within the food vacuole (Slater *et al.* 1991).

As no major deterioration in morphology was observed in drug-treated malaria-infected erythrocytes, treated parasites were assumed viable after actin disrupting drug exposure. The presence of punctate structures in drug-treated parasites could represent the accumulation of transport vesicles, while the reduced malaria pigment could signify a block in digestion brought about by actin disrupting drug treatment. These observations are based on light microscopy (limited resolution) and the following sections describe studies to further explore these findings.

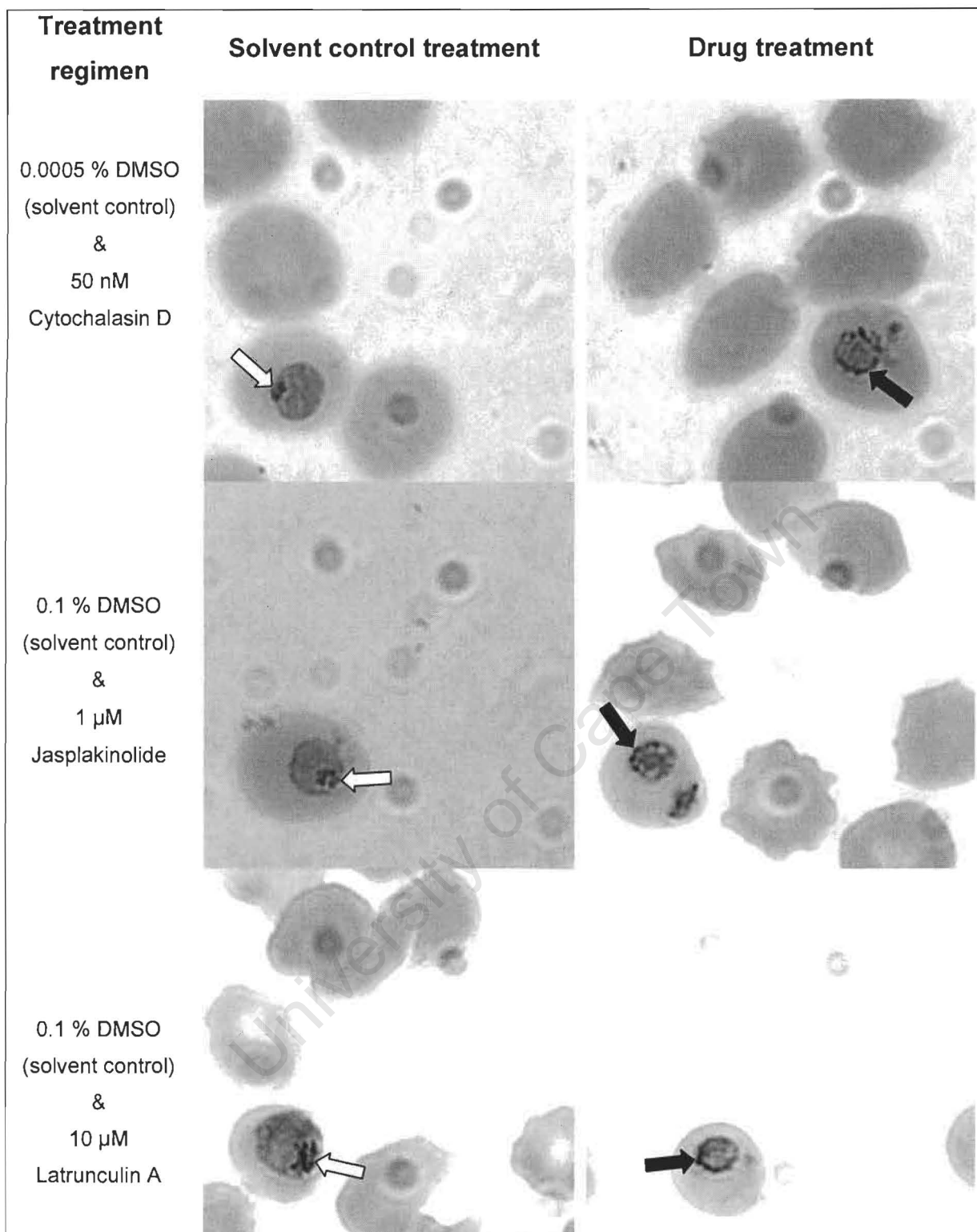


**Figure 2.** Representative Giemsa stained malaria parasitised red blood cells after 14 hours of 50 nM Cytochalasin D (0.0005 % DMSO), 1 μM Jasplakinolide (0.1 % DMSO) and 10 μM Latrunculin A (0.1 % DMSO) treatment. Treatment regimens are indicated on the left followed by representative images of solvent control (no drug) and drug-treated parasitised erythrocyte cultures. Densely localised malaria pigment of solvent control treated parasites are denoted by means of white arrows while postulated haemoglobin transport vesicles of drug-treated parasites are indicated with black arrows.

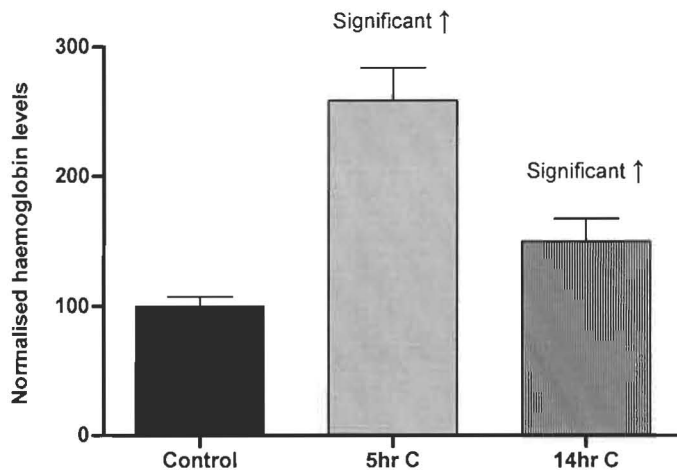
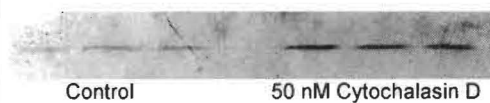
## 2.2.4 The effect of actin disrupting drug treatment on haemoglobin levels in malaria parasites

Malaria parasites endocytose large quantities of haemoglobin from the red blood cell cytoplasm. A reduction of parasite haemoglobin levels following drug treatment would be predictive of a block in endocytosis while an increase could signify inhibition of digestion. To determine the effects of actin disrupting drugs on the haemoglobin levels in the 3D7 strain of *P. falciparum*, a parasite culture at approximately 10 % parasitemia was split into two and exposed to either drug or solvent control. Parasites were either incubated in 50 nM Cytochalasin D, 1  $\mu$ M Jasplakinolide, or 10  $\mu$ M Latrunculin A for 5 or 14 hours, followed by Western blotting with anti-haemoglobin antiserum before comparisons were made between drug and control treated parasites.

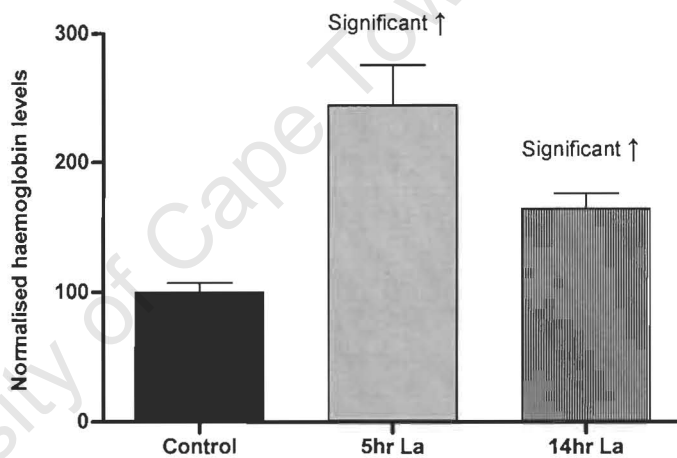
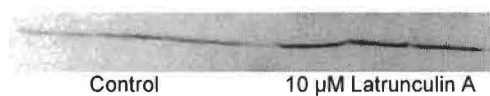
Cytochalasin D and Latrunculin A treated parasites showed significantly increased haemoglobin levels, represented graphically in Figure 3 A & B. By contrast Jasplakinolide treatment over both exposure times significantly reduced haemoglobin levels within the parasite (Figure 3 C). As Mefloquine is known to inhibit endocytosis and significantly reduce parasite haemoglobin levels (Hoppe *et al.* 2004), it was used as a positive control. Here, 156 nM of Mefloquine over both 5 and 14 hours of exposure to parasite cultures reduced haemoglobin levels significantly (Figure 3 D). Complete assay results are summarised in Table 3.

These results suggested that the actin filament stabilising Jasplakinolide, like Mefloquine, may inhibit haemoglobin endocytosis. By contrast, the actin depolymerising drugs Cytochalasin D and Latrunculin A raised haemoglobin levels, possibly by stimulating endocytosis or blocking haemoglobin digestion. The apparent reduction of malaria pigment observed in Cytochalasin D and Latrunculin A treated Giemsa-stained parasites, together with the significantly raised haemoglobin levels, suggest a block in digestion.

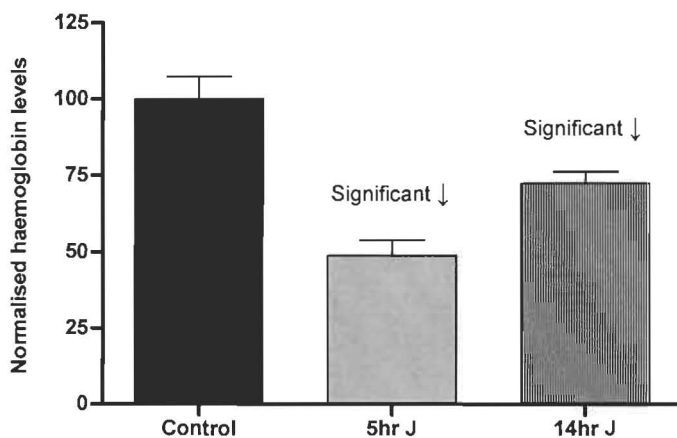
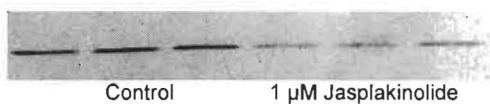
**A. 50 nM Cytochalasin D**



**B. 10 μM Latrunculin A**



**C. 1 μM Jasplakinolide**



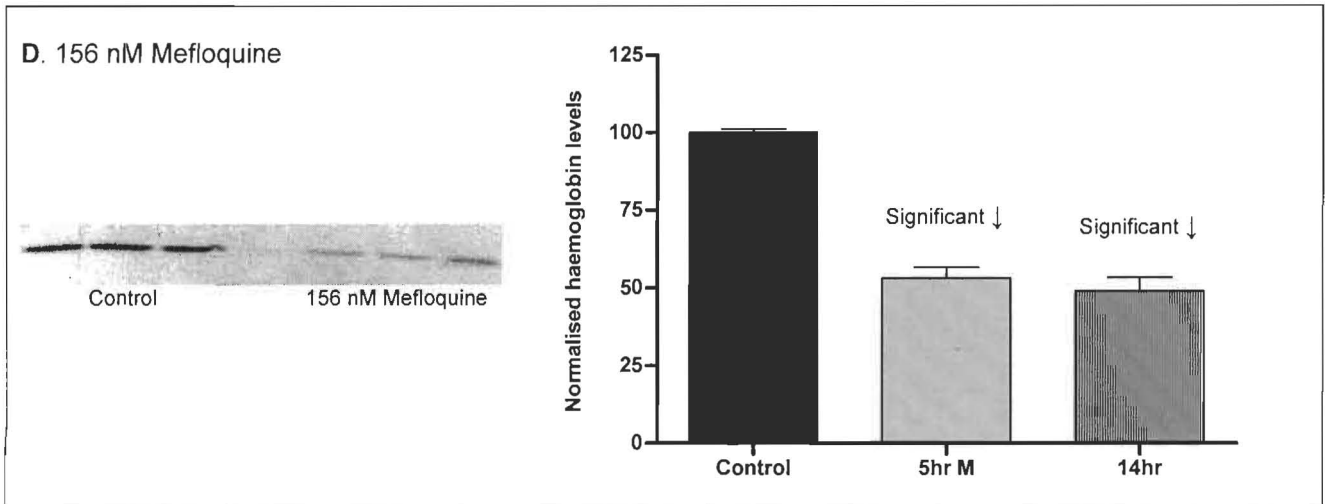


**Figure 3.** Haemoglobin levels in malaria parasites after various actin disrupting drug exposures. Parasite cultures (at approximately 10 % parasitemia) were split into two and either incubated with drug or solvent control for 5 or 14 hours. Malaria parasites were released from their host erythrocytes by saponin treatment, and washed extensively to remove unrelated extra-parasitic haemoglobin. Parasite pellets were run on SDS 10%-polyacrylamide gels, and the haemoglobin levels in the parasites were determined by Western blotting with anti-haemoglobin antiserum. Net intensities of individual haemoglobin bands were determined with Kodak ID image analysis software. Western blot representative images of haemoglobin levels accumulated by parasites exposed to 50 nM Cytochalasin D (A), 10  $\mu$ M Latrunculin A (B), 1  $\mu$ M Jasplakinolide (C) and 156 nM Mefloquine (as the experiment control) (D) are shown on the left. Summarised haemoglobin accumulated levels after 5 and 14 hour drug treatments are represented by means of bar graphs on the right of each representative western blot image. Experiments were performed in triplicate on at least 3 individual days. Intensity levels indicated were normalised to the control set at 100 and comparisons were made. Significance was set at  $\alpha = 0.05$ . Error bars indicate Standard Error of the Mean.

**Table 3.** Intra-parasitic haemoglobin levels after various actin disrupting treatments. n = number of observations.

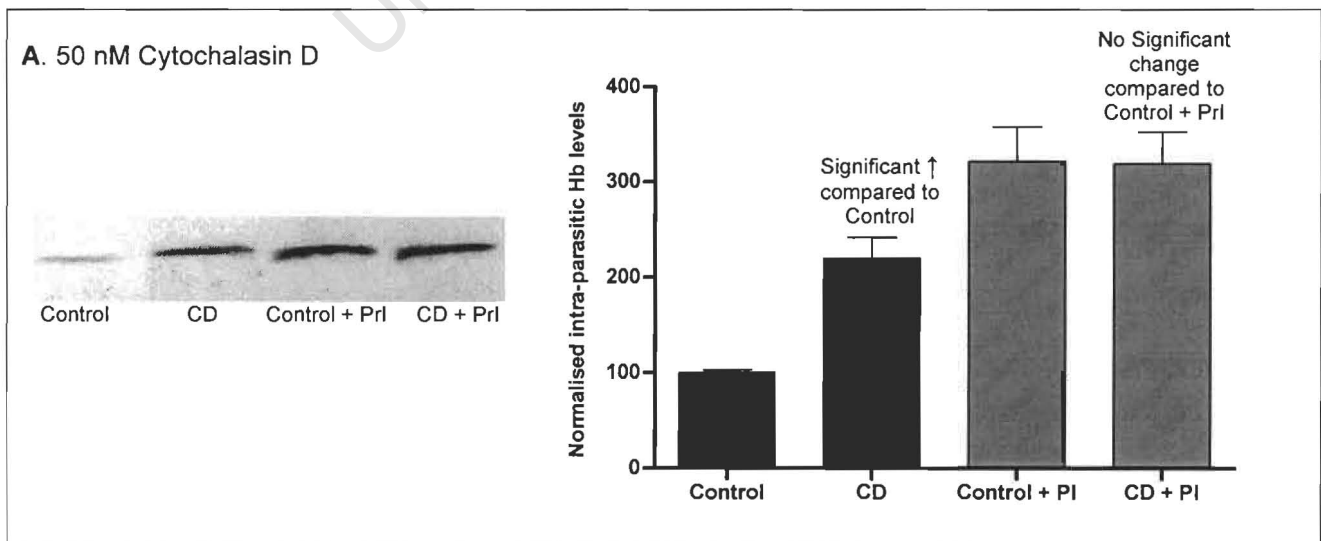
Treatment	Control	Drug	% Difference	n	Statistical test	Two tailed P value	Outcome
5 hr 50 nM Cytochalasin D	100 ± 7.32	258.41 ± 25.39	158 % ↑	21	Mann-Whitney	p < 0.0001	Significant increase
14 hr 50 nM Cytochalasin D	100 ± 2.11	149.95 ± 17.49	50 % ↑	15	Mann-Whitney	p = 0.0016	Significant increase
5 hr 10 µM Latrunculin A	100 ± 6.25	244.69 ± 31.29	145 % ↑	18	Mann-Whitney	p < 0.0001	Significant increase
14 hr 10 µM Latrunculin A	100 ± 8.67	164.48 ± 11.61	64 % ↑	15	Unpaired T test	p = 0.0001	Significant increase
5 hr 1 µM Jasplakinolide	100 ± 2.20	48.80 ± 4.97	51 % ↓	16	Mann-Whitney	p < 0.0001	Significant decrease
14 hr 1 µM Jasplakinolide	100 ± 4.66	72.35 ± 3.74	28 % ↓	15	Unpaired T test	p < 0.0001	Significant decrease
5 hr 156 nM Mefloquine	100 ± 1.24	53.13 ± 3.45	47 % ↓	47	Mann-Whitney	p < 0.0001	Significant decrease
14 hr 156 nM Mefloquine	100 ± 3.94	49.02 ± 4.41	51 % ↓	24	Unpaired T test	p < 0.0001	Significant decrease

### 2.2.5 Haemoglobin levels in the presence of protease inhibitors (PrI)

Total haemoglobin levels in the parasite are the result of a balance between uptake (endocytosis) and digestion in the digestive vacuole. To further investigate the effect which actin disrupting drugs have on the endocytosis of haemoglobin by the malaria parasite from its host cytosol, parasite cultures were treated with protease inhibitors (PrI) in an attempt to negate digestion and use haemoglobin levels within malaria parasites as a more accurate gauge of endocytosis. Mefloquine, having been shown to inhibit endocytosis of macromolecules in the malaria parasite *P. falciparum* (Hoppe *et al.* 2004), was again used as the positive control.

Five hour 50 nM Cytochalasin D treatment had no significant effect on haemoglobin levels within the malaria parasite when co-administered with PrI (Figure 4 A). Conversely, treatment with 1  $\mu$ M Jasplakinolide together with PrI significantly reduced haemoglobin uptake levels compared to PrI-treated controls (Figure 4 B). Similarly, 156 nM Mefloquine co-administered with PrI, significantly reduced haemoglobin uptake levels (Figure 4 C). Complete assay results are summarised in Table 4.

The similarity in haemoglobin levels in PrI-treated controls and PrI + Cytochalasin D treated parasites suggested that Cytochalasin D does not inhibit endocytosis. In addition, it suggested that Cytochalasin D raised haemoglobin levels in the absence of PrI by blocking haemoglobin digestion, not by stimulating endocytosis. The results further suggested that Jasplakinolide may inhibit endocytosis.



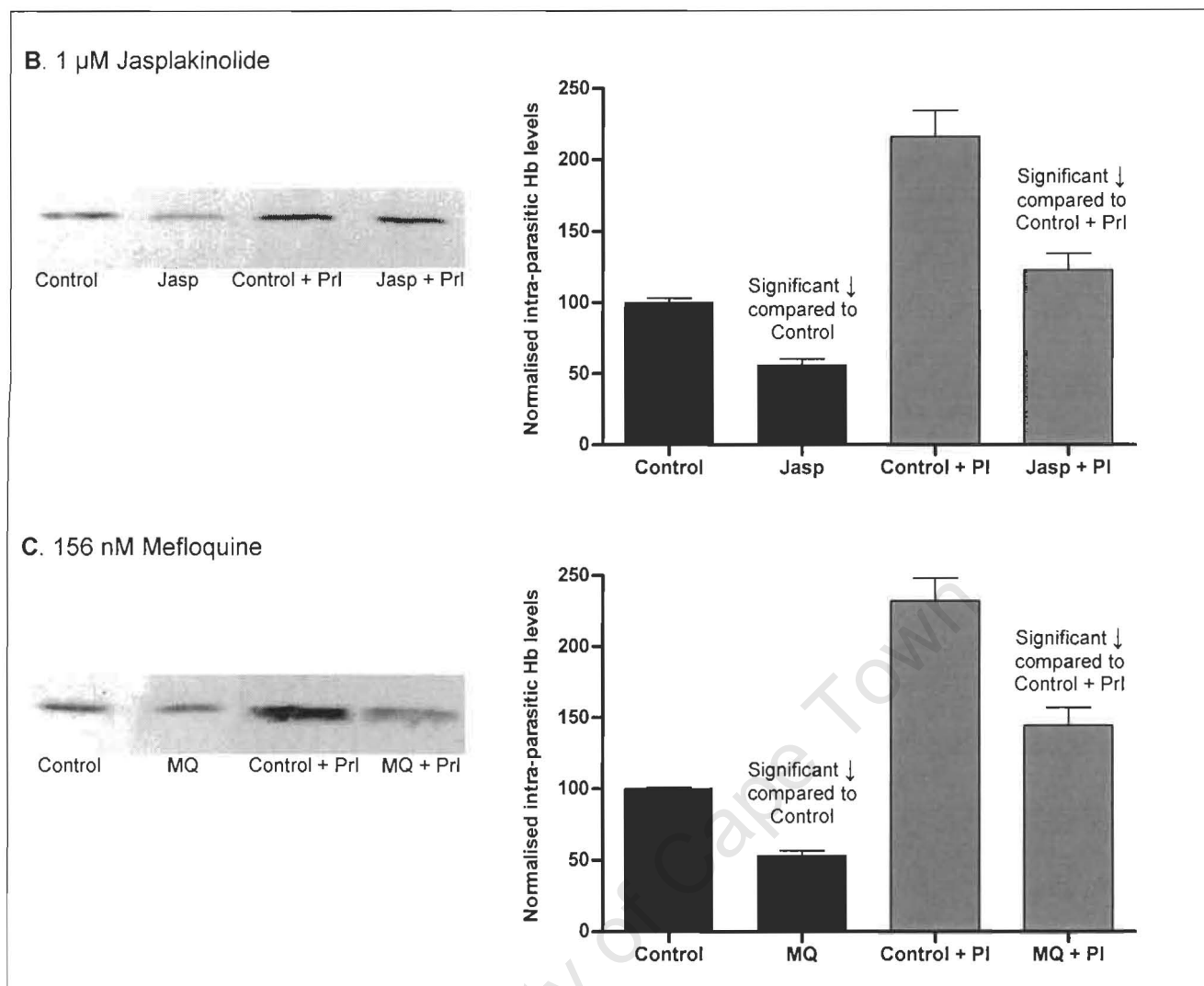


**Figure 4.** Haemoglobin levels in protease inhibitor treated malaria parasites after various actin perturbing drug exposures. Parasite cultures were incubated in either drug or solvent control for 5 hours with and without 40  $\mu$ M of protease inhibitors (PrI) ALLN and E64. Parasites were released from their host erythrocytes by saponin treatment, and washed extensively to remove extra-parasitic haemoglobin. Parasite pellets were run on SDS-polyacrylamide gels, and the haemoglobin levels in the parasites were determined by Western blotting with anti-haemoglobin antiserum. The net intensities of individual haemoglobin bands were determined with Kodak 1D image analysis software. Western blot representative images of haemoglobin levels accumulated by parasites exposed to 50 nM Cytochalasin D (A), 1  $\mu$ M Jasplakinolide (B) and 156 nM Mefloquine (as the experiment control) (C) with and without PrI are shown on the left. Summarised haemoglobin accumulated levels after various treatments are represented by bar graphs on the right of each representative western blot image. Experiments were performed in duplicate on at least 3 individual days. Intensity levels indicated were normalised to the control and comparisons were made using appropriate statistical tests. Significance was set at  $\alpha = 0.05$ . Error bars indicate Standard Error of the Mean.

**Table 4.** Haemoglobin levels within malaria parasites after various actin disrupting treatments with and without PrI. Experiments were performed in duplicate on at least 3 individual days. Intensity levels indicated were normalised to the control and comparisons were made using appropriate statistical tests. Significance was set at  $\alpha = 0.05$ . Error bars indicate Standard Error of the Mean. n = number of observations.

Treatment	Control	Drug	% Change	n	Statistical test	P value	Outcome
156 nM Mefloquine	100 ± 1.3	53.1 ± 3.4	47 % ↓	47	Mann Whitney	p < 0.0001	Significant decrease
Mefloquine + 40 µM PrI	232 ± 16.1	144.4 ± 12.6	38 % ↓	47	Mann Whitney	p < 0.0001	Significant decrease
50 nM Cytochalasin D	100 ± 3.3	219.7 ± 21.7	120 % ↑	21	Mann Whitney	p < 0.0001	Significant increase
Cytochalasin D + 40 µM PrI	321 ± 36.4	318.5 ± 33.6	0.2 % ↓	21	Unpaired T test	p = 0.9552	NO Significant change
1 µM Jasplakinolide	100 ± 3.0	56.0 ± 4.1	44 % ↓	27	Unpaired T test	p < 0.0001	Significant decrease
Jasplakinolide + 40 µM PrI	216 ± 18.3	122.6 ± 11.7	44 % ↓	27	Unpaired T test	p < 0.0001	Significant decrease

## 2.2.6 The effect of actin disrupting drugs on HRP uptake by malaria parasites

Supplementary investigation of the effect which actin disrupting drug treatment has on the uptake of macromolecules by the malaria parasite from the host cytosol, involved the preloading of erythrocytes with an exogenous endocytic tracer, horse radish peroxidase (HRP), and subsequent infection with enriched malaria parasites. Following 14 hours of drug and control exposure, parasites were isolated from their host red blood cells and intra-parasitic HRP levels determined by an enzymatic assay.

Cytochalasin D treatment showed no significant change in HRP levels, while Jasplakinolide significantly reduced HRP levels after 14 hours of treatment (Figure 5). Complete assay results are summarised in Table 5.

The results are consistent with those obtained by measuring haemoglobin levels after PrI treatment (Figure 4), suggesting that Jasplakinolide inhibits endocytosis while Cytochalasin D has no effect.

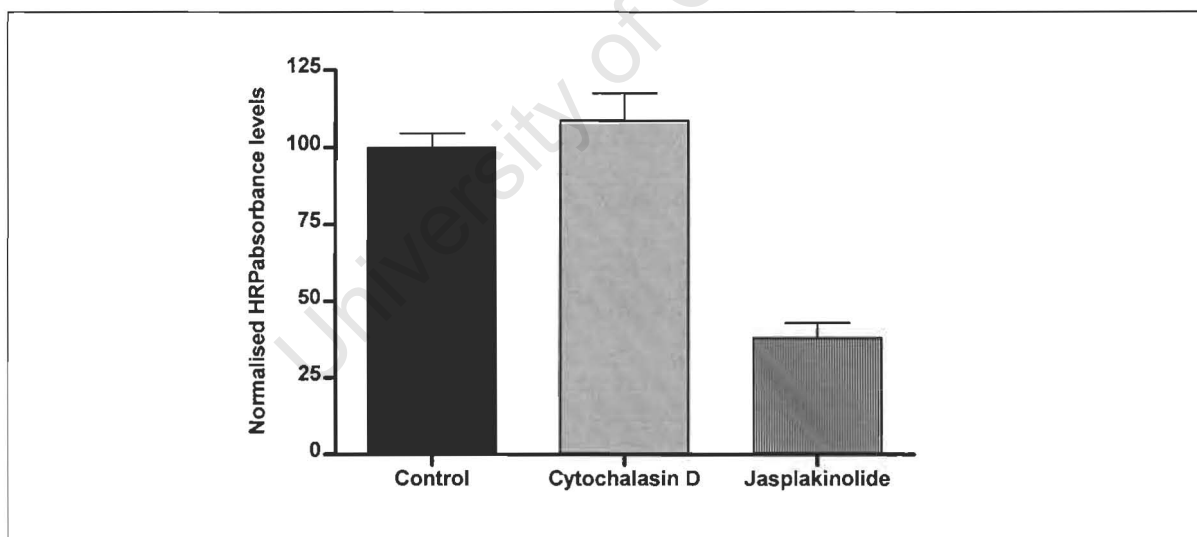


**Figure 5.** Quantitative HRP endocytosis assay for malaria parasites. Erythrocytes were preloaded with HRP, infected with parasites and treated with Cytochalasin D or Jasplakinolide for 14 hours. Subsequently, the parasites were released from their host red blood cells by saponin treatment and washed extensively to remove extra-parasitic HRP. Intra-parasitic HRP levels were determined spectrophotometrically, following incubation with the colorimetric HRP substrate *o*-phenylenediamine (OPD) and  $H_2O_2$  on a spectrophotometer set at 450 nm. Absorbance values were normalised to the solvent controls set at 100 and comparisons were made using appropriate statistical tests. Error bars indicate standard error of the mean.

**Table 5.** Quantitative HRP endocytosis assay for malaria parasites. n = number of observations.

Treatment	Control	Drug	% Change	n	Statistical test	Two tailed P value	Outcome
14 hr 50 nM Cytochalasin D	100 ± 4.64	108.76 ± 8.79	8 % ↑	3	Unpaired T test	p = 0.4276	NO Significant change
14 hr 1 µM Jasplakinolide	100 ± 9.07	38.12 ± 4.96	62 % ↓	3	Unpaired T test	p = 0.0008	Significant decrease

University of Cape Town

### 2.2.7 Immunofluorescence assay (IFA)

To determine the location of haemoglobin within the malaria parasite, control and drug-treated parasite cultures were fixed and reacted with anti-haemoglobin antiserum in an immunofluorescence assay (Figure 6). Average fluorescence intensity readings within parasite digestive vacuoles were obtained as a measure of haemoglobin levels in this compartment (Figure 7). In addition, transport vesicle counts were performed on randomly selected parasites by counting the amount of extra-digestive vacuolar fluorescent foci (Figure 8). All experimental results were normalised to their respective solvent controls set at 100 and comparisons were made using appropriate statistical tests (Table 6 & 7).

In solvent control treated parasites, haemoglobin was located predominantly in the digestive vacuole (Figure 6, black arrows). The digestive vacuole in each parasite is easily identifiable due to the presence of a large haemozoin crystal in this compartment. Significantly lower fluorescence intensities were recorded in the vacuoles of all actin disrupting drug-treated parasites except for Jasplakinolide (Figure 7). This suggests a reduction in haemoglobin levels in the vacuoles of Cytochalasin D and Latrunculin A treated parasites. Note there are no erythrocytes surrounding the parasite in the phase contrast images due to saponin lysis which was performed prior to parasite fixation in order to remove non-parasitic haemoglobin, reducing background levels and improving the quality of immunofluorescence signals in the corresponding TRITC-labelled anti-haemoglobin images.

In addition to the prominent haemoglobin fluorescence in the digestive vacuoles, fluorescent puncta or foci could also be observed in the parasite cytoplasm (Figure 6, white arrows). These presumably represent haemoglobin transport vesicles en route to the digestive vacuole from sites of endocytosis at the plasma membrane. All drug-treated parasites contained significantly more haemoglobin-filled transport vesicles compared to control parasites (Figure 6 & 8). Together with the reduction of haemoglobin levels within Cytochalasin D and Latrunculin A treated parasite vacuoles, the build up of haemoglobin-filled transport vesicles is likely to suggest a block in vesicle transport to the digestive vacuole, with a consequent block in haemoglobin digestion. Mefloquine, used as the positive control, showed a reduction in both fluorescence digestive vacuole intensity and

transport vesicle numbers (Figure 7 & 8), suggesting a block in endocytosis as previously reported (Hoppe *et al.* 2004).

University of Cape Town

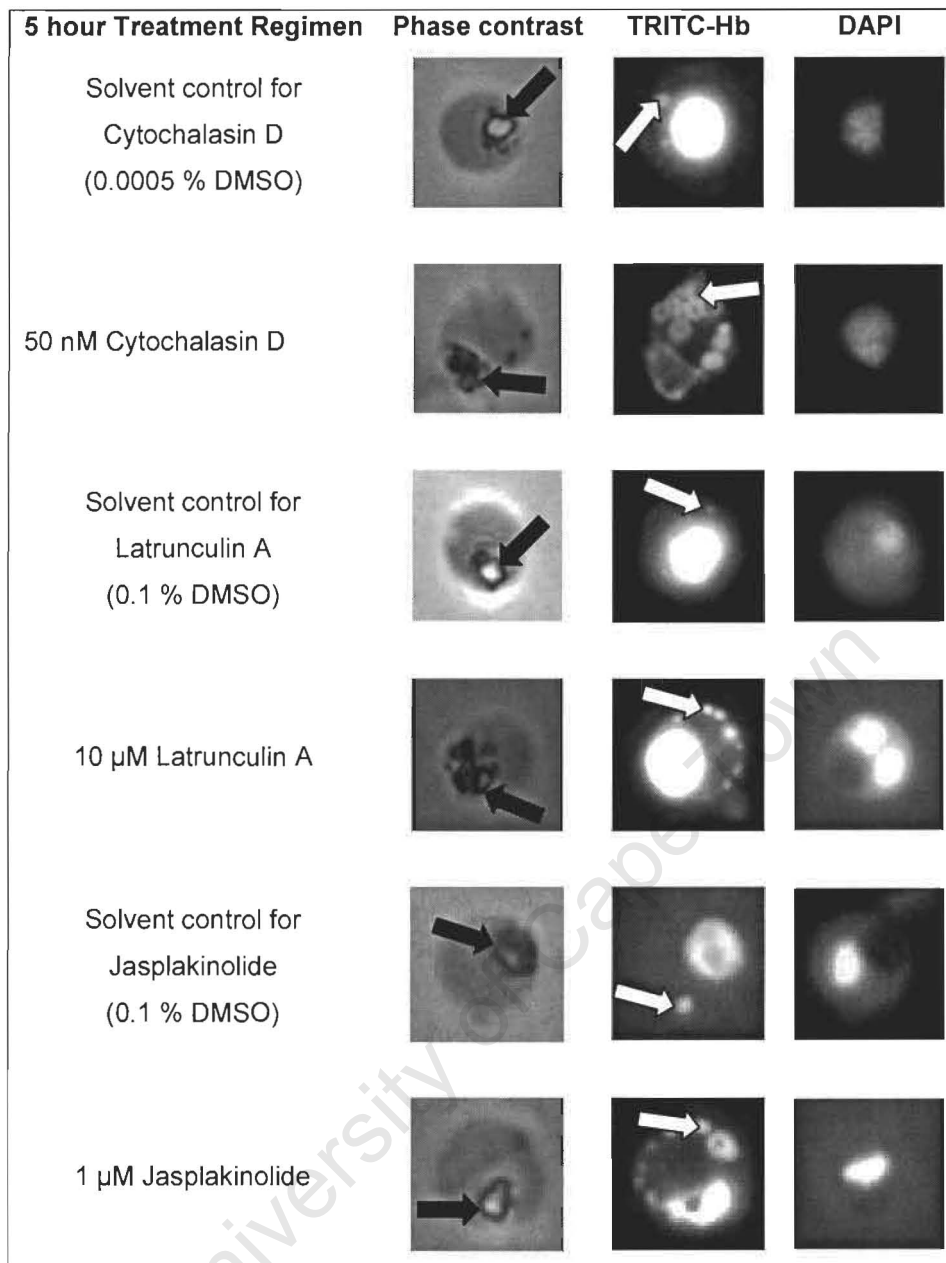


**Figure 6.** Representative microscope images demonstrating the effect of actin perturbing drugs on the sub-cellular localisation of haemoglobin in malaria parasites by immunofluorescence. Parasitised erythrocytes were drug and solvent control treated for 5 hours, before being saponin treated to release excess non-parasitic haemoglobin, followed by subsequent fixation and attachment of released parasites onto glass cover slips. Parasites were permeabilised and incubated with anti-haemoglobin antiserum and fluorescent secondary antibodies as well as DAPI (which stains nuclei). The panels represent from left to right: Treatment regimen, phase contrast image, corresponding TRITC-labelled anti-haemoglobin image followed by DAPI-stained nuclei images. A single erythrocyte-free parasite can be seen in each phase contrast image with its food vacuole (dark haemozoin crystal) denoted with a black arrow. Corresponding TRITC-labelled anti-haemoglobin parasite images have vesicle-like structures indicated by white arrows, with the digestive vacuole being the major site of haemoglobin fluorescence.

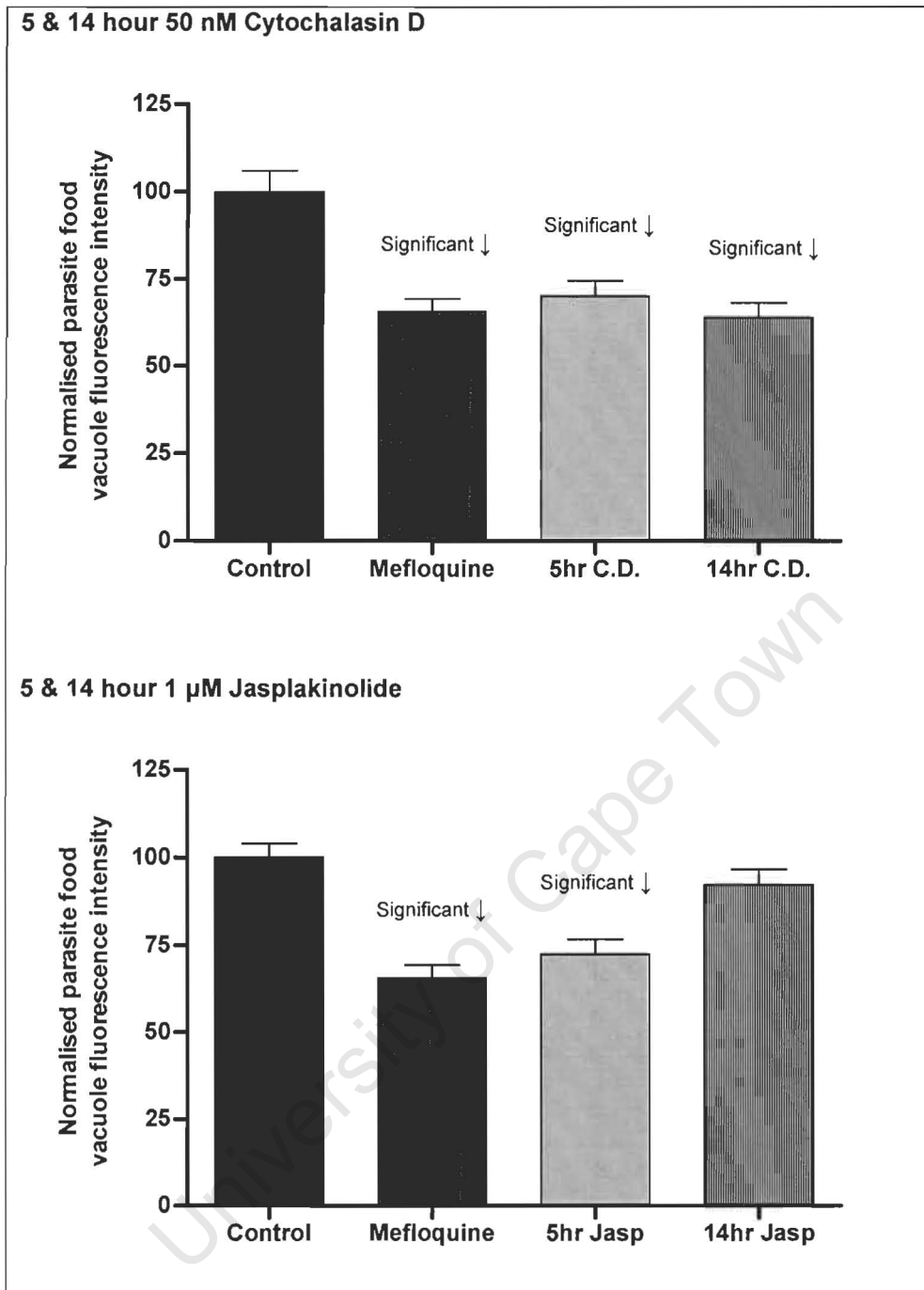


**Figure 7.** Malaria parasite digestive vacuole fluorescence intensity after drug and solvent control treatment. Fluorescence intensity was measured within > 60 (Table 7) randomly selected parasite digestive vacuoles on haemoglobin IFA slides, using Adobe Photoshop software (version 7.0). Readings were normalised to their respective controls set at 100 and comparisons were made using appropriate statistical tests. Due to heterogeneity of variances and the non-normal distribution of the data, comparisons were made using the Non-parametric Mann-Whitney U test for independent samples. Statistical significance was set at  $\alpha = 0.05$ . Error bars indicate standard error of the mean.

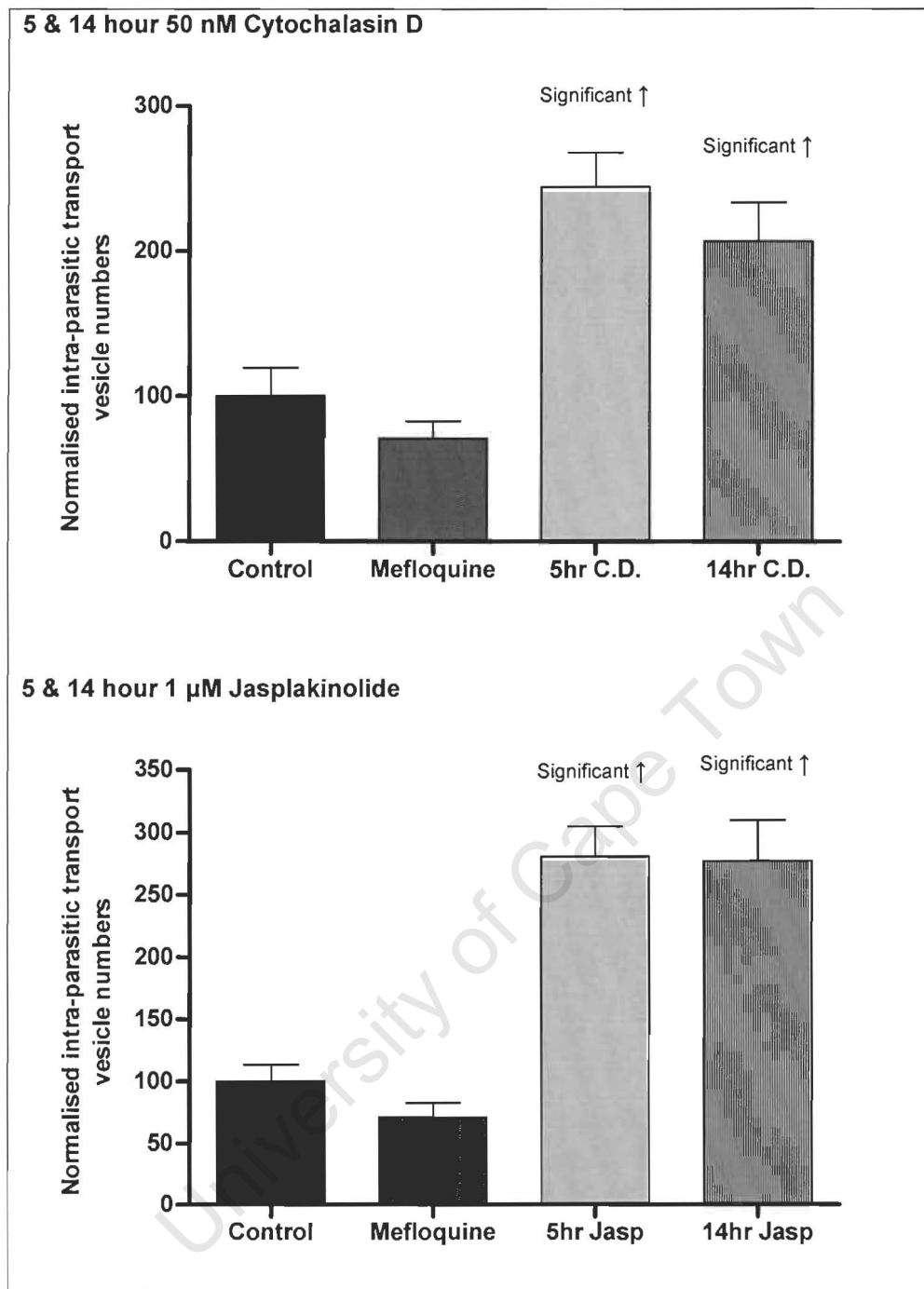


**Figure 8.** Malaria parasite transport vesicle numbers after drug and solvent control treatment. Average transport vesicle counts per parasite were compared between the various drug treatments and their respective solvent controls. Approximately 40 to 100 parasites (Table 8) were randomly selected on the haemoglobin IFA slides and the numbers of cytoplasmic fluorescent puncta (transport vesicles) outside the digestive vacuoles counted. Average transport vesicle counts were normalised to their respective solvent controls which were set at 100 and comparisons were made using appropriate statistical tests. Due to heterogeneity of variances and the non-normal distribution of the data, comparisons were made using the Non-parametric Mann-Whitney U test for independent samples. Statistical significance was set at  $\alpha = 0.05$ . Error bars indicate standard error of the mean.

**Table 6.** Normalised digestive vacuole haemoglobin fluorescence levels within malaria parasites after various actin disrupting treatments. n = number of observations.

Treatment	Control	Drug	% Change	n	Statistical test	Two tailed P value	Outcome
5 hr 50 nM Cytochalasin D	100 ± 5.976	70.204 ± 4.299	30 % ↓	151	Mann-Whitney	p < 0.0001	Significant decrease
14 hr 50 nM Cytochalasin D	100 ± 5.767	63.895 ± 4.265	36 % ↓	60	Mann-Whitney	p < 0.0001	Significant decrease
5 hr 1 µM Jasplakinolide	100 ± 4.011	72.408 ± 4.259	28 % ↓	108	Mann-Whitney	p < 0.0001	Significant decrease
14 hr 1 µM Jasplakinolide	100 ± 4.738	92.281 ± 4.337	8 % ↓	60	Mann-Whitney	p = 0.2069	No Significant change
14 hr 156 nM Mefloquine	100 ± 4.677	65.563 ± 3.748	34 % ↓	60	Mann-Whitney	p < 0.0001	Significant decrease

**Table 7.** Normalised transport vesicle numbers within malaria parasites after various actin disrupting treatments. n = number of observations.

Treatment	Control	Drug	% Change	n	Statistical test	Two tailed P value	Outcome
5 hr 50 nM Cytochalasin D	100 ± 19.11	244.27 ± 23.94	144 % ↑	66	Mann-Whitney	p < 0.0001	Significant increase
14 hr 50 nM Cytochalasin D	100 ± 18.40	206.80 ± 26.77	107 % ↑	102	Mann-Whitney	p = 0.0216	Significant increase
5 hr 1 µM Jasplakinolide	100 ± 13.44	280.85 ± 24.03	181 % ↑	71	Mann-Whitney	p < 0.0001	Significant increase
14 hr 1 µM Jasplakinolide	100 ± 19.67	277.08 ± 32.94	177 % ↑	60	Mann-Whitney	p < 0.0001	Significant increase
14 hr 156 nM Mefloquine	100 ± 19.46	70.97 ± 11.73	29 % ↓	40	Mann-Whitney	p = 0.5135	No significant change

### **2.2.8 Electron microscopy of malaria parasites exposed to actin disrupting drugs**

To confirm ultrastructurally that the punctate structures found in actin disrupting drug-treated parasites by IFA represented haemoglobin filled double membrane transport vesicles that had failed to deliver their contents to the digestive vacuole, control and drug-treated parasites were examined by electron microscopy. Transport vesicle numbers were counted in random cross sections of parasites, before comparisons were made using appropriate statistical tests with significance set at  $\alpha = 0.05$ . Additionally, transport vesicle size and distance from the periphery was estimated using a scale bar (1  $\mu\text{m}$ ) saved electronically onto digital images taken of parasitised erythrocytes on a Zeiss EM 912 transmission electron microscope.

Both Cytochalasin D and Jasplakinolide treated parasites contained significantly increased numbers of typical double membrane transport vesicles filled with ingested red blood cell cytosol, distinct from the digestive vacuole (Figure 9, asterisks & Figure 10). This is consistent with our findings from IFA, where actin disrupting drugs significantly raised transport vesicle numbers within treated parasites. Transport vesicle counts, conducted by electron microscopy, are summarised in Table 8.

Taking advantage of the higher resolution offered by the electron microscope, transport vesicle size and distance from the periphery was examined in addition to their numbers within the parasite. Transport vesicle size doubled after Cytochalasin D treatment, while Jasplakinolide treatment had no significant effect (Table 9). Conversely, transport vesicles were located closer the periphery after Jasplakinolide treatment, while Cytochalasin D had no significant effect on their distance from the periphery (Table 10). Interestingly, these findings may have implications on the role of the actin cytoskeleton during endocytosis which will be further explored in the discussion.

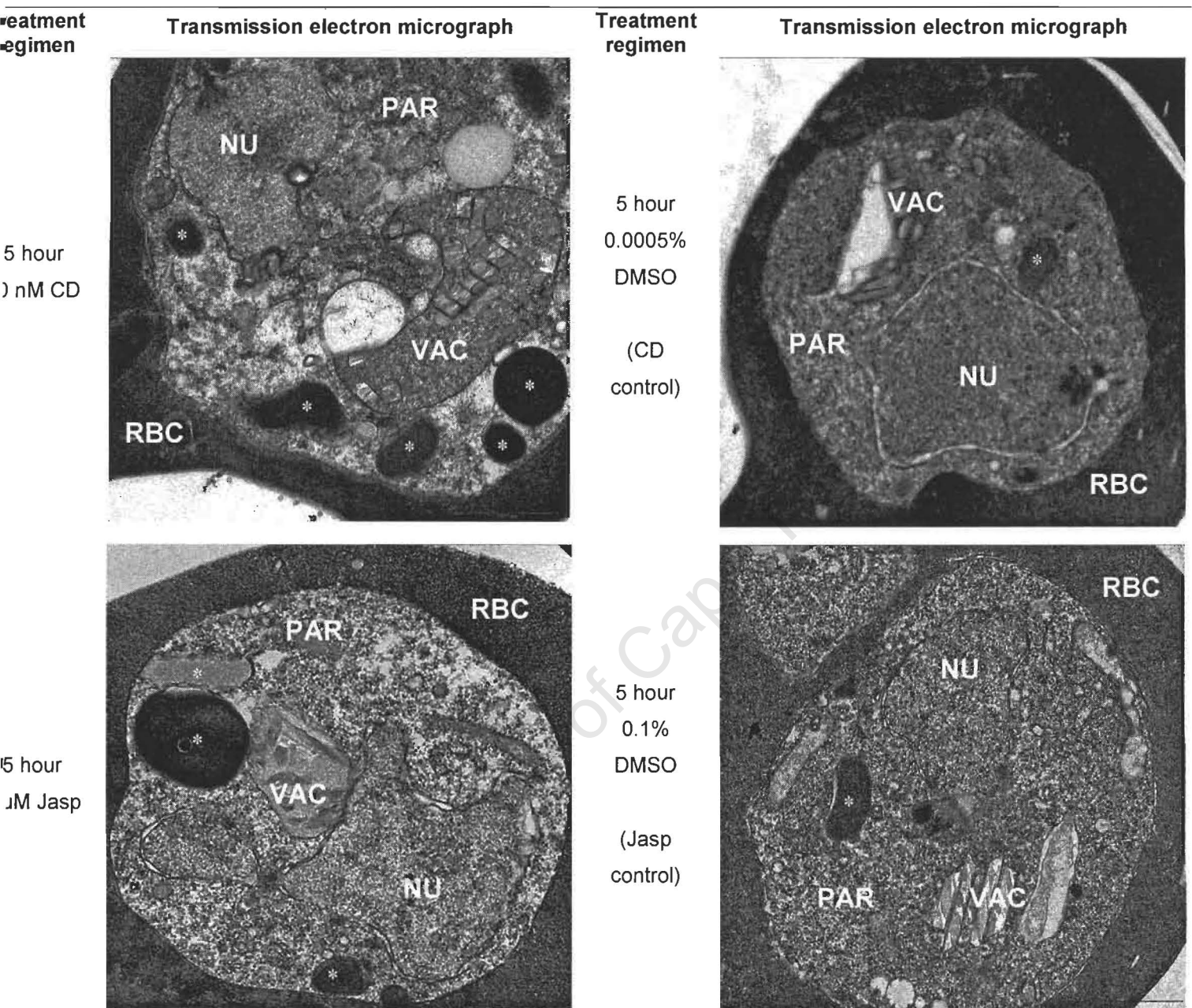


**Figure 9.** Transmission electron micrograph of a cross section of Cytochalasin D (CD) and Jasplakinolide (Jasp) treated trophozoite stage malaria parasites together with their respective controls. Labelled structures are the infected erythrocyte (RBC), parasite (PAR), parasite nucleus (NU), digestive vacuole (VAC), and transport vesicle (asterisks).

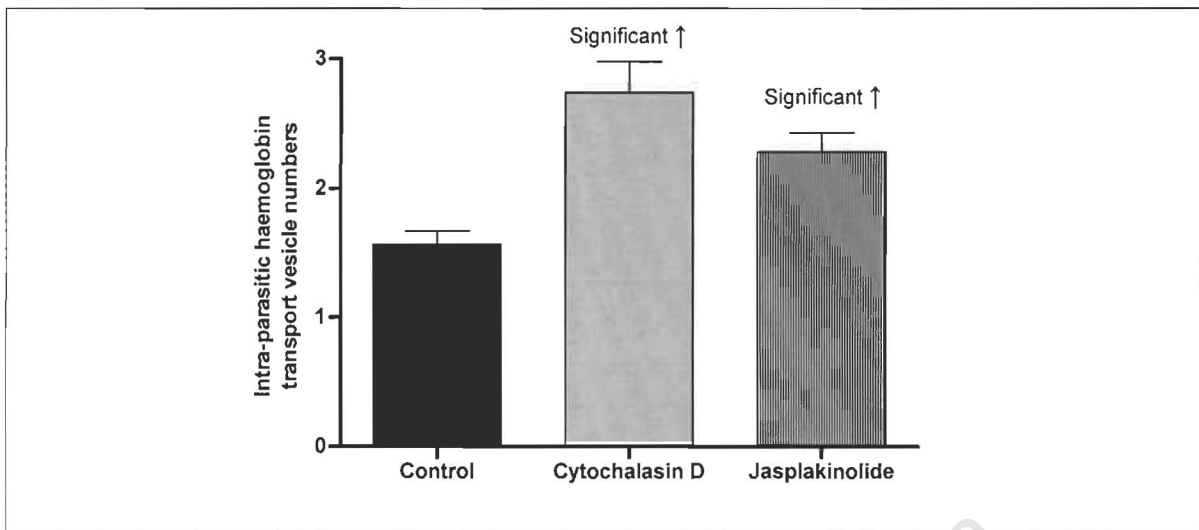


**Figure 10.** Transport vesicle numbers per malaria parasite after 5 hour actin disrupting drug exposure as observed by electron microscopy. Comparisons were made using the non-parametric Mann-Whitney U test for independent samples. Statistical significance was set at  $\alpha = 0.05$ . Error bars indicate standard error of the mean.

**Table 8.** Transport vesicle numbers per malaria parasite after 5 hours of actin disrupting drug exposure as observed by electron microscopy. Comparisons were made using appropriate statistical tests. Statistical significance was set at  $\alpha = 0.05$ . n = number of observations.

Treatment	Control	Drug	% Change	n	Statistical test	Two tailed P value	Outcome
5 hr 50 nM Cytochalasin D	1.56 ± 0.11	2.74 ± 0.24	75 % ↑	103	Mann Whitney	p = 0.0001	Significant increase
5 hr 1 μM Jasplakinolide	1.53 ± 0.12	2.28 ± 0.15	50 % ↑	131	Mann Whitney	p = 0.0004	Significant increase

**Table 9.** Transport vesicle size within malaria parasites after 5 hours of actin disrupting drug exposure as observed by electron microscopy. To avoid bias, all measurements (nm) were taken across the longest axis of each transport vesicle. Comparisons were made using appropriate statistical tests. Statistical significance was set at  $\alpha = 0.05$ . n = number of observations.

Treatment	Control (nm)	Drug (nm)	% Change	n	Statistical test	Two tailed P value	Outcome
5 hr 50 nM Cytochalasin D	310 ± 16	634 ± 35	105 % ↑	50	Mann Whitney	p < 0.0001	Significant increase
5 hr 1 μM Jasplakinolide	350 ± 25	408 ± 35	17 % ↑	50	Mann Whitney	p = 0.4101	No significant change

**Table 10.** Transport vesicle distance (nm) from the periphery of malaria parasites after 5 hours of actin disrupting drug exposure as observed by electron microscopy. To avoid bias, all measurements were taken across the shortest distance between the outer membrane of the vesicle and the parasite plasma membrane. Comparisons were made using appropriate statistical tests. Statistical significance was set at  $\alpha = 0.05$ . n = number of observations.

Treatment	Control (nm)	Drug (nm)	% Change	n	Statistical test	Two tailed P value	Outcome
5 hr 50 nM Cytochalasin D	370 ± 55	315 ± 49	15 % ↓	50	Unpaired T test	p = 0.4528	No significant change
5 hr 1 μM Jasplakinolide	371 ± 36	118 ± 18	68 % ↓	50	Mann Whitney	p < 0.0001	Significant decrease

### 2.2.9 The effect of actin disrupting drugs on the localisation of actin in *P. falciparum* infected erythrocytes as assessed by immunofluorescence assay (IFA)

Having established actin disrupting drug effects on the localisation of parasite haemoglobin, IFA, using anti-actin antiserum and fluorescent secondary antibodies, was performed to investigate the effects these drugs have on parasite actin localisation.

Control parasite actin appeared to be dispersed homogenously throughout the cytoplasm (Figure 11). Similar results were observed in parasites treated with Cytochalasin D. Contrastingly, Jasplakinolide treated parasites had a clearly distinguishable actin stain located all along the periphery of the majority of parasites. Treatment of *T. gondii* with the filament-stabilising drug Jasplakinolide has been shown to increase actin polymerisation (Schmitz *et al.* 2005). It is thus likely, that Jasplakinolide, by inducing and stabilising actin filaments within the malaria parasite, creates a cortical actin meshwork seen in Figure 11.

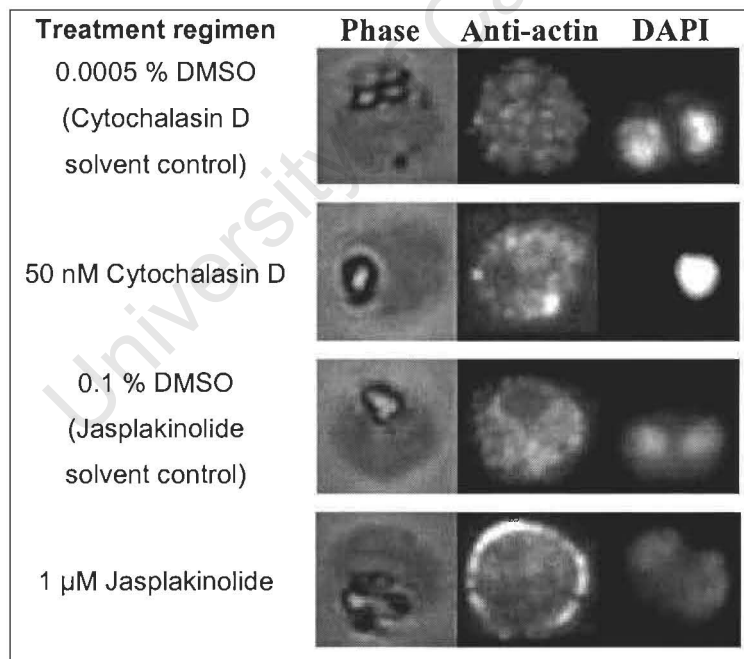


**Figure 11.** Microscope images of the effect of actin perturbing drugs on the sub-cellular localisation of actin in malaria parasites by immunofluorescence. Parasitised erythrocytes were drug and solvent control treated before being saponin treated to release the parasite with subsequent fixation onto glass cover slips. Parasites were permeabilised before incubation with anti-actin antiserum and fluorescent secondary antibodies as well as DAPI. The panels represent from left to right: Treatment regimen, phase contrast image, corresponding TRITC-labelled anti-actin image followed by DAPI-stained nuclei image.

## 2.3 Discussion

A genetic relationship between actin and endocytosis has been established in the budding yeast *S. cerevisiae* (Qualmann et al. 2000). Additionally, phagocytosis and macropinocytosis have been demonstrated to be actin dependent uptake pathways of solids and fluids respectively in mammalian cells (Grimmer et al. 2002, May & Machesky 2001). Furthermore, a dynamic actin cytoskeleton may be required for clathrin-dependent receptor-mediated endocytosis, as Latrunculin A (depolymerises actin filaments) was found to inhibit formation of clathrin-coated vesicles at the plasma membrane (Lamaze et al. 1997). Similarly, caveolae mediated endocytosis was impeded following disruption of actin assembly, implicating the requirement for actin during this uptake pathway (Conner & Schmid 2003).

In contrast, endocytic mechanisms in the malaria parasite *P. falciparum* are inadequately understood (Botero-Kleiven et al. 2001). Malaria parasites are, however, known to endocytose haemoglobin and fluid phase endocytic tracers through specialised endocytic sites termed cytosomes (Aikawa et al. 1966, Bannister et al. 2000). As the malaria parasite expresses a conventional actin gene (Pf-ACT1) throughout its life cycle (Wesseling et al. 1989), the use of actin disrupting drugs to elucidate endocytic mechanisms within the parasite seemed plausible. It is worth mentioning that the malaria parasite possesses two actin genes (Pf-ACT1 & Pf-ACTII), with the latter gene (Pf-ACTII) only expressed in the sexual stages (Wesseling et al. 1989). Based on the reported participation of actin in various modes of endocytosis in other eukaryotes, our initial hypothesis was that actin disrupting drug treatment would inhibit endocytosis of host cytoplasm by *P. falciparum*.

Parasite susceptibility to actin cytoskeleton disrupting drugs was established using growth inhibition assays, based on the measurement of parasite lactate dehydrogenase activity. As  $IC_{50}$  values for these drugs were in the nanomolar range, it was apparent that malaria parasites required a dynamic actin cytoskeleton for their survival, most notably for merozoite motility and invasion (Soldati & Meissner 2004). Our chosen final working concentrations (established from  $IC_{50}$  concentrations) for Cytochalasin D and

Jasplakinolide are comparable with concentrations reportedly used in malaria parasites (Bubb *et al.* 1994, Shaw & Tilney 1999, Kappa *et al.* 2004).

In this study we have established that contrary to our original hypothesis, the actin cytoskeleton is not required for endocytosis in the malaria parasite *P. falciparum*. Cytochalasin D, which depolymerises actin filaments, does not reduce haemoglobin uptake levels within malaria parasite after co-administration with protease inhibitors. Similarly, HRP endocytosis from host cytoplasm was not inhibited following Cytochalasin D treatment. This is consistent with some reports of Cytochalasin having no effect on clathrin-dependent internalisation in certain mammalian cells (Geli & Riezman 1998). It further suggests that haemoglobin endocytosis by parasites does not resemble phagocytosis or macropinocytosis, both of which are fundamentally actin dependent in mammalian cells and *Dictyostelium*.

At the outset, Jasplakinolide effects on parasite endocytosis may seem to contradict our findings established with Cytochalasin D. Unlike the latter drug, Jasplakinolide inhibits haemoglobin and HRP endocytosis by the parasite. This discrepancy, however, may be explained by its opposite effect on the actin cytoskeleton. Jasplakinolide, which stabilises and promotes actin polymerisation, creates a cortical actin meshwork along the periphery of the parasite. This actin meshwork was observed by IFA of parasites treated with Jasplakinolide using anti-actin antiserum and fluorescent secondary antibodies. The actin meshwork may physically impede the formation and subsequent trafficking of nascent endocytic vesicles towards the digestive vacuole. In agreement with this, in mammalian cells actin polymerisation has been proposed to negatively regulate endocytosis (Quallman *et al.* 2000, Schafer 2002) as it does in exocytosis (Eitzen 2003). A rigid cortical actin cytoskeleton may act as a physical barrier to endocytosis and will thus require its removal in order to allow for passage of nascent vesicles into the cytoplasm (Quallman *et al.* 2000, Schafer 2002). This is similar to a physical block imposed on endocytic vesicle movement by a hypothesised actin meshwork reported by Gaidarov *et al.* (1999). In further support of an actin meshwork barrier in Jasplakinolide treated parasites, transport vesicles, examined by electron microscopy, were found to lie closer to the periphery of treated trophozoites. A partial physical block, imposed on transport vesicle formation and subsequent trafficking towards the interior of the cell, can further account for reduced

haemoglobin uptake levels with and without PrI co-administration as well as reduced HRP levels in Jasplakinolide treated parasites. Intriguingly, immunofluorescence assays of Cytochalasin D and solvent control treated parasites, using anti-actin antiserum and fluorescent secondary antibodies, revealed homogeneously dispersed actin staining throughout the cytoplasm. This suggests that, under normal conditions, the parasite actin cytoskeleton is mostly depolymerised, existing primarily in the monomer state, or as very short filaments, too short to be resolved by conventional fluorescence microscopy (Schmitz *et al.* 2005, Schuler *et al.* 2005). This is in contrast to the extensive cortical actin filaments and stress fibres normally seen in mammalian cells by fluorescence microscopy. The actin IFA result suggests that Jasplakinolide promotes the formation of similar cortical actin fibres along the periphery of the malaria parasite.

The results further suggest that although actin is not required for endocytosis per se, it is required for subsequent transport vesicle trafficking within the malaria parasite. Punctate structures were found in Giemsa-stained thin blood smears of all actin disrupting drug treated parasites in addition to reduced malaria pigment. The results were interpreted as an accumulation of transport vesicles and a block in haemoglobin digestion. IFA of drug treated parasites, using anti-haemoglobin antiserum, confirmed a significant increase in haemoglobin filled transport vesicle numbers, a conclusion further supported by electron microscopy. Additionally, IFA of drug treated malaria parasites, using anti-haemoglobin antiserum, yielded lower fluorescence readings within parasite digestive vacuoles suggesting reduced haemoglobin levels within this compartment. This, together with a build up of haemoglobin-filled transport vesicles, suggests a block in vesicle transport and haemoglobin delivery to the digestive vacuole and a consequent block in haemoglobin digestion. The digestion block, brought about of transport vesicle accumulation, accounts for the elevated haemoglobin levels within Cytochalasin D treated parasites as found by Western blotting.

Trafficking of endocytic vesicles within the malaria parasite is thus likely to be actin dependent. In agreement with this, multiple roles have been suggested to be performed by the polymerisation of actin, including the propulsion of nascent vesicles away from the plasma membrane. The latter is supported by experimental reports of endosomes, pinosomes and clathrin coated vesicles associated with actin tails or plumes (comet tails)

in the cytoplasm (Merrifield *et al.* 1999, Taunton *et al.* 2000, Engqvist-Goldstein & Drubin 2003). Actin filaments may further facilitate vesicle trafficking within the cell (Schafer 2002), where motor proteins may link endocytosed cargo to actin filaments via rhodopsin or via linker proteins referred to as CLIPs (cytoplasmic linker proteins) (Schafer 2002, van Vliet *et al.* 2003). Additional proposed roles for actin in mammalian cell endocytosis include the pinching off and fission of nascent endocytic vesicles (Quallman *et al.* 2000). Interestingly, the electron microscopy results show that haemoglobin filled transport vesicles were significantly larger in Cytochalasin D treated parasites. Disruption of actin function in the parasites may delay closing and fission of the neck of the cytostome, the deep invagination of the plasma membrane where haemoglobin is endocytosed. Conceivably, this could result in an increase in vesicle size, without affecting the overall rate of endocytosis.

Interestingly, Cytochalasin D and Latrunculin A treated parasites, which contained significantly increased haemoglobin levels after 5 hours of treatment, showed less haemoglobin accumulation after 14 hours. This could be due to general detrimental effects exerted on the parasite over 14 hours of drug treatment, resulting in hampered growth with a consequent decrease in haemoglobin uptake. Similarly, Gaidarov *et al.* (1999) found high concentrations of Latrunculin B (25 mg / mL) partially blocked receptor-mediated endocytosis in mammalian cells, possibly due to non-specific toxic effects, while lower concentrations (0.3 mg / mL) did not. Alternatively, haemoglobin digestion inhibition caused by actin disrupting drug effects, could result in alternative (non actin dependent) degradative pathways being activated after 5 hours of treatment leading to a less pronounced increase in haemoglobin levels by 14 hours. Similarly, the differences observed between intra-parasitic haemoglobin accumulation levels after 5 and 14 hours of Jasplakinolide treatments, may be due to non-specific toxic effects or alternative degradative pathways activated after 5 hours of treatment.

In summary, our results infer that the actin cytoskeleton is not essential for endocytosis in the malaria parasite, but rather plays a role in subsequent trafficking of endocytosed vesicles to the parasite digestive vacuole. Future studies involving sub cellular fractionations could help elucidate the rate at which endosomes deliver their contents to the digestive vacuole. This could further clarify the effect which actin disrupting drugs

have on endocytic trafficking within the parasite. Additionally, further electron microscopy assays, using sample preparation procedures to enhance cytosome preservation, could more clearly illustrate the morphological effects which actin drug disrupting drugs have on the cytosome and endocytic vesicle formation.

University of Cape Town

## Chapter III

# Phosphoinositides and their role in endocytosis

### 3.1 Introduction

The membrane phospholipid, phosphatidylinositol (PtdIns), serves as a recruiter of protein machinery which regulates membrane trafficking and other cellular functions (Cavalli *et al.* 2001, Takenawa & Itoh 2001). The highly versatile hydrophilic inositol head-group of Phosphatidylinositol (PtdIns) localises on the cytoplasmic face of cellular membranes. Here it serves as a substrate for numerous enzymes including PtdIns kinases which phosphorylate either single or multiple sites, giving rise to a variety of phosphorylated stereoisomers collectively referred to as phosphoinositides (PI's) (Corvera *et al.* 1999). Certain of these inositol polyphosphates are soluble and serve as powerful second messengers whilst membrane bound phosphoinositides (PI's) are able to interact with budding, docking and fusion proteins regulating vesicular trafficking (Corvera *et al.* 1999).

There are nine currently known members of the mammalian 3' phosphorylating kinase enzyme (PI (3) kinase) family (De Camilli *et al.* 1996). As this enzyme is able to use PtdIns, PtdIns (4) P, or PtdIns (4, 5) P<sub>2</sub> as substrates to generate four different PI's (PI (3) P, PI (3,4) P<sub>2</sub>, PI (3,5) P<sub>2</sub> and PI (3,4,5) P<sub>3</sub>), it is more correctly termed a phosphoinositide (3) kinase enzyme rather than a phosphatidylinositol (3) kinase enzyme (De Camilli *et al.* 1996, Takenawa & Itoh 2001).

Studies in yeast have demonstrated a lipid signalling pathway which regulates a protein phosphorylation cascade required for endocytosis. Additionally genetic studies conducted in yeast have established a functional connection between a dynamic actin cytoskeleton and endocytosis (Qualmann *et al.* 2000). Thus, as the actin cytoskeleton plays a critical role in endocytosis, it is a postulated target for this lipid regulated cascade (Cavalli *et al.* 2001). In mammalian cells, Wortmannin, a PI (3) kinase inhibiting drug, was found not to effect the initial internalisation rate of certain endocytic markers, but only impeded their

trafficking from early to late endosomes (Clague 1998). Notably, Wortmannin caused significant down regulation of cell-surface transferrin receptors resulting from increased internalisation and decreased recycling rates (Spiro *et al.* 1996). Interestingly, *in vitro* studies have shown Wortmannin to inhibit constitutive endocytosis of HRP and transferrin as well as endosome fusion (Li *et al.* 1995). In agreement with this, Wortmannin and LY294002 were found to inhibit fluid-phase endocytosis but had little or no effect on clathrin-dependent internalisation pathways (Araki *et al.* 1996). Perhaps these seemingly contradictory findings regarding the role of Wortmannin may be due to it not only inhibiting PI (3) kinase, but additionally other enzymes including PI (4) kinase (Richards *et al.* 2004). Furthermore, various studies using Wortmannin made use of different cell types and concentrations.

PI (3) kinases are known as regulators of phagocytosis and are essential players in phagosome formation and maturation (Gillooly *et al.* 2001) (Table 1). Class I PI (3) kinase products, PI (3, 4) P<sub>2</sub> and PI (3, 4, 5) P<sub>3</sub>, are required for phagocytosis of large particles (>3 µm) by means of phagosome formation. Wortmannin, which inhibits endosome-endosome fusion (Li *et al.* 1995) and interferes with phagosome closure (Araki *et al.* 1996), suggests that PI (3) kinase may play a role during membrane formation of pseudopods and phagosomes as these membrane formations are postulated to be brought about by electron lucent vesicle fusion processes (Lennartz 1999). Class III PI (3) kinase, responsible for producing phosphoinositide (3) phosphate (PI (3) P), is located within phagosome membranes, and is required for phagosome maturation (Gillooly *et al.* 2001). Interestingly, PI (3) kinase does not appear to be essential for phagocytosis in *Dictyostelium*, yet is required for macropinocytosis (Cardelli 2001). Contrastingly, PI (3) kinase may play a role during phagocytosis in mammalian cells, however, this may be by means of another scenario involving the actin cytoskeleton (Lennartz 1999). Class I PI (3) kinase products may, additionally to phagocytosis, regulate actin polymerisation by binding either profilin or gelsolin. These actin binding proteins bind actin monomers and sever actin filaments, respectively, resulting in actin filament depolymerisation and subsequent inhibition of pseudopod extension (Lennartz 1999).

Recently, PI (3) kinase has been found to regulate various steps in endocytic trafficking (Spiro *et al.* 1996). PI (3) kinase is believed to regulate post-endosomal sorting and degradation as Wortmannin, in mammalian cells, inhibits the formation of specialised endocytic carrier vesicles (ECV's) resulting in an accumulation of swollen endosomes (Fernandez-Borja *et al.* 1999). In agreement with this, direct genetic evidence for an involvement of PI (3) kinase has been obtained for protein sorting to the yeast vacuole (Mukherjee *et al.* 1997). Here studies have shown PI signalling, via PI (3) kinase and its product PI (3) P, to play a critical role in ECV functioning (De Camilli *et al.* 1996). As PI (3) P is found in both early endosomes and within ECV's, Wortmannin is likely to inhibit membrane trafficking and sorting regulated by PI (3) kinase via FYVE-domain containing proteins (Cavalli *et al.* 2001). PI (3) P binds specifically to the early endosomal autoantigen 1 protein (EEA1) via a conserved zinc binding domain, known as the FYVE finger (Gagescu *et al.* 2000, Odorizzi *et al.* 2000). EEA1, essential for endosome fusion, provides an example of how PI (3) kinase may regulate membrane trafficking through FYVE-domain containing proteins, of which there are over 30 known to date (De Camilli *et al.* 1996).

As PI's are involved in signalling, trafficking and actin cytoskeleton remodelling, they function as key regulators at the interface between these major cellular processes (Takenawa & Itoh 2001). With this in mind, PI (3) kinase involvement in the endocytic pathway of the malaria parasite *Plasmodium falciparum* was investigated.

## 3.2 Results

### 3.2.1 The sensitivity of malaria parasites to PI (3) kinase inhibitors (IC<sub>50</sub>)

To determine the sensitivity and concentrations of Wortmannin and LY294002 required for examining the role of phosphoinositide-3-kinase (PI (3) kinase) in malaria parasites, growth inhibition assays, based on the measurement of parasite lactate dehydrogenase activity, were performed. The concentrations of the various study drugs which yield 50% parasite growth inhibition (IC<sub>50</sub>) are summarised in Table 11. Working concentrations for the various classes of drug were derived from the IC<sub>50</sub> values and are summarised together with their solvent concentrations in Table 11. With the actin drugs (Chapter II), final working concentrations for each drug were approximately 5 - 10 times that of their respective IC<sub>50</sub> values in an attempt to ensure observed parasite effects are the result of drug exposure and avoid non-specific effects of over-dosing. However, Wortmannin and LY294002 IC<sub>50</sub> concentrations were high compared to concentrations used in mammalian studies (Thelen *et al.* 1994), possibly because complete PI (3) kinase inhibition is less lethal in parasites. Wortmannin and LY294002 final working concentrations were therefore capped at 10 µM, as concentrations exceeding this were likely to result in non-specific overdose effects.

**Table 11.** IC<sub>50</sub> values generated for each drug together with their 95 % confidence intervals and final working and solvent concentrations used during experimentation.

Drug	IC <sub>50</sub>	95% Confidence Interval	Final working concentration used	Solvent concentration
LY294002	48.99 µM	41.06 – 58.45	10 µM	0.01 % DMSO
Wortmannin	54.91 µM	43.73 – 68.94	10 µM	0.1 % DMSO
Mefloquine	21.44 nM	14.87 – 30.91	156 nM	0.006 % MeOH
Methanol	1.01 %	0.659 – 1.684	0.006 %	0.006 %
Dimethyl-sulphoxide	0.835 %	0.653 – 1.069	0.01 – 0.1 %	0.01 – 0.1 %

### **3.2.2 The effect of PI (3) kinase inhibiting drugs on trophozoite morphology**

To establish whether trophozoite parasites were still viable after drug treatment, parasite and erythrocyte morphologies were observed by light microscopy of Giemsa-stained thin blood smears following drug and solvent control exposure of *in vitro* trophozoite infected red blood cells.

No major morphological differences were detected between control and drug treated trophozoite stage parasites and erythrocytes (Figure 12). Nonetheless, similar to actin disrupting drug treated parasites, punctate structures were peripherally located in Wortmannin and LY294002 treated parasites (Figure 12, black arrows), while malaria pigment was more readily identifiable in control treated parasites (Figure 12, white arrows).

As no major deterioration in morphology was observed in drug treated malaria infected erythrocytes, treated parasites were assumed viable after PI (3) kinase inhibiting drug exposure. Based on the similarity of the findings to those obtained with actin inhibitors (Chapter II), the presence of punctate structures in drug treated parasites was assumed to be an accumulation of transport vesicles, while reduced malaria pigment was assumed to reflect a block in haemoglobin digestion. These observations were again based on the limited resolution of light microscopy, and the following studies aim to further explore these findings.

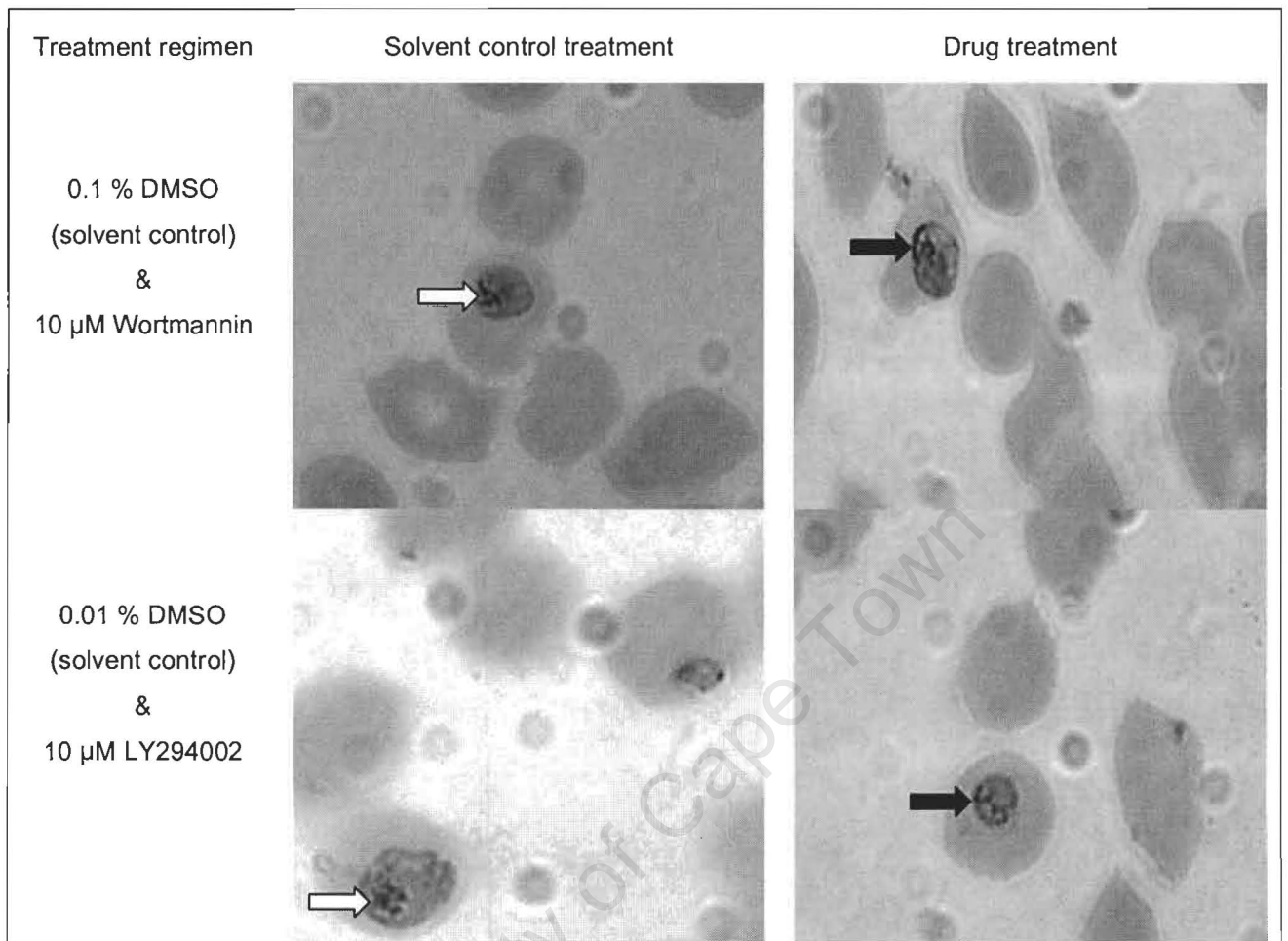


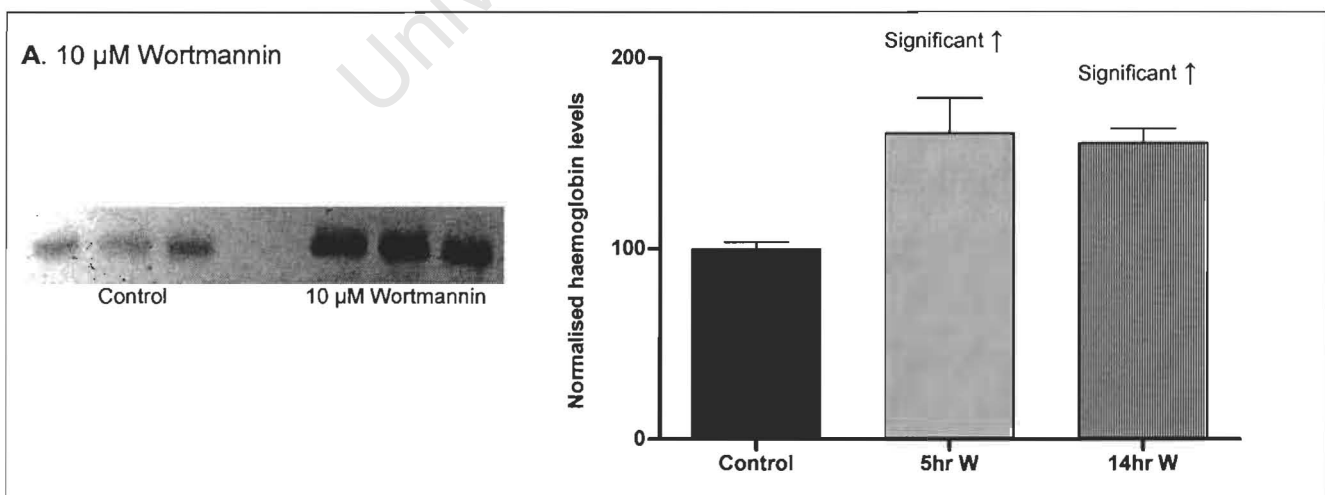
**Figure 12.** Giemsa stained parasitised red blood cells after various 5 hour phosphatidylinositol (3) kinase (PI (3) kinase) inhibiting drug treatments. Treatment regimens of 10  $\mu$ M Wortmannin (0.1 % DMSO) and 10  $\mu$ M LY294002 (0.01 % DMSO) are shown on the left followed by representative solvent control and drug treated malaria parasitised erythrocyte images. Densely localised malaria pigment of solvent control treated parasites are denoted by means of white arrows while postulated haemoglobin transport vesicles of drug treated parasites are indicated with black arrows.

### 3.2.3 The effect of PI (3) kinase inhibiting drug treatment on haemoglobin levels in malaria parasites

Malaria parasites endocytose large quantities of haemoglobin from their host erythrocyte cytoplasm. A reduction of parasite haemoglobin levels following drug treatment would be predictive of a block in endocytosis while an increase could signify inhibition of digestion. To determine the effects of PI (3) kinase inhibiting drugs on the haemoglobin levels in *P.falciparum*, parasites were incubated in 10  $\mu$ M Wortmannin and 10  $\mu$ M LY294002 for 5 and 14 hours, followed by Western blotting with anti-haemoglobin antiserum.

Wortmannin and LY294002 treated parasites showed significantly increased haemoglobin levels, represented graphically in Figure 13 A & B. Mefloquine was used as a positive control, and over both 5 and 14 hours of exposure, significantly reduced haemoglobin levels (Figure 13 D). Complete assay results are summarised in Table 12.

The PI (3) K inhibiting drugs, which raised parasite haemoglobin levels, may, similarly to Cytochalasin D, accomplish this by either stimulating endocytosis or blocking haemoglobin digestion. The apparent reduction of malaria pigment observed in Wortmannin and LY294002 treated Giemsa-stained parasites, together with the significantly raised haemoglobin levels, however, suggested a block in digestion.



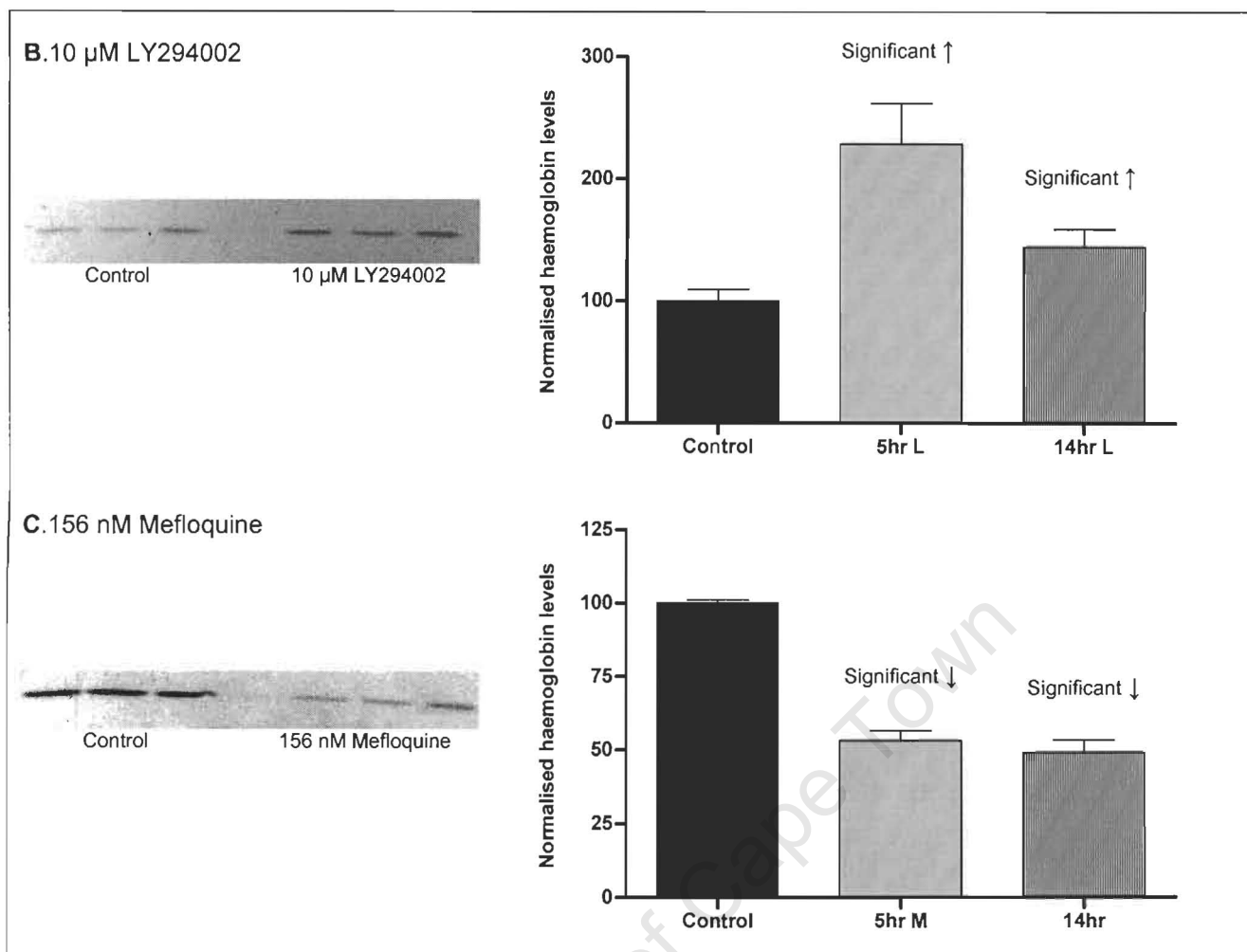


**Figure 13.** Haemoglobin accumulation levels in malaria parasites after various PI (3) kinase inhibiting drug exposures. Parasite cultures were incubated in either drug or solvent control for 5 and 14 hours. Malaria parasites were released from their host erythrocytes by saponin treatment, and washed extensively to remove unrelated extra-parasitic haemoglobin. Parasite pellets were run on SDS-polyacrylamide gels, and the haemoglobin levels in the parasites were determined by Western blotting with anti-haemoglobin antiserum. Net intensities of individual haemoglobin bands were determined with Kodak 1D image analysis software. Western blot representative images of haemoglobin levels accumulated by parasites exposed to 10  $\mu$ M Wortmannin (A), 10  $\mu$ M LY294002 (B) and 156 nM Mefloquine (as the experiment control) (C) are shown on the left. Summarised haemoglobin accumulated levels after 5 and 14 hour drug treatments are represented by means of bar graphs on the right of each representative western blot image. Experiments were performed in triplicate on at least 3 individual days. Intensity levels indicated were normalised to the control set at 100 and comparisons were made. Significance was set at  $\alpha = 0.05$ . Error bars indicate Standard Error of the Mean.

**Table 12.** Intra-parasitic haemoglobin levels after various PI (3) kinase inhibiting drug treatments. n = number of observations.

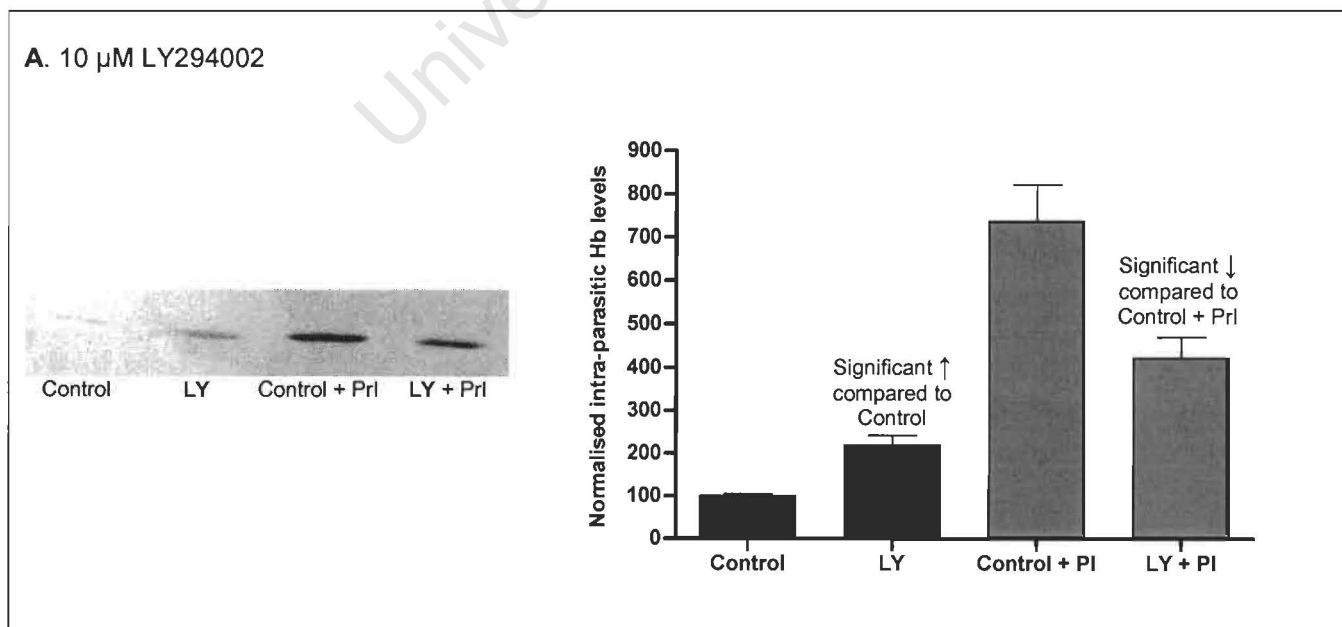
Treatment	Control	Drug	% Difference	n	Statistical test	Two tailed P value	Outcome
5 hr 10 $\mu$ M LY294002	100 $\pm$ 9.60	228.55 $\pm$ 33.52	129 % $\uparrow$	21	Mann-Whitney	p = 0.0010	Significant increase
14 hr 10 $\mu$ M LY294002	100 $\pm$ 5.39	144.55 $\pm$ 14.62	45 % $\uparrow$	15	Mann-Whitney	p = 0.0062	Significant increase
5 hr 10 $\mu$ M Wortmannin	100 $\pm$ 4.96	160.23 $\pm$ 18.71	60 % $\uparrow$	15	Mann-Whitney	p = 0.0014	Significant increase
14 hr 10 $\mu$ M Wortmannin	100 $\pm$ 3.43	155.05 $\pm$ 7.70	55 % $\uparrow$	27	Mann-Whitney	p < 0.0001	Significant increase
5 hr 156 nM Mefloquine	100 $\pm$ 1.24	52.68 $\pm$ 3.45	47 % $\downarrow$	47	Mann-Whitney	p < 0.0001	Significant decrease
14 hr 156 nM Mefloquine	100 $\pm$ 3.94	49.02 $\pm$ 4.41	51 % $\downarrow$	24	Unpaired T test	p < 0.0001	Significant decrease

### 3.2.4 Haemoglobin levels in the presence of protease inhibitors

As stated previously, haemoglobin levels within malaria parasites reflect a balance between endocytosis and digestion within the digestive vacuole. Thus, similar to the actin inhibiting drug assay, parasite cultures were treated with PrI in an attempt to negate digestion and use intra-parasitic haemoglobin levels as a more accurate measure of endocytosis. Mefloquine was again used as the positive control.

Five hour 10  $\mu$ M Wortmannin and 10  $\mu$ M LY294002 treatments significantly reduced haemoglobin levels within the malaria parasite when co-administered with PrI, compared to PrI-treated controls (Figure 14 A & B). Similarly, treatment with 156 nM Mefloquine co-administered with PrI significantly reduced haemoglobin levels (Figure 14 C). Complete assay results are summarised in Table 13.

The significant reduction in haemoglobin levels in PrI-treated controls and PrI + PI (3) kinase inhibiting drug treated parasites suggested that Wortmannin and LY294002 inhibited endocytosis. In addition, it suggested that Wortmannin and LY294002 raised haemoglobin levels in the absence of PrI by blocking haemoglobin digestion, not by stimulating endocytosis. The results further confirm that Mefloquine inhibited endocytosis as previously reported (Hoppe *et al.* 2004).



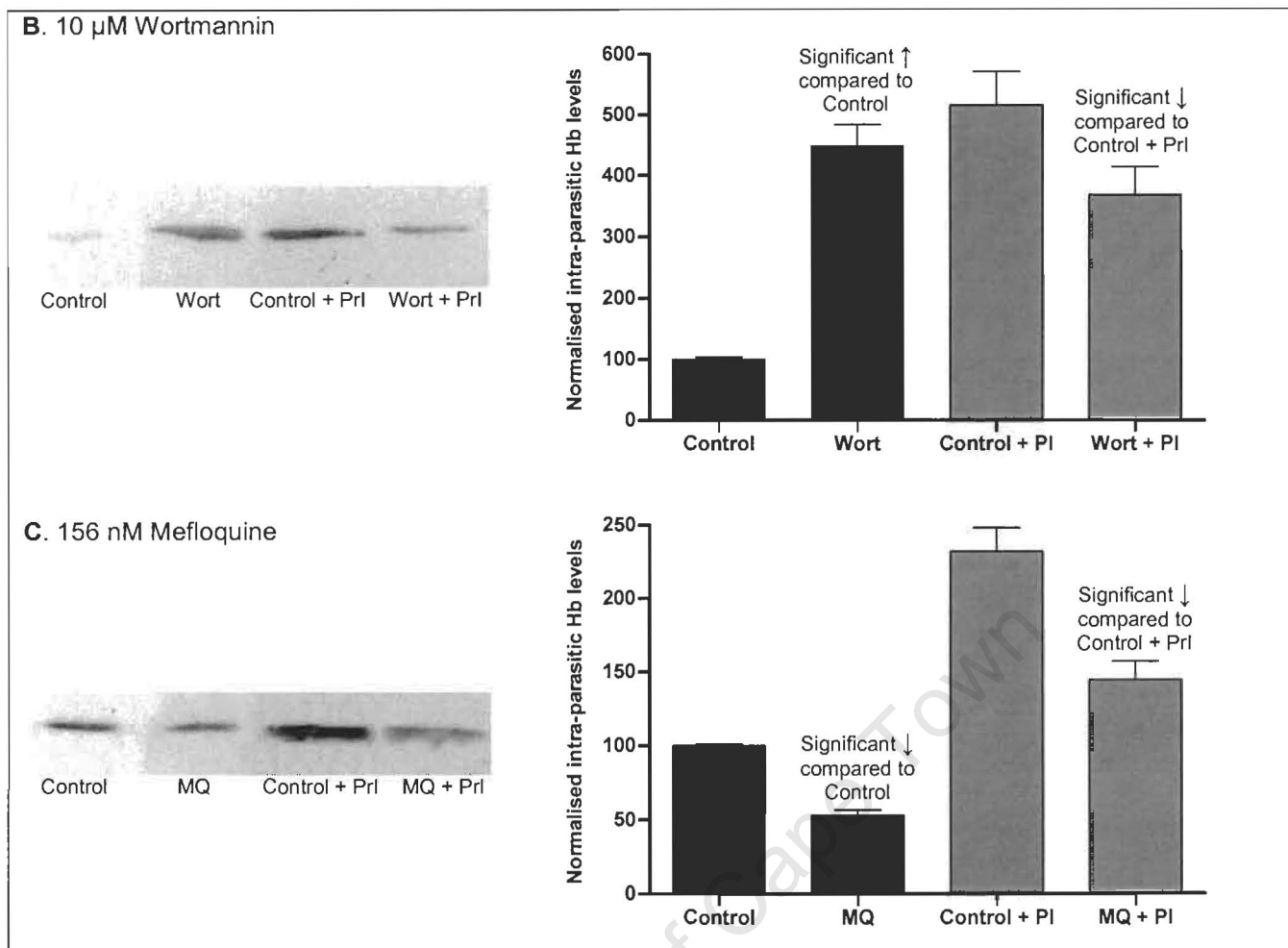


**Figure 14.** Haemoglobin levels in protease inhibitor treated malaria parasites after various PI (3) kinase inhibiting drug exposures. Parasite cultures were incubated in either drug or solvent control for 5 hours with and without 40  $\mu$ M of protease inhibitors (PrI) ALLN and E64. Parasites were released from their host erythrocytes by saponin treatment, and washed extensively to remove extra-parasitic haemoglobin. Parasite pellets were run on SDS-polyacrylamide gels, and the haemoglobin levels in the parasites were determined by Western blotting with anti-haemoglobin antiserum. The net intensities of individual haemoglobin bands were determined with Kodak 1D image analysis software. Western blot representative images of haemoglobin levels accumulated by parasites exposed to 10  $\mu$ M Wortmannin (A), 10  $\mu$ M LY294002 (B) and 156 nM Mefloquine (as the experiment control) (C) with and without PrI are shown on the left. Summarised haemoglobin accumulated levels after various treatments are represented by bar graphs on the right of each representative western blot image. Experiments were performed in duplicate on at least 3 individual days. Intensity levels indicated were normalised to the control and comparisons were made using appropriate statistical tests. Significance was set at  $\alpha = 0.05$ . Error bars indicate Standard Error of the Mean.

**Table 13.** Haemoglobin levels within malaria parasites after various PI (3) kinase inhibiting drug treatments with and without PrI. Experiments were performed in duplicate on at least 3 individual days. Intensity levels indicated were normalised to the control and comparisons were made using appropriate statistical tests. Significance was set at  $\alpha = 0.05$ . n = number of observations.

Treatment	Control	Drug	% Change	n	Statistical test	P value	Outcome
156 nM Mefloquine	100 ± 1.2	53.1 ± 3.4	47 % ↓	47	Mann Whitney	p < 0.0001	Significant decrease
Mefloquine + 40 µM PrI	232 ± 16.1	144.4 ± 12.6	38 % ↓	47	Mann Whitney	p < 0.0001	Significant decrease
10 µM LY294002	100 ± 4.7	219.3 ± 22.3	119 % ↑	25	Mann Whitney	p < 0.0001	Significant increase
LY294002 + 40 µM PrI	736 ± 84.6	420.4 ± 49.4	43 % ↓	25	Unpaired T test	p = 0.0023	Significant decrease
10 µM Wortmannin	100 ± 4.0	447.7 ± 35.9	348 % ↑	17	Mann Whitney	p < 0.0001	Significant increase
Wortmannin + 40 µM PrI	516 ± 55.0	367.8 ± 45.9	29 % ↓	19	Mann Whitney	p = 0.0410	Significant decrease

### 3.2.5 The effect of PI (3) kinase inhibiting drugs on HRP uptake by malaria parasites

Supplementary investigation of the effect which PI (3) kinase inhibiting drug treatment has on the uptake of macromolecules by the malaria parasite from the host cytosol, involved the preloading of erythrocytes with the exogenous endocytic tracer HRP, and subsequent infection with enriched malaria parasites. Following 14 hours of drug and control exposure, parasites were isolated from their host red blood cells and intra-parasitic HRP levels determined by an enzymatic assay.

Both LY294002 and Wortmannin significantly reduced intra-parasitic HRP levels after 14 hours of treatment (Figure 15). Complete assay results are summarised in Table 14.

In agreement with the results obtained by measuring haemoglobin levels after PrI treatment (Figure 15), these results confirmed Wortmannin and LY294002 to inhibit endocytosis in the parasite.

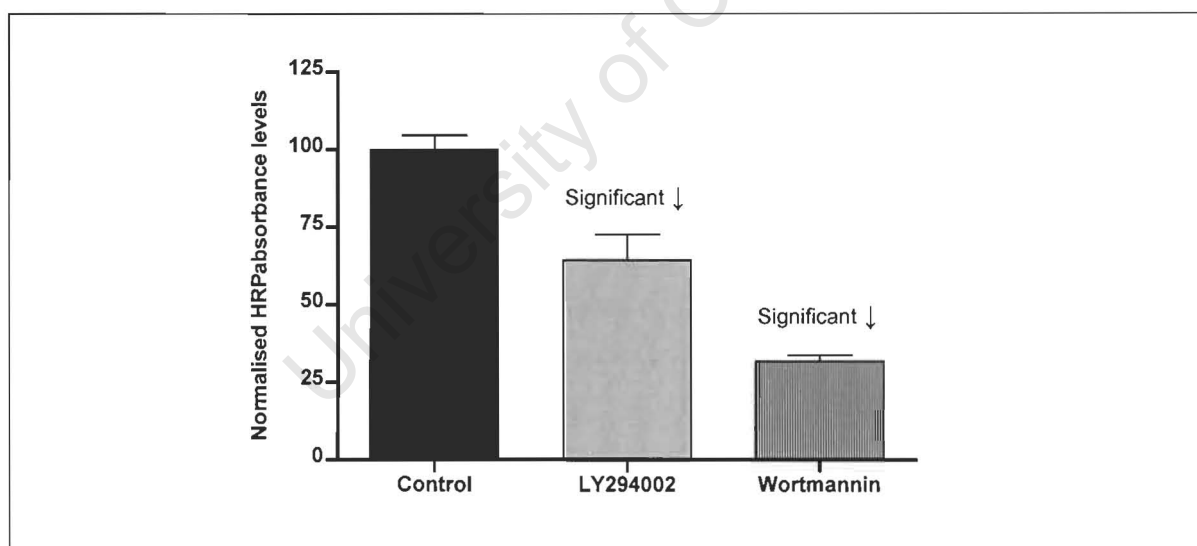


**Figure 15.** Quantitative HRP endocytosis assay for malaria parasites. Erythrocytes were preloaded with HRP; infected with parasites; and treated with LY294002 or Wortmannin for 14 hours. Subsequently, the parasites were released from their host red blood cells by saponin treatment and washed extensively to remove extra-parasitic HRP. Intra-parasitic horse radish peroxidase absorbance levels were determined photometrically, following incubation with the HRP substrate o-phenylenediamine (OPD), and  $H_2O_2$  on a spectrophotometer set at 450 nm. Absorbance values were normalised to the solvent controls set at 100 and comparisons were made using appropriate statistical tests. Error bars indicate standard error of the mean.

**Table 14.** Quantitative HRP endocytosis assay for malaria parasites. n = number of observations.

Treatment	Control	Drug	% Change	n	Statistical test	Two tailed P value	Outcome
14 hr 10 $\mu$ M LY294002	100 $\pm$ 3.12	64.35 $\pm$ 8.15	36 % $\downarrow$	3	Unpaired T test	p = 0.0191	Significant decrease
14 hr 10 $\mu$ M Wortmannin	100 $\pm$ 5.71	31.73 $\pm$ 1.97	68 % $\downarrow$	3	Unpaired T test	p = 0.0002	Significant decrease

University of Cape Town

### 3.2.6 Immunofluorescence assay (IFA)

Similarly to actin disrupting immunofluorescence assays, intra-parasitic haemoglobin localisation was determined with anti-haemoglobin antiserum in control and PI (3) kinase inhibiting drug treated parasite cultures in an IFA (Figure 16). Average fluorescence intensity readings measured within the parasite digestive vacuoles were used as a gauge of haemoglobin within this compartment (Figure 17). In addition, transport vesicle counts were performed on randomly selected parasites by counting the amount of extra-digestive vacuolar fluorescent foci (Figure 18). All experimental results were normalised to their respective solvent controls set at 100 and comparisons were made using appropriate statistical tests (Table 15 and 16).

In solvent control treated parasites, haemoglobin was located predominantly in the digestive vacuole (Figure 16, black arrows), identifiable by the digestive vacuole in each parasite is presence of a large haemozoin crystal in this compartment. Significantly lower fluorescence intensities were recorded in the vacuoles of Wortmannin and LY294002 treated parasites (Figure 17). This suggests a reduction in haemoglobin levels in the vacuoles of PI (3) kinase inhibiting drug treated parasites.

Wortmannin and LY294002 treated parasites contained significantly more haemoglobin-filled transport vesicles compared to control treated parasites (Figure 16, white arrows & 18). Together with the reduction of haemoglobin levels within drug treated parasite vacuoles, the build up of haemoglobin-filled transport vesicles is likely to reflect a block in vesicle transport to the digestive vacuole, with a consequent block in haemoglobin digestion. Mefloquine, used as the positive control, showed a reduction in both fluorescence digestive vacuole intensity and transport vesicle numbers (Figure 17 & 18).

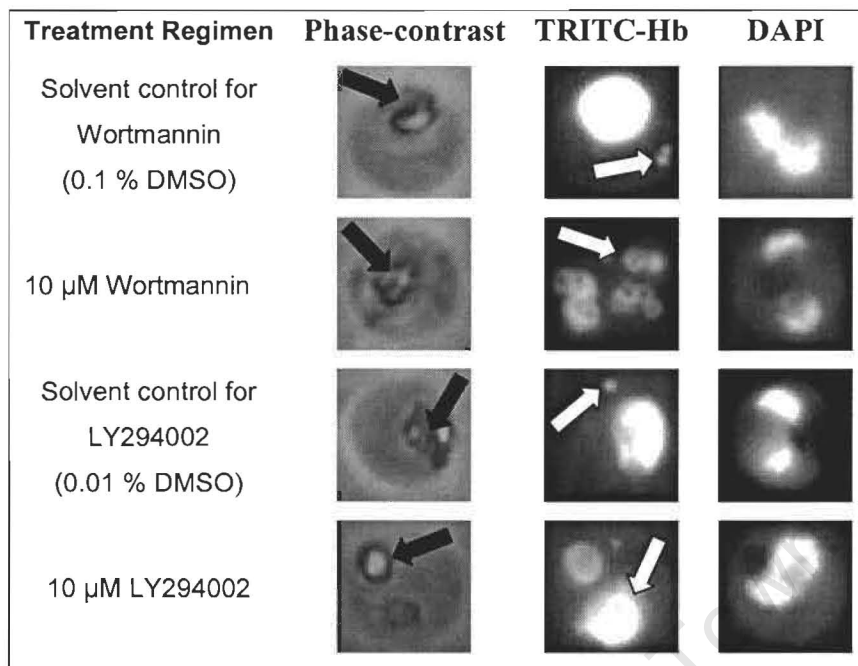


**Figure 16.** Microscope images demonstrating the effect of PI (3) kinase inhibiting drugs on the sub-cellular localisation of haemoglobin in malaria parasites by immunofluorescence. Parasitised erythrocytes were drug and solvent control treated, before being saponin treated to release excess non-parasitic haemoglobin, followed by subsequent fixation and attachment of released parasites onto glass cover slips. Parasites were permeabilised and incubated with anti-haemoglobin antiserum and fluorescent secondary antibodies as well as DAPI (which stains nuclei). The panels represent from left to right: Treatment regimen, phase contrast image, corresponding TRITC-labelled anti-haemoglobin image followed by DAPI-stained nuclei images. A single erythrocyte-free parasite can be seen in each phase contrast image with its food vacuole (dark haemozoin crystal) denoted with a black arrow. Corresponding TRITC-labelled anti-haemoglobin parasite images have vesicle-like structures indicated by white arrows, with the digestive vacuole being the major site of haemoglobin fluorescence.

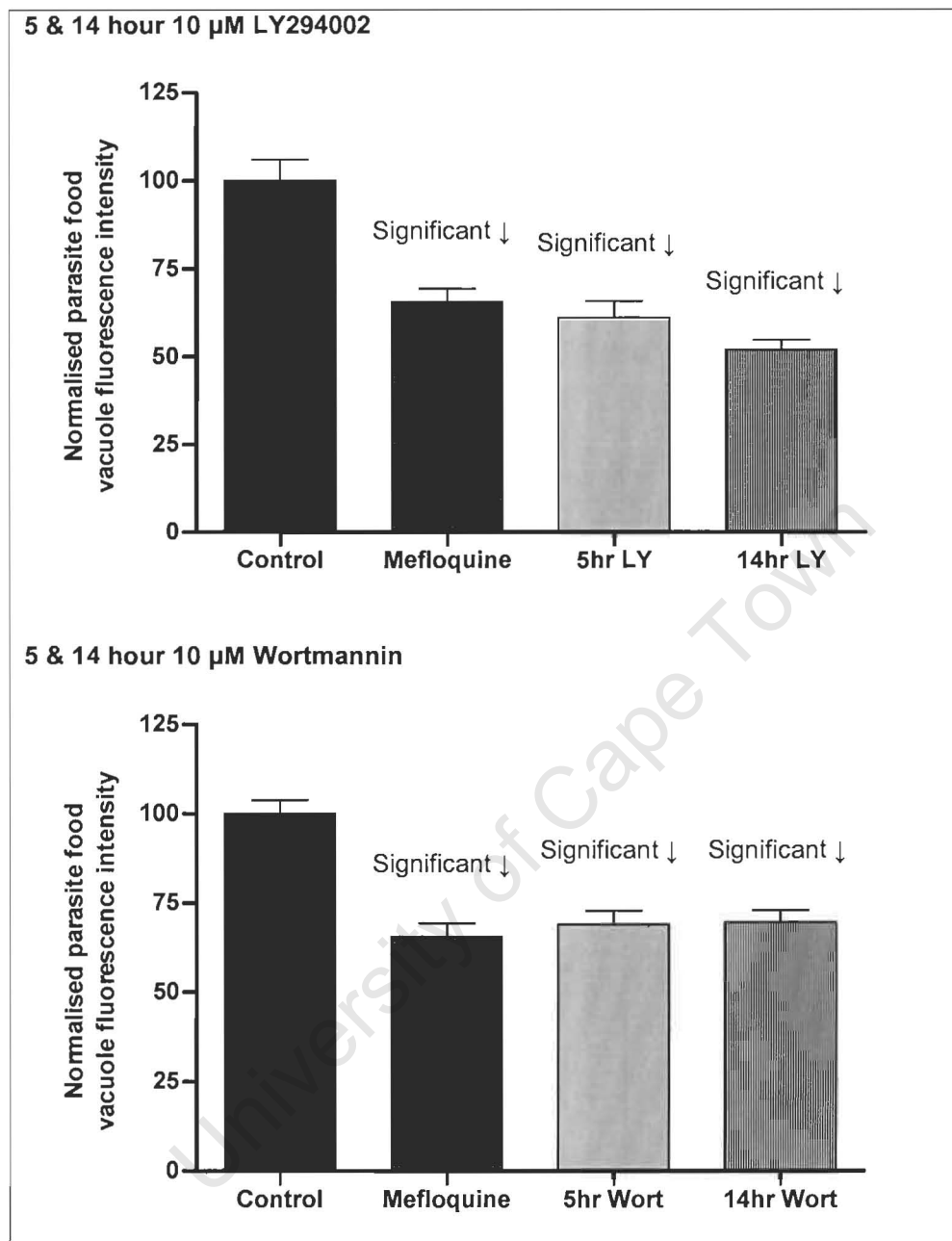


**Figure 17.** Malaria parasite digestive vacuole fluorescence intensity after drug and solvent control treatment. Fluorescence intensity was measured within  $\geq 60$  (Table 14) randomly selected parasite digestive vacuoles on haemoglobin IFA slides, using Adobe Photoshop software (version 7.0). Readings were normalised to their respective controls set at 100 and comparisons were made using appropriate statistical tests. Due to heterogeneity of variances and the non-normal distribution of the data, comparisons were made using the Non-parametric Mann-Whitney U test for independent samples. Statistical significance was set at  $\alpha = 0.05$ . Error bars indicate standard error of the mean.

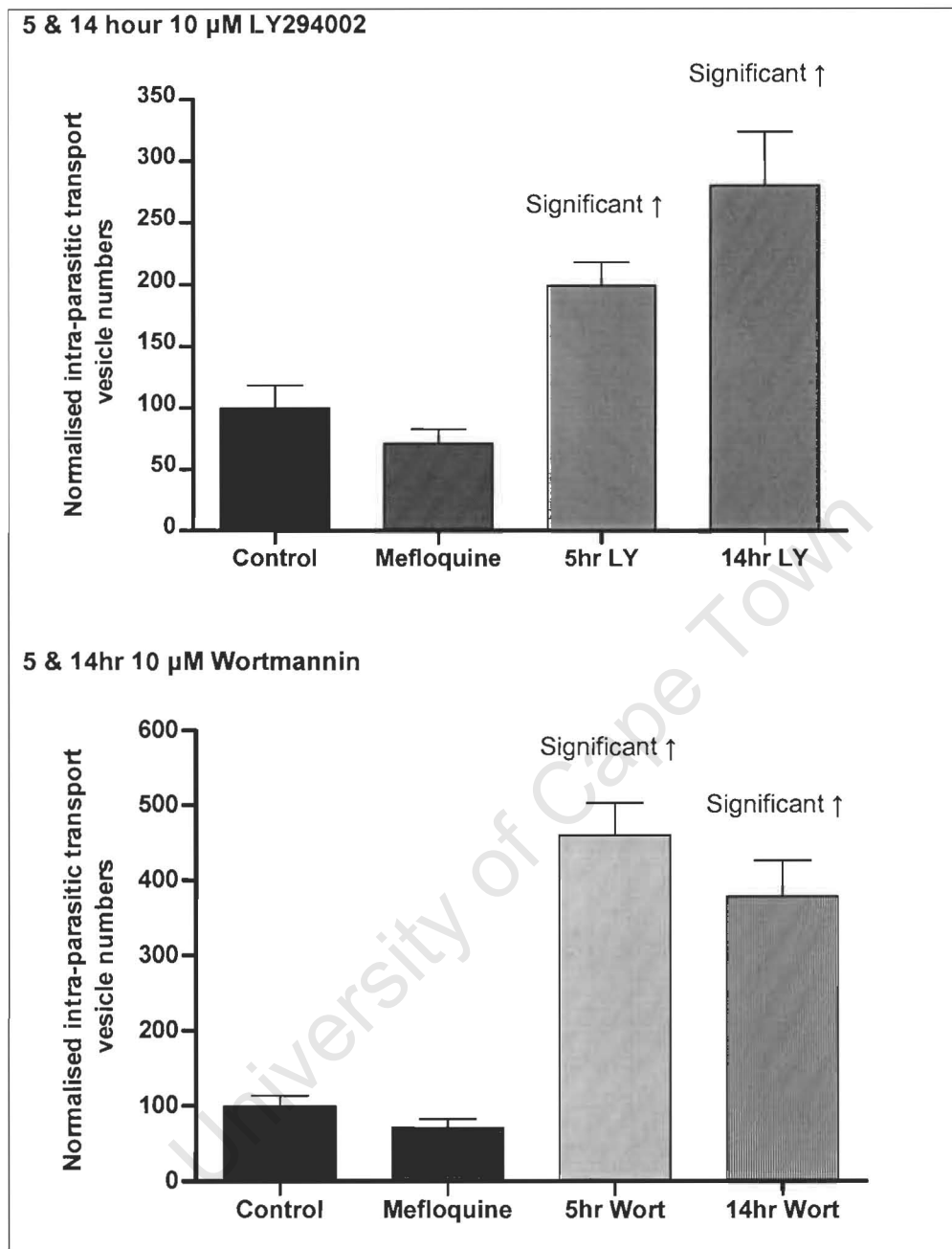


**Figure 18.** Malaria parasite transport vesicle numbers after drug and solvent control treatment. Average transport vesicle counts per parasite were compared between the various drug treatments and their respective solvent controls. Between 40 and 60 parasites (Table 15) were randomly selected on the haemoglobin IFA slides and the numbers of cytoplasmic fluorescent puncta (transport vesicles) outside the digestive vacuoles counted. Average transport vesicle counts were normalised to their respective solvent controls which were set at 100 and comparisons were made using appropriate statistical tests. Due to heterogeneity of variances and the non-normal distribution of the data, comparisons were made using the Non-parametric Mann-Whitney U test for independent samples. Statistical significance was set at  $\alpha = 0.05$ . Error bars indicate standard error of the mean.

**Table 15.** Digestive vacuole haemoglobin fluorescence levels within malaria parasites after various PI (3) kinase inhibiting drug treatments. n = number of observations.

Treatment	Control	Drug	% Change	n	Statistical test	Two tailed P value	Outcome
5 hr 10 $\mu$ M LY294002	100 $\pm$ 5.974	61.126 $\pm$ 4.641	39 % $\downarrow$	107	Mann-Whitney	p < 0.0001	Significant decrease
14 hr 10 $\mu$ M LY294002	100 $\pm$ 2.841	51.962 $\pm$ 2.789	48 % $\downarrow$	60	Mann-Whitney	p < 0.0001	Significant decrease
5 hr 10 $\mu$ M Wortmannin	100 $\pm$ 3.938	68.956 $\pm$ 3.836	31 % $\downarrow$	130	Mann-Whitney	p < 0.0001	Significant decrease
14 hr 10 $\mu$ M Wortmannin	100 $\pm$ 4.328	69.548 $\pm$ 3.277	30 % $\downarrow$	60	Mann-Whitney	p < 0.0001	Significant decrease
14 hr 156 nM Mefloquine	100 $\pm$ 4.677	65.563 $\pm$ 3.748	34 % $\downarrow$	60	Mann-Whitney	p < 0.0001	Significant decrease

**Table 16.** Transport vesicle numbers within malaria parasites after various PI (3) kinase inhibiting drug treatments. n = number of observations.

Treatment	Control	Drug	% Change	n	Statistical test	Two tailed P value	Outcome
5 hr 10 $\mu$ M LY294002	100 $\pm$ 18.31	199.19 $\pm$ 18.43	99 % $\uparrow$	60	Unpaired T test	p = 0.0002	Significant increase
14 hr 10 $\mu$ M LY294002	100 $\pm$ 24.69	280 $\pm$ 43.70	180 % $\uparrow$	40	Mann-Whitney	p = 0.0012	Significant increase
5 hr 10 $\mu$ M Wortmannin	100 $\pm$ 13.97	459.52 $\pm$ 42.99	360 % $\uparrow$	58	Mann-Whitney	p < 0.0001	Significant increase
14 hr 10 $\mu$ M Wortmannin	100 $\pm$ 23.80	377.78 $\pm$ 47.87	278 % $\uparrow$	40	Mann-Whitney	p < 0.0001	Significant increase
14 hr 156 nM Mefloquine	100 $\pm$ 19.46	70.97 $\pm$ 11.73	29 % $\downarrow$	40	Mann-Whitney	p = 0.5135	No significant change

### **3.2.7 Electron microscopy of malaria parasites exposed to the PI (3) kinase inhibiting drug Wortmannin**

To confirm ultrastructurally that the punctuated structures found in Wortmannin treated parasites represented haemoglobin filled double membrane transport vesicles that had failed to deliver their contents to the food vacuole, control and drug treated parasites were examined by electron microscopy. Transport vesicle numbers were counted in random cross sections of parasites, before comparisons were made using appropriate statistical tests with significance set at  $\alpha = 0.05$ . Additionally, transport vesicle size and distance from the periphery was estimated using a scale bar (1  $\mu\text{m}$ ) saved electronically onto digital images taken of parasitised erythrocytes on a Zeiss EM 912 transmission electron microscope.

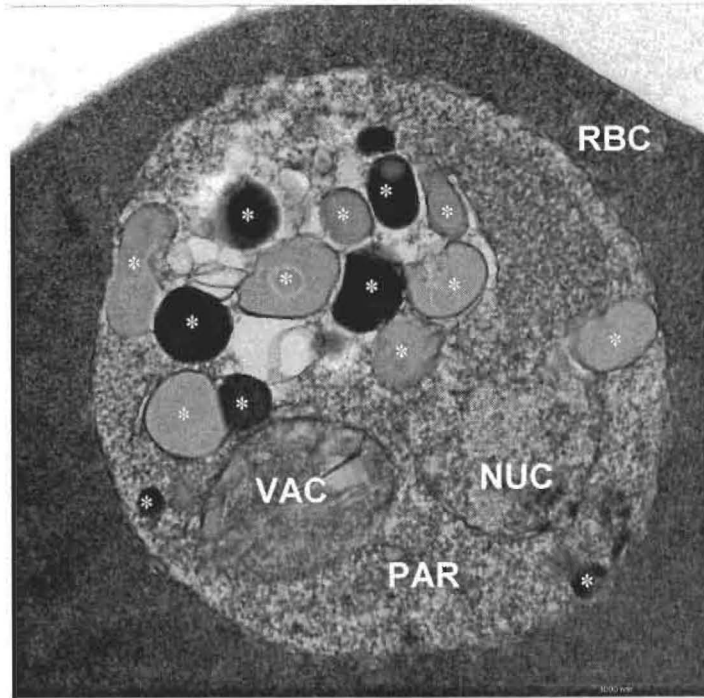
Wortmannin treated parasites contained significantly increased numbers of double membrane transport vesicles filled with ingested red blood cell cytosol, distinct from the digestive vacuole (Figure 19, asterisks & Figure 20). This is consistent with our findings from IFA, where PI (3) kinase inhibiting drugs significantly raised transport vesicle numbers within treated parasites. Transport vesicle counts, conducted by electron microscopy, are summarised in Table 17.

Taking advantage of the higher resolution offered by the electron microscope, transport vesicle size and distance from the periphery was examined in addition to their numbers within the parasite. Transport vesicle size increased by approximately 70% after Wortmannin treatment (Table 18), while their distance from the periphery did not change (Table 19). Interestingly, transport vesicles accumulated within Wortmannin treated parasites, appeared to bundle together. These findings may have implications on the role of PI (3) kinase during endocytosis which will further be explored in the discussion.

Treatment regimen

Transmission electron micrograph

5 hour  
10  $\mu$ M  
Wortmannin



5 hour  
0.1% DMSO  
Solvent control  
for Wortmannin

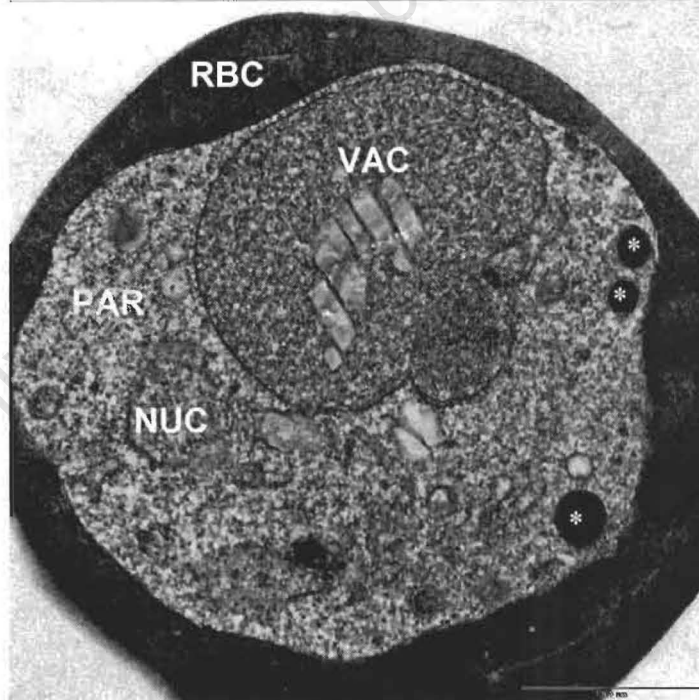


**Figure 19.** Transmission electron micrograph of a cross section of 10  $\mu$ M Wortmannin and solvent control treated trophozoite stage malaria parasites. Labelled structures are the infected erythrocyte (RBC), parasite (PAR), parasite nucleus (NUC), digestive vacuole (VAC), and transport vesicle (asterisks).

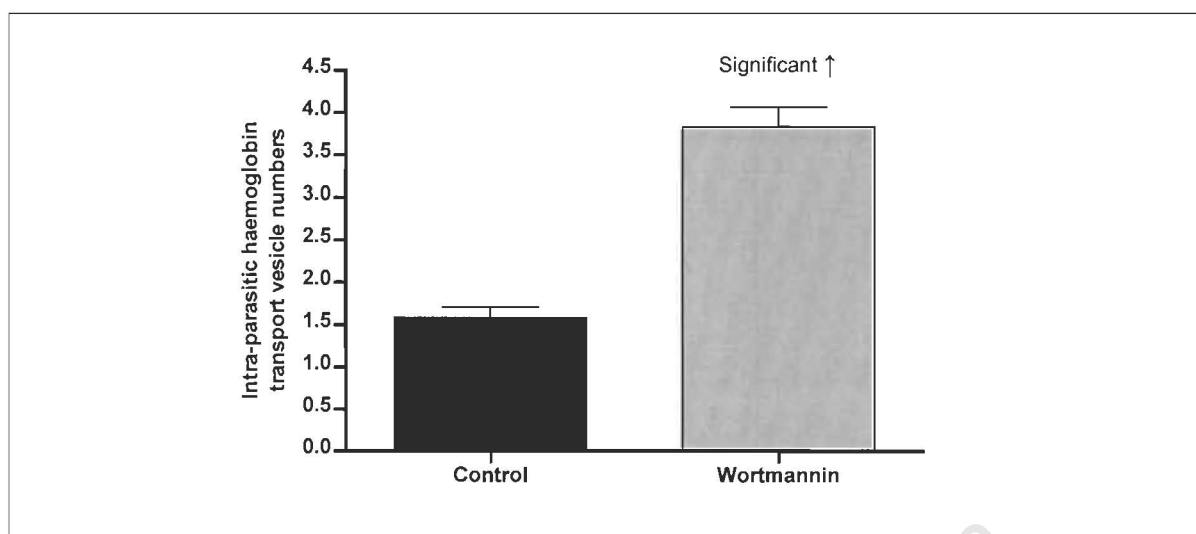


**Figure 20.** Transport vesicle numbers per malaria parasite after 5 hours of 10  $\mu$ M Wortmannin exposure as observed by electron microscopy. Comparisons were made using the non-parametric Mann-Whitney U test for independent samples. Statistical significance was set at  $\alpha = 0.05$ . Error bars indicate standard error of the mean.

**Table 17.** Transport vesicle numbers per malaria parasite after 5 hours of 10  $\mu$ M Wortmannin exposure as observed by electron microscopy. Comparisons were made using appropriate statistical tests. Statistical significance was set at  $\alpha = 0.05$ . n = number of observations.

Treatment	Control	Drug	% Change	n	Statistical test	Two tailed P value	Outcome
5 hr 10 $\mu$ M Wortmannin	1.58 $\pm$ 0.12	3.83 $\pm$ 0.23	142 % $\uparrow$	112	Mann Whitney	p < 0.0001	Significant increase

**Table 18.** Transport vesicle size within malaria parasites after 5 hours of Wortmannin treatment as observed by electron microscopy. To avoid bias, all measurements (nm) were taken across the longest axis of each transport vesicle. Comparisons were made using appropriate statistical tests. Statistical significance was set at  $\alpha = 0.05$ . n = number of observations.

Treatment	Control (nm)	Drug (nm)	% Change	n	Statistical test	Two tailed P value	Outcome
5 hr 10 $\mu$ M Wortmannin	322 $\pm$ 33	543 $\pm$ 26	69 % $\uparrow$	50	Mann Whitney	p < 0.0001	Significant increase

**Table 19.** Transport vesicle distance (nm) from the periphery of malaria parasites after 5 hours of Wortmannin treatment as observed by electron microscopy. To avoid bias, all measurements were taken across the shortest distance between the outer membrane of the vesicle and the parasite plasma membrane. Comparisons were made using appropriate statistical tests. Statistical significance was set at  $\alpha = 0.05$ .

Treatment	Control (nm)	Drug (nm)	% Change	n	Statistical test	Two tailed P value	Outcome
5 hr 10 $\mu$ M Wortmannin	370 $\pm$ 48	344 $\pm$ 53	7 % $\downarrow$	50	Unpaired T test	p = 0.7173	No significant change

### **3.2.8 The effect of PI (3) kinase inhibiting drugs on the localisation of actin in *P. falciparum* infected erythrocytes as assessed by immunofluorescence assay (IFA)**

As some results observed in Wortmannin and LY294002 treated parasites mirrored those seen in Cytochalasin D treated parasites, and as PI (3) kinases are known to regulate actin cytoskeleton remodelling, immunofluorescence assays were performed to investigate the effects these drugs could have on parasite actin localisation, using anti-actin antiserum and fluorescent secondary antibodies.

Control parasite actin appeared to be dispersed homogenously throughout the cytoplasm (Figure 21). Similar results were observed in parasites treated with both Wortmannin and LY294002.

These results suggest that PI (3) kinase has no altering effects on trophozoite actin localisation, at least not that which can be resolved by fluorescence microscopy.

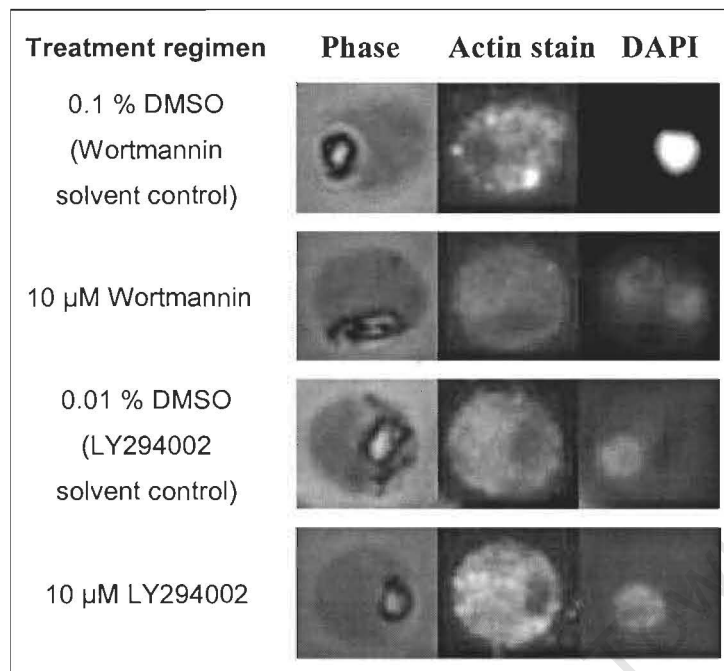


**Figure 21.** Microscope images showing the effect of PI (3) kinase inhibiting drugs on the sub-cellular localisation of actin by immunofluorescence. Parasitised erythrocytes were drug and solvent control treated before being saponin treated to release the parasite with subsequent fixation onto glass cover slips. Parasites were permeabilised before incubation with anti-actin antiserum and fluorescent secondary antibodies as well as DAPI. The panels represent from left to right: Treatment regimen, phase contrast image, TRITC-labelled anti-actin image and lastly the DAPI-stained nuclei image.

### 3.3 Discussion

In *Dictyostelium*, Phosphoinositide (3) kinase (PI (3) K) is required for macropinocytosis, a type of fluid-phase endocytosis (Maniak 2001). Additionally, Wortmannin and LY294002 were found to inhibit fluid-phase endocytosis within mammalian cells (Araki *et al.* 1996). By contrast, endocytic mechanisms in the malaria parasite *P. falciparum* are inadequately understood (Botero-Kleiven *et al.* 2001). Nonetheless, host erythrocyte cytoplasm is internalised through vacuole formations at the base of specialised endocytic sites termed cytostomes (Bannister *et al.* 2000, Hempelmann *et al.* 2002). Based on the reported participation of PI (3) kinase in fluid phase endocytosis in other eukaryotes, our initial hypothesis was that PI (3) kinase inhibition would inhibit endocytosis of host cytoplasm via the cytostome in the malaria parasite.

IC<sub>50</sub> curves were used to establish parasite sensitivity and working concentrations to the various PI (3) kinase inhibiting drugs. Interestingly, Wortmannin was found active at nanomolar concentrations in mammalian cells (Thelen *et al.* 1994), with a reported IC<sub>50</sub> of 25 nM (Spiro *et al.* 1996). Contrastingly, in the malaria parasite, Wortmannin and LY294002 had IC<sub>50</sub> concentrations of approximately 50 µM. This suggests that malaria parasites are not as sensitive to PI (3) kinase inhibition as mammalian cells are, or possibly due to differences in enzyme structures, the drugs do not inhibit malaria PI (3) kinase as well as they do their mammalian counterparts.

In this study we have partially addressed our hypothesis by showing that trophozoite stage malaria parasites require either PI (3) kinase or another Wortmannin-sensitive factor during endocytosis. These results were established by means of two assays involving the measurement of haemoglobin uptake within parasites whilst under the influence of protease inhibitors, and horseradish peroxidase uptake from pre-loaded host erythrocytes. Both LY294002 and Wortmannin significantly reduced intra-parasitic HRP levels after 14 hours of treatment. Additionally, PI (3) kinase inhibition (when co-administered with protease inhibitors) significantly reduced haemoglobin levels within the malaria parasite after 5 hours of treatment. Consistent with our findings, Wortmannin was found to inhibit constitutive endocytosis of HRP and transferrin in mammalian cells (Li *et al.*

1995). Furthermore, macropinocytosis in *Dictyostelium* is known to be PI (3) kinase dependent (Maniak 2003).

In addition for the requirement during endocytosis, our results suggest subsequent trafficking events within the malaria parasite are sensitive to either PI (3) kinase inhibition or another Wortmannin-sensitive factor. Initially, Giemsa-stained thin blood smears of trophozoite stage parasites were observed to have an apparent increase in punctuate structures and a decrease of haemozoin crystal. These results (similarly to the actin inhibiting results) suggested an accumulation of transport vesicles and a block in haemoglobin digestion. Supporting these findings, immunofluorescence assays conducted on Wortmannin and LY294002 treated parasites using anti-haemoglobin antiserum and fluorescent secondary antibodies, demonstrated a significant increase in transport vesicle numbers with a significant reduction of haemoglobin within the digestive vacuole. Subsequent electron microscopy assays further confirmed an increase in haemoglobin filled transport vesicles following drug treatment. Together these results inferred a block in transport vesicle trafficking to the digestive vacuole with a consequent decrease in haemoglobin delivery, and thus digestion within this compartment. These results explain the initial Western blots with anti-haemoglobin antiserum, which demonstrated significantly elevated intra-parasitic haemoglobin levels following drug treatment. Consistent with the block in trafficking, Fernandez-Borja *et al.* (1999) similarly inferred PI (3) kinase to regulate post-endosomal sorting and degradation in mammalian cells, as endocytosed molecules intended for degradation are transported to lysosomes inside transport intermediates which themselves required PI (3) kinase for their formation. Additionally, *in vitro* studies have demonstrated Wortmannin (100 ng / mL) to reduce early endosome fusion by 80 % by blocking PI (3) kinase activity (Li *et al.* 1995). It was therefore suggested that PI (3) P (an essential membrane component and product of PI (3) kinase), was likely responsible for membrane budding and / or fusion events required for constitutive membrane trafficking through interaction with FYVE-domain containing proteins. In light of this, it is therefore conceivable that Wortmannin and LY294002 treatment blocks membrane fusion events within the malaria parasite, resulting in the build up of transport vesicles which are unable to dock and fuse with the digestive vacuole. This leads to reduced levels of haemoglobin delivered to the digestive vacuole and consequently increased numbers of haemoglobin filled transport vesicles.

Interestingly, transport vesicle measurements, taken across the longest axis of each vesicle within Wortmannin treated parasites, were observed by electron microscopy to be significantly larger than those observed in control treated parasites. As PI (3) kinases are reported essential for phagosome and macropinosome closure into intracellular organelles within mammalian cells (Araki *et al.* 1996), transport vesicles could similarly require PI (3) kinase for their closure within the malaria parasite. PI (3) kinase-hindered closure of endocytic vesicles pinching off from the cytostome could result in greater quantities of cytoplasm collecting into the subsequently larger vesicles, observed within Wortmannin treated parasites. Alternatively, as PI (3) kinase is known to regulate actin polymerisation (Lennartz 1999, Takenawa & Itoh. 2001), PI (3) kinase inhibition may (similarly to the actin disrupting drug effects) result in the delayed closure of and or fission at the cytostome neck with consequently larger transport vesicle formation.

The “bundled” nature of the accumulated endocytic vesicles in the electron micrograph of Wortmannin treated parasites may reflect an interesting phenomenon. Parasite endocytic vesicles are surrounded by a double membrane. The outer membrane is derived from the parasite plasma membrane and the inner membrane from the parasite vacuole membrane (PVM) which surrounds the parasite and separates it from the host erythrocyte cytoplasm. Although not conclusive, the bundled structure may suggest that the outer membranes of the accumulated vesicles in close proximity fuse together in a homotypic fusion event, leading to a single large vacuole containing numerous haemoglobin-filled vesicles surrounded only by their inner membrane. This would suggest that unlike in mammalian cells (Li *et al.* 1995), PI (3) kinase inhibition does not prevent homotypic fusion of endocytic vesicles in parasites. However, PI (3) kinase activity is required for maturation of the outer membrane of the vesicles, in order for heterotypic fusion to the digestive vacuole to occur. If correct, this would be the first demonstration of vesicle maturation and homotypic fusion in the malaria parasite. Future studies, using serial cross-sectioning electron microscopy assays of parasite transport vesicles and cytostome organelles, could clarify the morphology of these structures following Wortmannin treatment. *In vitro* fusion assays, examining Wortmannin effects on homotypic and heterotypic fusion, could further elucidate the effect which either PI (3) kinase or another Wortmannin-sensitive factor has on membrane maturation and trafficking within the malaria parasite.

In summary, we have demonstrated PI (3) kinase to mediate endocytosis within the malaria parasite. Furthermore, trafficking of endocytosed haemoglobin within transport vesicles to the digestive vacuole was dependent on PI (3) kinase activity. This was possibly due to the inhibition of membrane fusion events, resulting in the inhibition of vesicle membrane maturation. This inhibition prevented transport vesicles from fusing with and consequently delivering their contents into the digestive vacuole, resulting in an accumulation of undigested haemoglobin filled transport vesicles.

University of Cape Town

## Chapter IV

### Conclusion

Published reports generally agree that actin dynamics may play several roles during endocytosis in eukaryotic cells, including vesicle formation and subsequent trafficking (Engqvist-Goldstein & Drubin 2003). Additionally, phosphoinositides (PI's) are reported to function as key regulators in major cellular processes, including signalling, trafficking and actin cytoskeleton remodelling (Takenawa & Itoh 2001). In this study, Cytochalasin D and Latrunculin A which depolymerise and prevent actin filament formation, Jasplakinolide which, by contrast, stabilises actin filaments, and Wortmannin and LY294002 which inhibit PI (3) kinase, were used to study actin disrupting and PI (3) kinase inhibiting drug effects on haemoglobin endocytosis and transport vesicle trafficking within the malaria parasite *P. falciparum*.

Mammalian cells on the whole have more evidence supporting actin in endocytic vesicle formation compared to PI (3) kinase dependence during this process. Contrastingly, in the malaria parasite, our results suggest the actin cytoskeleton is not essential for endocytosis whereas PI (3) kinase is. Interestingly, both classes of drug significantly elevate transport vesicle numbers within the parasite, suggesting they both effect subsequent vesicle trafficking. However, the mechanisms by which they accomplish this is suggested to be different. Future studies demonstrating a dose-dependent effect for each drug could bolster our findings and conclusions thereof.

Actin disruption is likely to prevent endocytic vesicle transport by blocking the formation of actin rockets or plumes which are proposed to drive endocytic vesicles further into the cell away from the plasma membrane in mammalian cells (Merrifield *et al.* 1999). Similarly, endocytic vesicle attachment to actin fibres via linker proteins (CLIPS) would be inhibited by actin disruption, thereby preventing their attachment and subsequent movement via motor proteins along actin microfilaments (Goode *et al.* 2000). This could result in an accumulation of endocytic vesicles which have failed to deliver their contents to the digestive vacuole, observed in the malaria parasite following actin disrupting drug treatment in this study.

Additionally, trafficking of endocytic vesicles may be impeded by PI (3) kinase inhibition by an alternative mechanism. Enzyme inhibition would prevent PI (3) P formation. Membrane budding and or fusion events, brought about by interactions between PI (3) P and FYVE-domain containing proteins, could thus be inhibited and result in a block in constitutive vesicle membrane maturation. This block in membrane maturation would conceivably prevent membrane fusion events within the malaria parasite, resulting in the build up of transport vesicles which are unable to dock and fuse with the digestive vacuole following PI (3) kinase inhibition treatment.

Therefore, trafficking within the malaria parasite is regulated by both actin and PI (3) kinase, similarly to mammalian cells (Richards *et al.* 2004). Interestingly, Leverrier & Ridley (2001) report actin dynamics to occur upstream of PI (3) kinase during endocytosis. Actin is required for initial phagosome / macropinosome or endocytic vesicle formation, while PI (3) kinase is required for subsequent phagosome / endosome maturation via membrane fusion / fission events. In contrast, as actin is potentially not required in the malaria parasite for endocytosis per se, while PI (3) kinase is potentially required, PI signalling seems to occur upstream of actin events. An alternative or additional explanation for the similarity in actin and PI (3) kinase inhibitor effects (i.e. build-up of transport vesicle and block in digestive vacuole fusion) could be that PI (3) kinase, in addition to PI (3) P formation and membrane maturation, regulates actin dynamics, as has been proposed in some studies in mammalian cells (Lennartz 1999, Takenawa & Itoh. 2001). A summary of actin disrupting and PI (3) kinase inhibiting drug effects on *Plasmodium* endocytic and trafficking events can be seen in Table 20.

**Table 20.** Drug effects on malaria parasite endocytic and trafficking events.

<b>Drug</b>	<b>Endocytosis (HRP)</b>	<b>Transport vesicle trafficking</b>
Cytochalasin D	Has no effect	Impedes trafficking
Jasplakinolide	Reduces uptake (barrier)	Impedes trafficking
Wortmannin / LY294002	Reduces uptake	Impedes trafficking

# Chapter V

## Materials and methodology

### 5.1 *P. falciparum* strain used in this study

The *P. falciparum* strain 3D7 (cloned from NF54 isolated in the Netherlands (Walliker *et al.* 1987)) was used during this thesis.

### 5.2 Drugs used during this study

All actin cytoskeleton disrupting and Phosphoinositide-3-kinase (PI (3) kinase) inhibiting drugs were dissolved in dimethyl-sulphoxide (DMSO). Mefloquine was dissolved in methanol (MeOH) with additional dilutions performed in culture medium (CM). Protein digestion inhibiting enzymes, ALLN and E64 were dissolved in DMSO and distilled deionised water (dH<sub>2</sub>O) respectively. All drugs were stored between -20 and -80 °C.

#### 5.2.1 Actin cytoskeleton disruptors:

- 1 mg of Cytochalasin D (*Zygosporium mansonii*) (Calbiochem-Novabiochem, La Jolla, Calif.), having a molar mass of 507.6 grams per mole (g / mol), was dissolved in 1970 µL DMSO yielding a 1 mM stock.
- 50 µg of Jasplakinolide (*Jaspis johnstoni*) (Calbiochem-Novabiochem, La Jolla, Calif.), having a molar mass of 709.7 g / mol, was dissolved in 70.4 µL DMSO resulting in a 1 mM stock.
- 100 µg of Latrunculin A (*Latrunculia magnifica*) (Calbiochem-Novabiochem, La Jolla, Calif.), having a molar mass of 421.6 g / mol, was dissolved in 23.7 µL DMSO generating a 10 mM stock.

### **5.2.2 PI (3) kinase inhibitors:**

- 1 mg of Wortmannin (Calbiochem-Novabiochem, La Jolla, Calif.), having a molar mass of 428.4 g / mol, was dissolved in 233.4  $\mu$ L DMSO making a 10 mM stock.
- 5 mg of LY294002 (Calbiochem-Novabiochem, La Jolla, Calif.), having a molar mass of 307.4 g / mol, was dissolved in 1626  $\mu$ L DMSO making a 10 mM stock.

### **5.2.3 Malaria endocytosis inhibitor:**

- 1 mg of Mefloquine hydrochloride (Roche Diagnostics, Mannheim, Germany), having a molar mass of 378.312 g / mol, was dissolved in 1 mL methanol and diluted a further 1000 fold in culture medium yielding a 2.6  $\mu$ M stock.

### **5.2.4 Haemoglobin digesting inhibiting drugs (protease inhibitors (PrI)):**

- 5 mg of ALLN (Calbiochem-Novabiochem, La Jolla, Calif.), having a molar mass of 383.5 g / mol, was dissolved in 326  $\mu$ L DMSO yielding a 40 mM stock.
- 1 mg of E64 protease inhibitor (Calbiochem-Novabiochem, La Jolla, Calif.), having a molar mass of 357.4 g / mol, was dissolved in 140  $\mu$ L distilled deionised water ( $\text{dH}_2\text{O}$ ) yielding a 20 mM stock.

### **5.2.5 Horseradish Peroxidase (endocytic tracer):**

- A 5 mg / mL stock was prepared in culture medium and stored at 4°C covered in light shielding tinfoil wrapping. Horseradish peroxidase (HRP) was purchased from Sigma-Aldrich.

The above mentioned drugs, with their respective solvent controls and the endocytic marker HRP, were added to parasite cultures at final concentrations summarised in Table 21.

**Table 21.** Drugs used during experimentation together with their respective solvent controls at final concentrations.

Treatment	Final drug concentration	Final solvent concentration
Cytochalasin D	50 nM	0.0005 % DMSO
Latrunculin A	10 $\mu$ M	0.1 % DMSO
Jasplakinolide	1 $\mu$ M	0.1 % DMSO
Wortmannin	10 $\mu$ M	0.1 % DMSO
LY294002	10 $\mu$ M	0.01 % DMSO
Mefloquine	156 nM	0.006 % MeOH
ALLN	40 $\mu$ M	0.1 % DMSO
E-64	40 $\mu$ M	dH <sub>2</sub> O
HRP (5 mg / mL)	200 $\mu$ g / mL	Culture medium

### 5.3 *P. falciparum* in vitro cell culture

Parasites were cultivated under sterile conditions according to a modified method of Trager and Jensen (1977). The parasites were maintained in RPMI 1640 culture medium (Biowhittaker Highveld Biologicals, Johannesburg, South Africa) supplemented with 25 mM sodium bicarbonate, gentamycin sulphate [50  $\mu$ g / L], 22 mM glucose, 25 mM Hydroxyethane Piperazine Sulphonic Acid (HEPES), 5 g / L Albumax II (GIBCO BRL) and 323  $\mu$ M hypoxanthine. The cells were routinely maintained at a haematocrit (hct) between 2 and 4 % and a parasitemia (pst) falling between 5 and 10 %. Culture medium (CM) was changed daily and parasites were diluted with O<sup>+</sup> human erythrocytes (Western Province Blood Transfusion Service, Cape Town, South Africa) during the trophozoite stage. Culture flasks harbouring the suspended parasites were maintained in an atmosphere of filtered 4 % CO<sub>2</sub>, 3 % O<sub>2</sub>, and 93 % N<sub>2</sub> and stored in a NUAIR™ incubator at 37 °C.

Thin blood smears, fixed on glass slides with methanol, were stained with 10 % Giemsa stain (Merck, Darmstadt, Germany) in phosphate-buffered saline (composed of 8.0 g / L sodium chloride, 0.2 g / L potassium chloride, 1.15g / L di-sodium hydrogen phosphate and 0.2 g / L potassium dihydrogen phosphate) (PBS) for 3 minutes. The slides were

rinsed with water and air dried before viewing under a Leitz microscope fitted with an oil immersion objective. The number of parasitised RBC's divided by the total number of erythrocytes, both parasitised and non-parasitised, yielded the parasitemia.

## 5.4 Parasite synchronisation

Parasite cultures were routinely synchronised during ring phase of development using the D-sorbitol method described by Lambros & Vanderberg (1979). Suspensions were centrifuged at 750 rcf (relative centrifugation force) for 3 minutes with the resulting pellet, comprised of parasitised and non-parasitised erythrocytes, incubated in 5 volumes of 5 % D-sorbitol (Sigma) for 10 minutes at 37 °C. The newly sorbitol treated parasite pellets were re-suspended in CM, causing preferential lysis of erythrocytes infected with trophozoite stage parasites and resulting in a predominantly ring phase infected culture (Figure 22 (Panel A)). Parasite cultures were predominantly in the trophozoite stage of development 24 hours after synchronisation as seen in Figure 22 (Panel B).

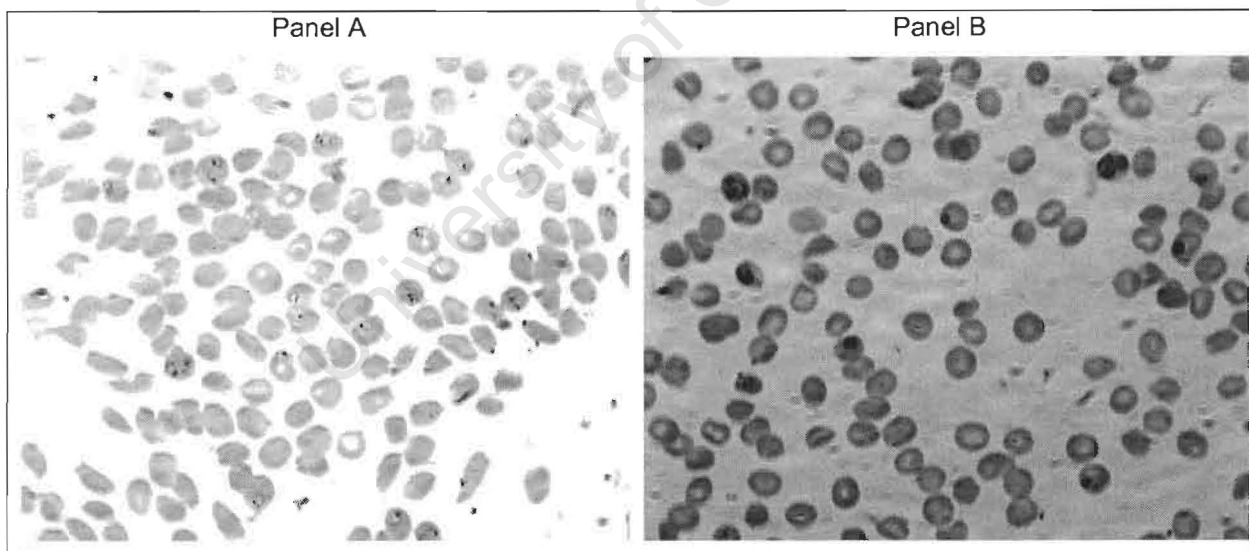


**Figure 22.** Giemsa stained ring infected parasite culture after synchronisation using 5 % sorbitol (A). A predominantly trophozoite infected culture 24 hours after sorbitol synchronisation (B).

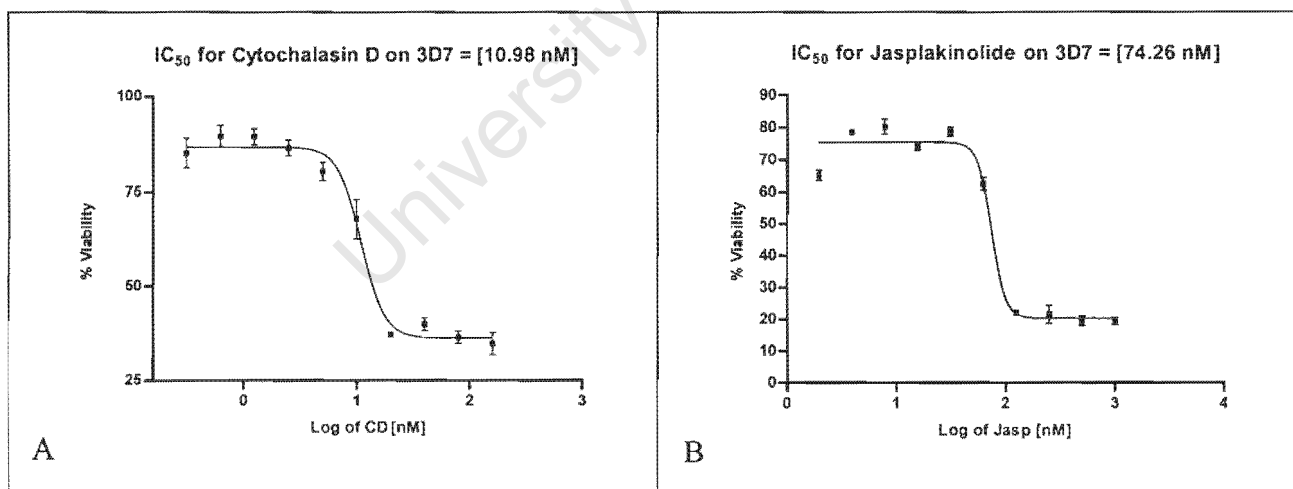
## 5.5 Growth inhibition assays (IC<sub>50</sub>)

In order to establish working concentrations for the various classes of drug, IC<sub>50</sub> values for each were generated (Figure 23). The sensitivity of *P. falciparum* to the various drugs was assayed in vitro using a colorimetric method which measures the activity of the parasite enzyme lactate dehydrogenase (Makler *et al.* 1993, Fivelman *et al.* 1999). This enzyme catalyses the conversion of lactate to pyruvate and is dependent on the co-factor NAD<sup>+</sup> which is itself reduced by a hydride anion (H<sup>-</sup>) derived from the lactate molecule to form NADH. As *Plasmodium* lactate dehydrogenase (pLDH) specifically reacts with 3-acetyl pyridine adenine dinucleotide (APAD<sup>+</sup>), an analogue of NAD, and human LDH isozymes do not (Makler *et al.* 1993), the enzymatic assay described by Piper *et al.* (1999) was used to measure pLDH activity in presence of human LDH found in erythrocytes. In order to visualise the parasite specific enzymatic formation of APADH from APAD (Malstat™), a visualisation solution containing Nitroblue Tetrazolium (NBT) (1.6 mg / mL) and Phenazine Ethosulphate (PES) (0.08 mg / mL) was added. NBT reduction to the blue / purple formazan salt can be monitored and quantified spectrophotometrically at 620 nm. Thus, lactate dehydrogenase activity is used as a measure of parasite viability, with the greatest colour production produced by the most viable parasites.

Using a similar method described by Desjardins *et al.* (1979), parasites obtained from continuous stock cultures were sub cultured into flat bottomed 96-well microtitration plates. 200µL of non-parasitised erythrocytes, maintained at 1 % haematocrit, suspended in CM containing no drug were added to the plate as the blank. Each drug, at double its final concentration in CM, was added in triplicate in 200 µL aliquots to the microtitre plate. Next, 100 µL volumes of CM were added to all wells excepting those harbouring the drug and the blank mentioned above. Two-fold serial dilutions of each drug were made across the plate. Parasite cultures, in trophozoite stage of development, sub cultured to 2 % parasitemia in a 2 % erythrocyte suspension, were added in 100 µL aliquots to all columns in the plate excepting the blank. The control constituted a 2 % parasitised erythrocyte suspension, containing no drug, in CM at a haematocrit of 1 %. The microtitre plates, once prepared, were placed into dessiccator cabinets and flushed with gas as previously described, before storage in a NUAIR™ incubator at 37 °C for 48 hours. The concentration ranges for each drug over the two-fold serial dilution series were as follows:

Cytochalasin D (160 nM to 0.3125 nM); Latrunculin A (39 nM to 0.076172 nM); Jaspplakinolide (1000 nM to 1.953125 nM); Wortmannin (1000  $\mu$ M to 1.953125  $\mu$ M); LY294002 (200  $\mu$ M to 0.390625  $\mu$ M); Mefloquine (250 nM to 0.488251 nM); Dimethylsulphoxide (20 % to 0.039063 %) and Methanol (9.5 % to 0.01855 %).

After the 48 hour incubation period during which parasites grew in the presence of drug or control, 15  $\mu$ L from each well were transferred into a duplicate plate containing 100  $\mu$ L Malstat™ reagents (APAD and lactate) and 25  $\mu$ L NBT / PES. Parasite viability was then determined by measuring the generation of a blue / purple coloured Tetrazolium salt with a spectrophotometer at a wavelength ( $\lambda$ ) of 620 nm. To cancel out the erythrocytes LDH ability to produce the blue coloured formazan salt, all readings were subtracted from the blank giving a more specific reflection of parasite viability. The percentage viability was calculated by dividing the absorbance of the drug exposed parasites by the absorbance of the control parasites, multiplied by 100. Results were entered into the GraphPad Prism 4 computer package and growth inhibition curves were constructed for each drug as well as for the solvents, DMSO and methanol.



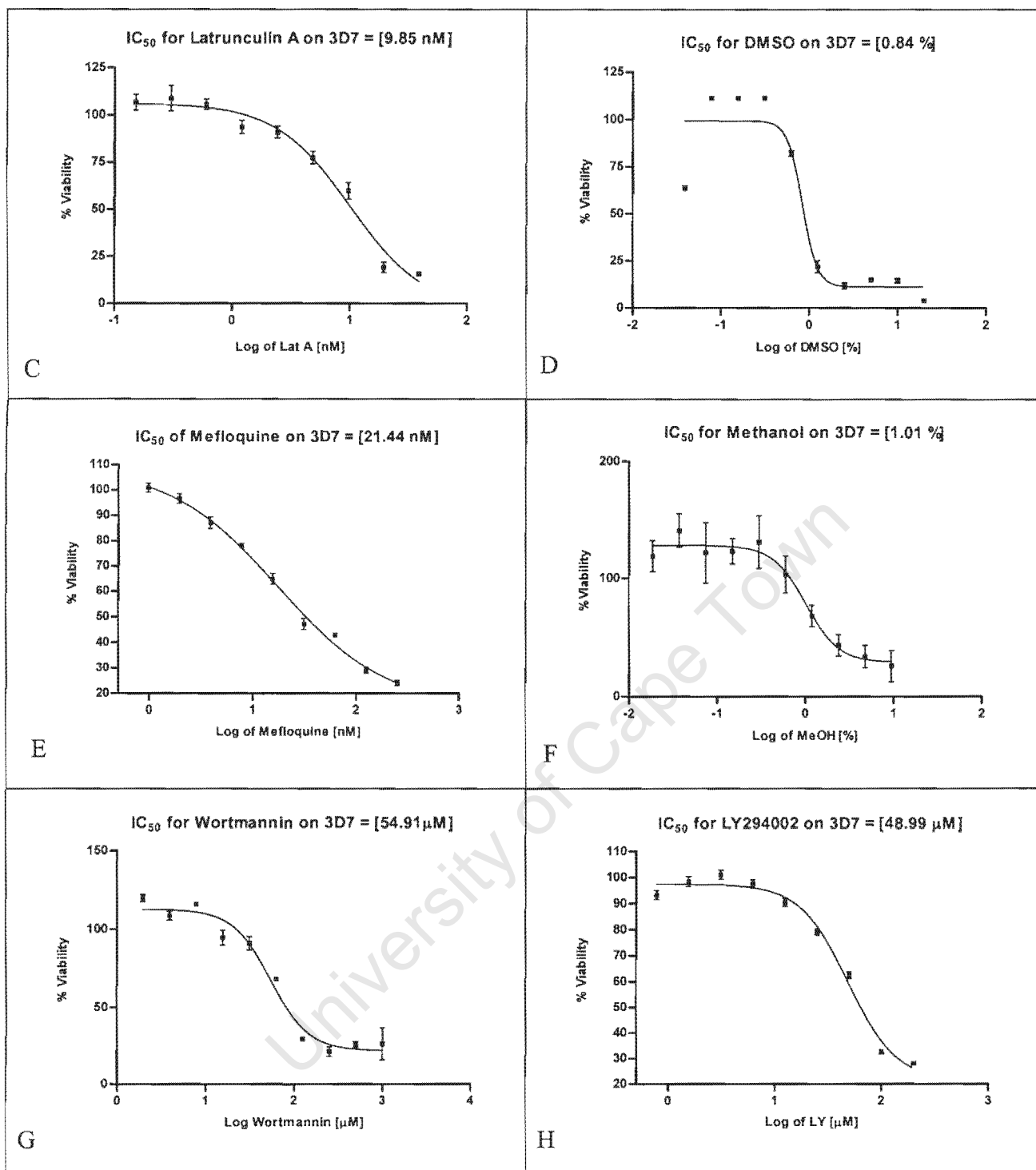


**Figure 23.**  $IC_{50}$  graphs for the various drugs and their solvents used during the course of this study.

## 5.6 Enrichment of trophozoite infected erythrocytes

Cultures were enriched either by density centrifugation using a modified version of Ginsburg et al. (1984) or by a magnetic separation of haemazoin-containing parasites using a MACS system (Miltenyi Biotec GmbH, Bergisch Gladbach, Germany) (Uhlemann *et al.* 2000). The prior, density gradient centrifugation enrichment method, involved trophozoite infected erythrocytes being isolated from ring and non-infected red blood cells based on their unique density profile. An 80 % (v/v) Percoll (Sigma-Aldrich, St. Louis, Mo.) solution was prepared in 5 x RPMI solution at 25 % w/v sorbitol. A 60 % (v/v) Percoll solution was prepared in equal volumes of 5 x RPMI at 25 % w/v sorbitol and 1 x RPMI at 5 % w/v sorbitol. 500  $\mu$ L of 60 % percoll solution was carefully layered onto 500  $\mu$ L 80 % percoll solution within a microcentrifuge tube. Between 200 and 300  $\mu$ L of an approximately 10 % parasitised erythrocyte pellet was layered onto the 60 % percoll solution. The percoll / parasite mixture was then centrifuged at 10 000 rcf for 15 minutes in a microfuge with slow acceleration / deceleration activated. The enriched trophozoite layer was situated at the interface between the two percoll gradients. The layer of trophozoite stage parasites were removed and added to 3 x volume of CM drop-wise with swirling to prevent hypertonic lysis of the infected erythrocytes. The parasites were centrifuged on a microfuge at 4500 rpm for 3 minutes and added to 5 x volume CM drop-wise with swirling to the pellet before re-suspending them in 15 mL CM for further experimentation.

Trophozoite enrichment by magnetic property involved passing approximately 200  $\mu$ L of packed parasite culture through an LD column (Miltenyi Biotec) whilst within the magnetic field of a MACS Separator magnet (Miltenyi Biotec). This technique utilised the magnetic property of iron located within haem harboured within trophozoite stage parasites. Non-infected and ring infected erythrocytes having less magnetic properties passed through the column, while trophozoite infected erythrocytes remained within the magnetic column and were later eluted with 2 mL culture supernatant from the LD column by removing the magnetic field. Both techniques regularly yielded cultures at greater than 90 % parasitemia as confirmed by light microscopy of Giemsa stained trophozoite stage parasite cultures (Figure 24 (Panel B)).

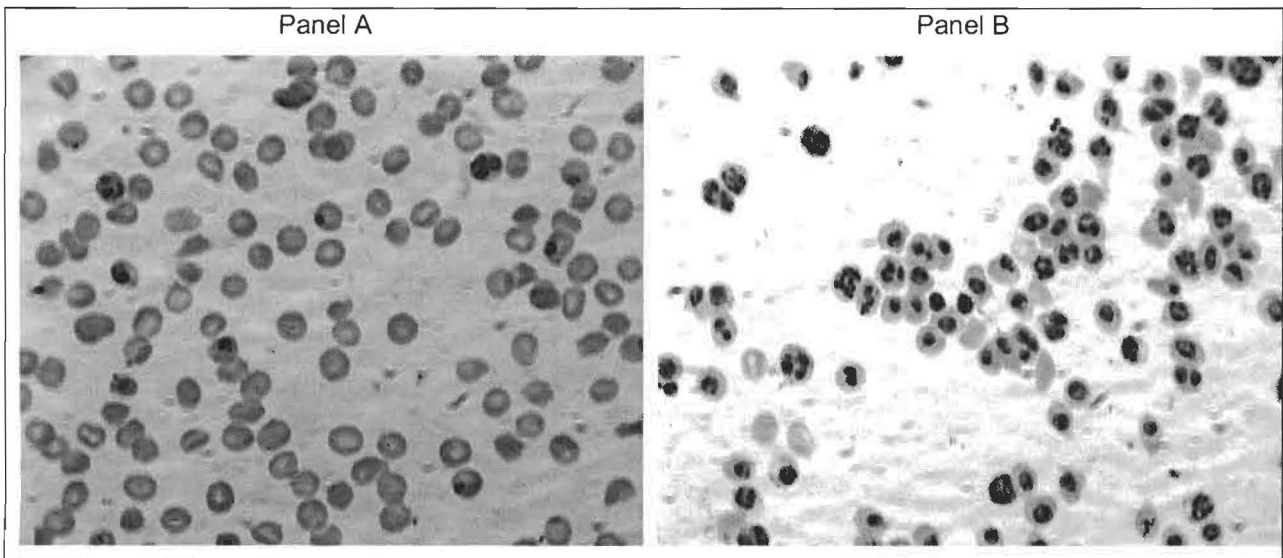


**Figure 24.** Microscope images of Giemsa stained trophozoite infected erythrocytes. Panel A represents a non-enriched trophozoite culture whilst Panel B represents an enriched trophozoite infected erythrocyte culture.

## 5.7 Trophozoite isolation from host erythrocytes by saponin lysis

Mid to late trophozoite stage parasites were isolated from their host erythrocytes using saponin lysis. Approximately 1 mL of parasite culture (roughly 10 % parasitemia) having a haematocrit of 2 % (i.e. about 20  $\mu$ L of pRBC pellet) was centrifuged at 700 rcf for 3 minutes before aspirating off the supernatant leaving behind the pellet of parasitised erythrocytes. Parasitised red blood cells collected into microcentrifuge tubes were re-suspended into 500  $\mu$ L of 0.1 % (w/v) saponin (Sigma) in PBS. Thereafter the parasite pellet was centrifuged on a microfuge at 5000 rpm for 3 minutes. The parasite pellet was washed 4 times in 1 mL CM to remove excess haemoglobin.

## **5.8 The effect of actin disrupting drugs on red blood cell integrity**

Erythrocytes were treated with either 50 nM Cytochalasin D or 1  $\mu$ M Jasplakinolide for 5 hours. Erythrocyte pellets were collected from the various suspensions by bench-top centrifugation at 4500 rcf for 3 minutes and diluted 5 fold in CM. Erythrocyte numbers were counted in triplicate both before and after drug exposure by means of a haemocytometer viewed under a Leitz Laborlux light microscope using a 40 times objective. Small aliquots of diluted red cell suspensions were applied to haemocytometer slides under glass cover slips. Erythrocytes located in five randomly selected grids on the haemocytometer were counted. This procedure was performed in triplicate. The mean number for each count was then multiplied by the dilution factor of 5. This number was then multiplied by 25 (total number of grids) before multiplying by 10 000 yielding the total number of erythrocytes located within 10 mL of red blood cell suspension. Erythrocyte counts were normalised to their respective solvent controls which were set at 100. As the data sets were normally distributed and had equal variances, parametric Unpaired T-tests were used to compare erythrocyte numbers before and after drug exposure. Statistical significance was set at  $\alpha = 0.05$ .

## **5.9 Morphology of parasitised erythrocyte cultures before and after 14 hour actin perturbing drug exposure**

In order to visualise possible gross morphological changes in parasitised erythrocyte cultures, Giemsa stained thin blood smears were performed. Light microscopy of air dried and methanol fixed infected erythrocytes were conducted on a Leitz Laborlux microscope under a 100 times magnification oil immersion objective. Images of the various parasite cultures were captured using a Media Cybernetics CoolSNAP-Pro monochrome cooled charge-coupled device camera.

## **5.10 Sodium dodecyl sulphate polyacrylamide gel electrophoresis (SDS-PAGE)**

SDS-PAGE was performed according to the standard procedure of (Laemmli 1970). A single culture of malaria parasites maintained at approximately 10 % parasitemia was split in two and exposed to either drug or control. Trophozoite phase parasites, harboured within red blood cells, were then pelleted after drug and control exposure in a microfuge at 4500 rpm for 3 minutes. Trophozoite stage parasites were isolated from their host cells by saponin lysis and excess haemoglobin removed as described above. The resulting pellets, comprised of parasites harbouring endocytosed haemoglobin, were re-suspended in 80  $\mu$ L of distilled deionised water (dH<sub>2</sub>O) resulting in hypotonic parasite lysis. The mixture was added to 20  $\mu$ L of 4 x concentration reducing SDS-PAGE sample buffer (10 mL stacking buffer, 8 mL glycerol, 0.8 g SDS, 0.8 mL 2-mercapto-ethanol, 0.2 mg bromophenol blue and 1.2 mL distilled water) and boiled for 5 minutes. In order to pellet haemozoin, triplicate samples were centrifuged at 13000 rpm for 1 minute on a microfuge before application to a SDS-10%-PAGE gel. The stacking buffer used was comprised of 6.05 g Tris, 0.4 g SDS and made up to 100 mL water with the pH adjusted to 6.8. The resolving gel buffer (lower gel) was made of 18.2 g Tris, 0.4 g SDS and mad up to 100 mL water with the pH adjusted to 8.8.

Electrophoresis was performed at a constant 20 mA in a Bio-Rad Mini PROTEAN<sup>®</sup> II electrophoresis apparatus. After the loading dye front approached the gel edge, the gel was removed and used for Western blotting.

## **5.11 Western blotting**

Parasite proteins (performed in triplicate) resolved by passage through an SDS polyacrylamide gel, was transferred onto a Hybond-ECL Nitrocellulose membrane (Amersham Pharmacia Biotech) in a Bio-Rad Mini Trans-Blot Electrophoretic Transfer Cell at a constant 100 Volts for 60 minutes in transblot buffer (3.029 g / L Tris (0.303 %), 14.4 g / L glycine (1.44 %) and 200 mL / L of methanol (20 %) in water). Block solution

(5 % (w/v) fat-free milk powder and 0.1 % (v/v) Tween 20 (Sigma) in PBS) was added to each membrane for 45 minutes before incubation with rabbit anti-haemoglobin antiserum (Sigma-Aldrich, St. Louis, Mo.) diluted 1:1000 in block solution for 1 hour. The membrane was rinsed in wash buffer (0.1 % (v/v) Tween 20 in PBS) before 4 additional rinses in block solution for 5 minutes each.

The washed membrane was incubated with secondary antibody (peroxidase-conjugated goat anti-rabbit immunoglobulin (Calbiochem-Novabiochem, La Jolla, Calif.) diluted 1:5000 in 10 mL block solution, for an hour before rinsing 5 times for 5 minutes each in wash buffer.

To visualise membrane bound peroxidase, the membrane was soaked in LumiGlo chemiluminescent substrate (KPL, Gaithersburg, MD) wrapped in cling wrap and exposed to Kodak BioMax Light autoradiography film. Exposure times between 5 and 20 seconds were used. Western blot images on developed autoradiograph film were captured using a Kodak EDAS 290 gel documentation system incorporating a Kodak DC290 digital camera. Net intensities of individual haemoglobin bands were quantified with a Kodak 1D image analysis software package version 3.5.

All experiments were performed in duplicate or triplicate on at least three separate days. Haemoglobin band intensity readings analysed with Kodak 1D image analysis software, were normalised to their respective solvent controls. Due to non-normal distribution of data and significant differences of variances between data sets, normalised net intensity readings of drug and control bands were compared using the non-parametric Mann-Whitney U test for independent samples. Those data sets having normal distribution and equal variances were analysed using the parametric Unpaired T-test. Statistical significance was set at  $\alpha = 0.05$ .

## **5.12 Horseradish Peroxidase endocytosis assay**

Red blood cells were pre-loaded with horseradish peroxidase (HRP) by hypotonic lysis (Krogstad & Schlesinger 1986). One volume of 30°C pre-heated packed erythrocytes was

rapidly mixed with one and half volumes 30°C pre-heated hypotonic solution (5 mM HEPES, 11 mM glucose, 2 mM MgCl<sub>2</sub> and 2 mM Na<sub>2</sub>ATP) containing 200 µg / mL horseradish peroxidase, and incubated for 10 minutes at 30°C. Erythrocyte membranes were re-sealed by rapidly mixing them with one and a half volumes of 37°C pre-heated hypertonic solution (280 mM NaCl, 40 mM KCl and 11 mM glucose) and incubating for 5 minutes at 37 °C. Packed erythrocytes (600 µL) were pre-loaded with the endocytic tracer, HRP, and added to approximately 30 µL of enriched trophozoite infected erythrocytes in 15 mL culture medium. Trophozoite infected erythrocytes were enriched by the previously described percoll density gradient centrifugation method. The mixture was returned to culture, allowing the malaria parasites to invade the HRP pre-loaded erythrocytes and develop into late rings. Drug and solvent controls were added for 14 hours. After incubation, parasitised red blood cells were pelleted in a microfuge at 4500 rpm for 3 minutes before being isolated by saponin lysis and washed to remove extra-parasitic HRP described previously. Isolated trophozoite phase parasites were permeabilised in 1 mL of 0.1 M phosphate citrate buffer (pH 4.8) containing 1 % Triton. The samples were centrifuged for 30 seconds in a Beckman bench-top centrifuge at top speed to pellet haemozoin crystals. Next we added 100 µL of the supernatant to 100 µL phosphate citrate buffer containing 3 mg / mL o-phenylenediamine (OPD) and 1 µL / mL H<sub>2</sub>O<sub>2</sub> (HRP substrate) in a 96-well plate. Each experiment was performed in triplicate and absorbance measured at 450 nm on a spectrophotometer. The use of a blank (i.e. non-HRP pre-loaded RBC's) to control for background calometric readings was initially done (data not shown). As the absorbance levels for these blanks were virtually undetectable, experiments were conducted as stated above. Absorbance values were normalised to the control and comparisons were made using appropriate statistical tests. Due to normal distribution of data and equal variances between data sets, normalised absorbance readings of drug and control bands were compared using the parametric Unpaired T-test. Statistical significance was set at  $\alpha = 0.05$ .

### 5.13 Immunofluorescence assay (IFA)

In order to visualise the location of haemoglobin harboured within drug pressured parasites, immunofluorescence assays were performed on mid to late trophozoite stage parasites (identifiable by the DAPI-stained nuclei, which should be  $\leq 2$ ).

A 1 mg / mL poly-L-lysine mixture (poly-L) was made in PBS. Glass cover slips were incubated in 50  $\mu$ L of poly-L for 15 minutes. Poly-L treated cover slips were then placed into the wells of a 24-well plate containing 300  $\mu$ L of PBS in each well. Erythrocyte pellets were collected from various drug and control treated cultures by centrifugation at 4500 rpm for 3 minutes using a microfuge. Trophozoite stage parasites were isolated and excess haemoglobin removed as described previously. Parasite pellets, collected from each drug and control treated culture, were re-suspended in 30  $\mu$ L PBS. Re-suspended parasites were transferred into the 24-well plate wells containing poly-L treated cover slips in 300  $\mu$ L PBS. Parasites were pelleted onto the glass cover slips by centrifugation at 700 rcf for 2 minutes. Loosely bound parasites were removed by rinsing the cover slips 4 times with 1 mL of PBS. Parasites were then fixed in 0.5 mL PBS containing 4 % paraformaldehyde and 0.25 % gluteraldehyde for 15 minutes. The glass cover slips, with attached parasites, were rinsed 4 times with 1 mL PBS before being permeabilised with 0.5 mL of 0.5 % Triton X-100 (Sigma) in PBS for 5 minutes. Following another 4 rinses with 1 mL PBS, the parasites were treated with 0.5 mL of 0.15 M glycine for 20 minutes to quench possible reactive aldehyde groups before being rinsed a further 4 times in 1 mL PBS.

The newly permeabilised parasites, fixed onto cover slips, were incubated in block solution for 30 minutes within a moist chamber. The block solution was composed of 2 % Bovine Serum Albumin Factor V (Boehringer Mannheim), 50 % Foetal calf serum (Highveld Biological), 1 mM magnesium chloride (Sigma), 1 mM calcium chloride (BDH) and 0.1 % Tween 20 (Sigma) in PBS.

Rabbit anti-haemoglobin antiserum (primary antibody) (Sigma-Aldrich St. Louis MO) diluted 1:200 in block solution, was used to probe the various parasite samples. The cover slips were incubated for an hour with primary antibody within moist chambers before

being rinsed 4 times in 1 mL wash. Wash was composed of 0.1 % BSA and 0.1 % Tween 20 in PBS.

The light sensitive secondary antibody (Tetramethylrhodamine B Isothiocyanate (TRITC)-conjugated anti-rabbit antibody) (Invitrogen, Frederick, MA) diluted 1:250 in block solution, was incubated with the cover slips for a further hour within a light sheltered moist chamber. Again the cover slips were rinsed 4 times with 1 mL of wash.

Lastly, parasite nuclei were stained by rinsing the cover slips in 1  $\mu\text{g}$  / mL 4',6'-diamidino-2-phenylindole (DAPI) for 1 minute. The cover slips were then rinsed in dH<sub>2</sub>O before being dabbed dried on tissue and mounted onto glass microscope slides on drops of anti-fading polyvinyl alcohol mounting medium (Permafluor) (Immunotech, Marseille, France). Parasites were examined the following day on a Nikon Eclipse E600 fluorescence microscope using a 100 times oil-immersion objective. Images of malaria parasites were captured using a Media Cybernetics CoolSNAP-Pro monochrome cooled charge-coupled device camera. The fluorescence microscope settings for the visualisation of TRITC and DAPI fluorescence are as follows: TRITC (EX 540/25, DM 565, BA 605/55) and DAPI (EX 340 – 380, DM 400, BA 435 – 485).

Average transport vesicles per parasite counts were obtained by randomly selecting parasites and counting the amount of extra-digestive vacuolar fluorescent foci. Average transport vesicle counts obtained from each drug treated parasite sample were normalised to their respective solvent controls. Additionally fluorescence intensity readings within the parasite digestive vacuoles were quantified using the histogram function of Adobe Photoshop software (Version 7.0). Intensity readings in treated samples were normalised to their respective controls and comparisons were made using appropriate statistical tests. Due to heterogeneity of variances and the non-normal distribution of the data, comparisons were made using the non-parametric Mann-Whitney U test for independent samples. Conversely, those data sets which had normal distribution and equal variances were analysed using the parametric Unpaired T-test. Statistical significance was set at  $\alpha = 0.05$ .

## 5.14 Electron microscopy

Erythrocytes from a *P. falciparum* culture were centrifuged after 5 hours of drug and control exposure in a microfuge at 4500 rpm for 3 minutes. Erythrocytes infected with trophozoite stage parasites were enriched by means of a magnetic column as described earlier. The enriched parasite cultures eluted from the column were washed in 1mL of fixing buffer comprised of 0.1 M sodium cacodylate, 0.1 M sucrose, 2 mM calcium chloride, and 2 mM magnesium chloride adjusted to a pH between 7.2 and 7.4. The parasitised erythrocytes were fixed by tumbling in 1 mL fixing buffer containing 4 % paraformaldehyde and 2 % glutaraldehyde before washing in 1 mL fixing buffer. The parasites were further fixed by tumbling for an hour in 1 mL fixing buffer containing 1 % tannic acid before being washed twice with 1 mL fixing buffer. The infected erythrocytes were lastly fixed in 1 % osmium tetroxide in 1 mL fixing buffer whilst being tumbled for an hour and again washed twice with 1 mL fixing buffer. Fixed cells were subsequently pelleted, immobilized in 2 % low melting point agarose, and dehydrated in a series of ascending ethanol concentrations comprised of 30, 50, 75 and 100 % for 10 minutes each whilst tumbling. Cells were further dehydrated in 50 and 100 % propylene oxide in ethanol for 10 minutes each whilst tumbling. Spurr resin was allowed to infiltrate the dehydrated cells in a series of ascending concentrations of resin in propylene oxide (50, 75 and 100 %). Resin infiltration was carried out for 2 hours whilst tumbling in 50 and 75 % resin and overnight in 100 % Spurr resin. The parasite sample was transferred into freshly prepared 100 % Spurr resin the following day and tumbled for the day. The sample was then left overnight in fresh Spurr resin at 60 °C in a heating block.

Ultra thin sections (60 -80 nm) were prepared the following day with an ultramicrotome. Parasite sections were contrasted with uranyl acetate for 8 minutes and lead citrate for 4 minutes before viewing them on a JEOL 1200EXII transmission electron microscope (for transport vesicle counts) or Zeiss EM910 transmission electron microscope (for capturing digital images).

Transport vesicle numbers, as well as size and distance from the periphery were measured and comparisons were made using appropriate statistical tests. As variances between data

sets were significantly different, the non-parametric Mann-Whitney U test for independent samples was used. Significance was set at  $\alpha = 0.05$ . Transport vesicle size and distance to the periphery was measured by reference to a 1  $\mu\text{m}$  scale bar captured along with the digital image. To avoid bias, transport vesicle size was estimated by measuring the longest axis across each double membrane vesicle. Similarly, transport vesicle distance from the parasite periphery was estimated by measuring the shortest distance between the parasite plasma membrane and the outer membrane of the double membrane vesicle.

University of Cape Town

## References

- Aikawa, M., Hepler, P.K., Huff, C.G., and H. Sprinz. 1966. The feeding mechanism of avian malarial parasites. *Journal of Cell Biology*. **28**:355-373.
- Anderson, R. G. 1998. The caveolae membrane system. *Annual Review of Biochemistry*. **67**:199–225.
- Apodaca, G. 2001. Endocytic traffic in polarised epithelial cells: Role of the actin and microtubule cytoskeleton. *Traffic*. **2**:149-159.
- Araki, N., Johnson, M.T., and J.A. Swanson. 1996. A role for Phosphoinositide 3-kinase in the completion of macropinocytosis and phagocytosis by macrophages. *The Journal of Cell Biology*. **135**:1249-1260.
- Ayscough, K.R. 2004. Endocytosis: Actin in the driving seat. *Current Biology*. **14**:R124-R126.
- Ayscough, K.R., Pokala, J.S.N., Sanders, M., Crews, P., and D.G. Drubin. 1997. High rates of actin filament turnover in budding yeast and roles for actin in establishment and maintenance of cell polarity revealed using the actin inhibitor Latrunculin-A. *The Journal of Cell Biology*. **137**:399–416.
- Bannister, L., Hopkins, J., Fowler, R., Krishna, S., and G. Mitchell. 2000. A brief illustrated guide to the ultrastructure of *Plasmodium falciparum* asexual blood stages. *Parasitology Today*. **16**:427-433.
- Botero-Kleiven, S., Fernandez, V., Lindh, J., Richter-Dahlfors, A., von Euler, A., and M. Wahlgren. 2001. Receptor-mediated endocytosis in an Apicomplexan parasite (*Toxoplasma gondii*). *Experimental Parasitology*. **98**:134-144.
- Brown, D.A., and E. London. 1998. Functions of lipid rafts in biological membranes. *Annual Review of Cell Developmental Biology*. **14**:111–136.
- Bubb, M.R., Senderowicz, A.M.J., Sausville, E.A., Duncan, K.L.K., and E.D. Korn. 1994. Jasplakinolide, a cytotoxic natural product, induces actin polymerisation and competitively inhibits the binding of phalloidin to F-actin. *The Journal of Biological Chemistry*. **269**:14869-14871.
- Cardelli, J. 2001. Phagocytosis and macropinocytosis in *Dictyostelium*: Phosphoinositide-based processes, biochemically distinct. *Traffic*. **2**:311-320.

- Cassimeris, L., McNeill, H., and S.H. Zigmond. 1990. Chemottractant-stimulated polymorphonuclear leukocytes contain two populations of actin filaments that differ in their spatial distributions and relative stabilities. *The Journal of Cell Biology*. **110**:1067-1075.
- Cavalli, V., Corti, M., and J. Gruenberg. 2001. Endocytosis and signalling cascades: a close encounter. *FEBS Letters*. **498**:190-196.
- Clague, M.J. 1998. Molecular aspects of the endocytic pathway. *The Biochemical Journal*. **336**:271-282.
- Clarke, M., Kohler, J., Heuser, J., and G. Gerisch. 2002. Endosome fusion and microtubule-based dynamics in the early endocytic pathway of *Dictyostelium*. *Traffic*. **3**:791-800.
- Conner, S.D., and S.L. Schmid. 2003. Regulated portals of entry into the cell. *Nature*. **422**:37-44.
- Corvera, S., D'Arrigo, A., and H. Stenmark. 1999. Phosphoinositides in membrane traffic. *Current Opinion in Cell Biology*. **11**:460-465.
- Coue, M., Brenner, S.L., Spector, I., and E.D. Korn. 1987. Inhibition of actin polymerization by Latrunculin A. *FEBS letters*. **231**:316-318.
- Damm, E., Pelkmans, Kartenbeck, J., Mezzacasa, A., Kurzchalia, T., and A. Helenius. 2005. Clathrin- and caveolin-1-independent endocytosis: entry of simian virus 40 into cells devoid of caveolae. *The Journal of Cell Biology*. **168**:477-488.
- De Camilli, P., Emr, S. D., McPherson, P. S., and P. Novick. 1996. Phosphoinositides as regulators in membrane traffic. *Science*. **271**:1533-1539.
- Desjardins, R.E., Canfield, C.J., Haynes, J.D., and J.D. Chulay. 1979. Quantitative assessment of antimalarial activity *In Vitro* by a semiautomated microdilution technique. *Antimicrobial Agents and Chemotherapy*. **16**:710-718.
- Dobrowolski, J.M., and L.D. Sibley. 1996. *Toxoplasma* invasion of mammalian cells is powered by the actin cytoskeleton of the parasite. *Cell*. **84**:933-939.
- Dunn, K.W., McGraw, T.E., and F.R. Maxfield. 1989. Iterative fractionation of recycling receptors from lysosomally destined ligands in an early sorting endosome. *The Journal of Cell Biology*. **109**: 3303-3314.
- Durrbach, A., Louvard, D., and E. Coudrier. 1996. Actin filaments facilitate two steps of endocytosis. *Journal of Cell Science*. **109**:457-465.

- Eitzen, G. 2003. Actin remodelling to facilitate membrane fusion. *Biochimica et Biophysica Acta*. **1641**:175-181.
- Engqvist-Goldstein, A.E.Y. and D.G. Drubin. 2003. Actin assembly and endocytosis: From yeast to mammals. *Annual Review in Cell Development Biology*. **19**:287-332.
- Fernandez-Borja, M., Wubbolts, R., Calafat, J., Janssen, H., Divecha, N., Dusseljee, S., and J. Neefjes. 1999. Multivesicular body morphogenesis requires phosphatidylinositol 3-kinase activity. *Current Biology*. **9**:55-58.
- Fitch, C.D. 2004. Ferriprotoporphyrin IX, phospholipids, and the antimalarial actions of quinoline drugs. *Life Sciences*. **74**:1957-1972.
- Fivelman, Q.L., Walden, J.C., Smith, P.J., Folb, P.I., and K.I. Barnes. 1999. The effect of artesunate combined with standard antimalarials against chloroquine-sensitive and chloroquine-resistant strains of *Plasmodium falciparum* *in vitro*. *Transactions of the Royal Society of Tropical Medicine and Hygiene*. **93**:429-432.
- Francis, S.E., Gluzman, I.Y., Oksman, A., Knickerbocker, A., Mueller, R., Bryant, M.L., Sherman, D.R., Russell, D.G., and D.E. Goldberg. 1994. Molecular characterization and inhibition of a *Plasmodium falciparum* aspartic hemoglobinase. *The EMBO Journal*. **13**:306-317.
- Gagescu, R., Gruenberg, J., and E. Smythe. 2000. Membrane dynamics in endocytosis: Structure-function relationship. *Traffic*. **1**:84-88.
- Gaidarov, I., Santini, F., Warren, R. A., and J. H. Keen. 1999. Spatial control of coated-pit dynamics in living cells. *Nature Cell Biology*. **1**:1-7.
- Gavigan, G.S., Dalton, J.P., and A. Bell. 2001. The role of aminopeptidases in haemoglobin degradation in *Plasmodium falciparum*-infected erythrocytes. *Molecular & Biochemical Parasitology*. **117**:37-48.
- Geli, M.I., and H. Riezman. 1998. Endocytic internalisation in yeast and animal cells: similar and different. *Journal of Cell Science*. **111**:1031-1037.
- Gillooly, D., J., Simonsen, A., and H. Stenmark. 2001. Phosphoinositides and phagocytosis. *The Journal of Cell Biology*. **155**:15-17.
- Ginsburg, H., Kutner, S., Krugliak, M., and Z.I. Cabantchik. 1984. Characterization of permeation pathways appearing in the host membrane of

- Plasmodium falciparum* infected red blood cells. *Molecular and Biochemical Parasitology*. **14**:313-322.
- Grimmer, S., van Deurs, B., and K. Sandvig. 2002. Membrane ruffling and macropinocytosis in A431 cells require cholesterol. *Journal of Cell Science*. **115**:2953-2962.
  - Goddette, D.W., and C. Frieden. 1986. The mechanism of action of Cytochalasin D. *The Journal of Biological Chemistry*. **261**:15974-15980.
  - Goldberg, D.E. 1993. Hemoglobin degradation in *Plasmodium*-infected red blood cells. *Seminars in Cell Biology*. **4**:355-361.
  - Goode, B.L., Drubin, D.G., Barnes, G., 2000. Functional cooperation between the microtubule and actin cytoskeletons. *Current Opinion in Cell Biology* **12**: 63–71.
  - Goodyer, I.D., Pouvelle, B., Schneider, T.G., Trelka, D.P., and T.F. Taraschi. 1997. Characterization of macromolecular transport pathways in malaria-infected erythrocytes. *Molecular and Biochemical Parasitology*. **87**:13-28.
  - Gruenberg, J. 2001. The endocytic pathway: A mosaic of domains. *Nature Reviews*. **2**:721-730.
  - Gruenberg, J., Griffiths, G., and K.E. Howell. 1989. Characterization of the early endosome and putative endocytic carrier vesicles in vivo and with an assay of vesicle fusion in vitro. *The Journal of Cell Biology*. **108**:1301-1316.
  - Hakansson, S., Charron, A.J., and L.D. Sibley. 2001. *Toxoplasma* vacuoles: a two step process of secretion and fusion forms the parasitophorous vacuole. *EMBO Journal*. **20**:3132–3144.
  - Haldar, K., de Amorim, A.F., and G.A.M. Cross. 1989. Transport of fluorescent phospholipid analogues from the erythrocyte membrane to the parasite in *Plasmodium falciparum*-infected cells. *The Journal of Cell Biology*. **108**:2183-2192.
  - Haldar, K., Samuel, B.U., Mohandas, N., Harrison, T., and N.L. Hiller. 2001. Transport mechanisms in *Plasmodium*-infected erythrocytes: lipid rafts and a tubovesicular network. *International Journal for Parasitology*. **31**:1393-1401.
  - Hempelmann, E., Motta, C., Hughes, R., Ward, S.A., and P. G. Bray. 2003. *Plasmodium falciparum*: sacrificing membrane to grow crystals? *Trends in Parasitology*. **19**:23–26.

- Hoppe, H.C., van Schalkwyk, D.A., Wiehart, U.I.M., Meredith, S.A., Egan, J., and B.W. Weber. 2004. Antimalarial quinolines and artemisinin inhibit endocytosis in *Plasmodium falciparum*. *Antimicrobial Agents and Chemotherapy*. **48**:2370-2378.
- Kappe, S.H.I., Buscaglia, C.A., Bergman, L.W., Coppens I., and V. Nussenzweig. 2004. Apicomplexan gliding motility and host cell invasion: overhauling the motor model. *TRENDS in Parasitology*. **20**:13-16.
- Kirk, K. 2001. Membrane transport in the malaria-infected erythrocyte. *Parasitological Reviews*. **81**:495-537.
- Kirkham, M., and R.G. Parton. 2005. Clathrin-independent endocytosis: New insights into caveolae and non-caveolar lipid raft carriers. *Biochimica et Biophysica Acta*. **1745**:273-286.
- Kirkham, M., Fujita, A., Chadda, R., Nixon, S.J., Kurzchalia, T.V., Sharma, D.K., Pagano, R.E., Hancock, J.F., Mayor, S. and R.G. Parton. 2005. Ultrastructural identification of uncoated caveolin-independent early endocytic vehicles. *The Journal of Cell Biology*. **168**: 465-476.
- Kolakovich, K.A., Gluzman, I.Y., Duffin, K.L., and D.E. Goldberg. 1997. Generation of haemoglobin peptides in the acidic digestive vacuole of *Plasmodium falciparum* implicates peptide transport in amino acid production. *Molecular & Biochemical Parasitology*. **87**:123-135.
- Krogstad, D.J., and P.H. Schlesinger. 1986. A perspective on antimalarial action: effects of weak bases on *Plasmodium falciparum*. *Biochemical Pharmacology* **35**:547-552.
- Krugliak, M., Zhang, J., and H. Ginsburg. 2002. Intraerythrocytic *Plasmodium falciparum* utilizes only a fraction of the amino acids derived from the digestion of host cell cytosol for the biosynthesis of its proteins. *Molecular & Biochemical Parasitology*. **119**:249-256.
- Laemmli, U.K. 1970. Cleavage of structural proteins during the assembly of the head of bacteriophage T4. *Nature*. **227**:680 - 685.
- Lamaze, C., Fujimoto, L.M., Yin, H.L., and S.L. Schmid. 1997. The actin cytoskeleton is required for receptor-mediated endocytosis in mammalian cells. *The Journal of Biological Chemistry*. **272**:20332-20335.
- Lambros, C., and J.P. Vanderberg. 1979. Synchronisation of *Plasmodium falciparum* intraerythrocytic stages in culture. *Journal of Parasitology* **65**:418-420.

- Lauer, S., Rathod, P., Ghori, N. and K. Haldar. 1997. A membrane network for nutrient import in red cells infected with the malaria parasite. *Science*. **276**: 1122-1125.
- Lennartz, M.R. 1999. Phospholipases and phagocytosis: the role of phospholipid derived second messengers in phagocytosis. *The International Journal of Biochemistry and Cell Biology*. **31**:415-430.
- Leverrier, Y., and A.J. Ridley. 2001. Requirement for Rho GTPases and PI 3-kinases during apoptotic cell phagocytosis by macrophages. *Current Biology*. **11**:195–199.
- Li, G., D'Souza-Schorey, C., Barbieri, M.A., Roberts, R.L., Klippel, A., Williams, L.T., and P.D. Stahl. 1995. Evidence for Phosphatidylinositol 3-kinase as a regulator of endocytosis via activation of Rab5. *Proceedings of the National Academy of Sciences of the United States of America*. **92**:10207-10211.
- Magowan, C., Brown, J.T., Liang, J., Heck, J., Coppel, R.L., Mohandas, N., W. Meyer-Ilse. 1997. Intracellular structures of normal and aberrant *Plasmodium falciparum* malaria parasites imaged by Soft-X-Ray microscopy. *Proceedings of the National Academy of Sciences of the United States of America*. **94**:6222-6227.
- Makler, M.T., Ries, J.M., Williams, J.A., Bancroft, J.E., Piper, R.C., Gibbins, B.L., and D.J. Hinrichs. 1993. Parasite lactate dehydrogenase as an assay for *Plasmodium falciparum* drug sensitivity. *American Journal of Tropical Medicine and Hygiene*. **48**:739-741.
- Maniak, M. 2003. Fusion and fission events in the endocytic pathway of *Dictyostelium*. *Traffic*. **4**:1–5.
- Maniak, M. 2001. Fluid-phase uptake and transit in axenic *Dictyostelium* cells. *Biochimica et Biophysica Acta*. **1525**:197-204.
- Martin, R.E., and K. Kirk. 2006. Transport of the essential nutrient isoleucine in human erythrocytes infected with the malaria parasite *Plasmodium falciparum*. *Blood*. **109**:2217-2224.
- May, R.C., and L.M. Machesky. 2001. Phagocytosis and the actin cytoskeleton. *Journal of Cell Science*. **114**:1061-1077.
- Merrifield, C.J., Feldman, M.E., Wan, L., and W. Almers. 2002. Imaging actin and dynamin recruitment during invagination of single clathrin-coated pits. *Nature Cell Biology*. **4**:691–698.

- Merrifield, C.J., Moss, S.E., Ballestrem, C., Imhof, B.A., Giese, G., Wunderlich, I., and W. Almers. 1999. Endocytic vesicles move at the tips of actin tails in cultured mast cells. *Nature Cell Biology*. 1:72-74.
- Mukherjee, S., Ghosh, R.N., and F.R. Maxfield. 1997. Endocytosis. *Physiological Reviews*. 77:759-803.
- Nabi, I.R., and P.U. Le. 2003. Caveolae/raft-dependent endocytosis. *Journal of Cell Biology*. 161:673–677.
- Nichols, B.A., Chiappino, M.L., and C.E. Pavesio. 1994. Endocytosis at the micropore of *Toxoplasma gondii*. *Parasitology research*. 80:91-98.
- Niedergang, F., and F. Chavrier. 2004. Signaling and membrane dynamics during phagocytosis: many roads lead to the phagos(R)ome. *Current Opinion in Cell Biology*. 16:422-428.
- Odorizzi, G., Babst, M., and S.D. Emr. 2000. Phosphoinositide signalling and the regulation of membrane trafficking in yeast. *Trends in Biochemical Sciences*. 25:229-235.
- Oliveira, C.A., Chedraoui, S., and B. Mantovani. 1997. Latrunculin A is a potent inducer of aggregation of polymorphonuclear leukocytes. *Life Sciences*. 61:603-609.
- Olliaro, P.L., and D.E. Goldberg. 1995. The *Plasmodium* digestive vacuole: Metabolic headquarters and choice drug target. *Parasitology Today*. 11:294-297.
- Piper, R., Lebras, J., Wentworth, L., Hunt-Cook, A., Houze, S., Chiodini, P., and M. Makler. 1999. Immunocapture diagnostic assays for malaria using *Plasmodium* lactate dehydrogenase (pLDH). *The American Journal of Tropical Medicine and Hygiene*. 60:109-118.
- Pouvelle, B., Gormley, J.A., and T.F. Taraschi. 1994. Characterization of trafficking pathways and membrane genesis in malaria-infected erythrocytes. *Molecular and Biochemical Parasitology*. 66:83-96.
- Pouvelle, B., Spiegel, R., Hsiao, L., Howard, R., Morris, R., Thomas, A. and T. Taraschi. 1991. Direct access to serum macromolecules by intraerythrocytic malaria parasites. *Nature*. 353:73-75.
- Prescott, D.M. 1988. *Cells* (1<sup>st</sup> edition). Jones and Bartlett Publishers, Boston, Portola Valley, pp 621.

University of Cape Town

- Seastone, D.J., Lee, E., Bush, J., Knecht, D., and J. Cardelli. 1998. Overexpression of a novel Rho family GTPase, RacC, induces unusual actin-based structures and positively affects phagocytosis in *Dictyostelium discoideum*. *Molecular Biology of the Cell*. **9**:2891-2904.
- Shaw, M.K., and L.G. Tilney. 1999. Induction of an acrosomal process in *Toxoplasma gondii*: Visualization of actin filaments in a protozoan parasite. *Proceedings of the National Academy of Sciences of the United States of America*. **96**:9095-9099.
- Sibley, L.D. 2003. *Toxoplasma gondii*: Perfecting an intracellular life style. *Traffic*. **4**:581-586.
- Simonsen, A., Lippe, R., Christoforidis, S., Gaullier, J., Brech, A., Callaghani, J., Toh, B., Murphy, C., Zerial, M., and H. Stenmark. 1998. EEA1 links PI(3)K function to Rab5 regulation of endosome fusion. *Nature*. **394**:494-498.
- Singh, R.D., Puri, V., Valiyaveetil, J.T., Marks, D.L., Bittman, R. and R.E. Pagano. 2003 Selective caveolin-1-dependent endocytosis of glycosphingolipids. *Molecular Biology of the Cell*. **14**: 3254– 3265.
- Slater, A.F.G., Swiggard, W.J., Orton, B.R., Flitter, W.D., Goldberg, D., Serami, E. and G.B. Henderson. 1991. An iron-carboxylate bond links heme units of malaria pigment. *Proceedings of the National Academy of Sciences of the United States of America*. **88**:325-329.
- Soldati, D., and M. Meissner. 2004. *Toxoplasma* as a novel system for motility. *Current Opinion in Cell Biology*. **16**:32-40.
- Spiro, D.J., Boll, W., Kirchhausen, T., and M. Wessling-Resnick. 1996. Wortmannin alters the transferrin receptor endocytic pathway *In Vivo* and *In Vitro*. *Molecular Biology of the Cell*. **7**:355-367.
- Stenmark, H., Aasland, R., Toh, B., and A D'Arrigo. 1996. Endosomal localization of the autoantigen EEA1 is mediated by a zinc-binding FYVE finger. *The Journal of Biological Chemistry*. **271**:24048-24054.
- Takenawa, T., and T. Itoh. 2001. Phosphoinositides, key molecules for regulation of actin cytoskeletal organisation and membrane traffic from the plasma membrane. *Biochimica et Biophysica Acta*. **1533**:190-206.

- Taunton, J., Rowning, B.A., Coughlin, M.L., Wu, M., Moon, R.T., Mitchison, T.J., and C.A. Larabell. 2000. Actin-dependent propulsion of endosomes and lysosomes by recruitment of N-WASP. *The Journal of Cell Biology*. **148**:519-530.
- Thelen, M., Wymann, M.P., and H. Langen. 1994. Wortmannin binds specifically to 1-phosphatidylinositol 3-kinase while inhibiting guanine nucleotide-binding protein-coupled receptor signalling in neutrophil leukocytes. *Proceedings of the National Academy of Sciences of the United States of America*. **91**:4960-4964.
- Trager, W., and J.B. Jensen. 1976. Human malaria parasites in continuous culture. *Science*. **193**:673-675.
- Uhlemann, A., Staalsoe, T., Klinkert, M., and L. Hviid. 2000. Analysis of *Plasmodium falciparum*-infected red blood cells. *MACS and more*. 4:7-8.
- van Vliet, C., Thomas, E.C., Merino-Trigo, A., Teasdale, R.D., and P.A. Gleeson. 2003. Intracellular sorting and transport of proteins. *Progress in Biophysics and Molecular Biology*. **83**:1-45.
- Walliker, D., Quakyi, I.A., Wellems, T.E., McCutchan, T.F., Szarfman, A., London, W.T., Cororan, L.M., Burkot, T.R., and R. Carter. 1987. Genetic analysis of the human malaria parasite *Plasmodium falciparum*. *Science*. **236**:1661-1666.
- Wang, C.C., and P.M. Simashkevich. 1981. Purine metabolism in the protozoan parasite *Eimeria tenella*. *Proceedings of the National Academy of Sciences of the United States of America*. **78**:6618-6622.
- Wesseling, J.G., Smits, M.A., and J.G.G. Schoenmakers. 1988. Extremely diverged actin proteins in *Plasmodium falciparum*. *Molecular and Biochemical Parasitology*. **30**:143-153.
- Wesseling, J.G., Snijders, J.F., van Someren, P., Jansen, J., Smits, M.A., and G.G. Schoenmakers. 1989. Stage-specific expression and genomic organisation of the actin genes of the malaria parasite *Plasmodium falciparum*. *Molecular and Biochemical Parasitology*. **35**:167-176.